PHYSICAL REVIEW D **76,** 126010 (2007)

Explaining the electroweak scale and stabilizing moduli in *M* theory

Bobby S. Acharya

Abdus Salam International Centre for Theoretical Physics, Strada Costiera 11, Trieste, Italy and INFN, Sezione di Trieste

Konstantin Bobkov, Gordon L. Kane, Piyush Kumar, and Jing Shao

Michigan Center for Theoretical Physics, University of Michigan, Ann Arbor, Michigan 48109, USA

(Received 24 May 2007; published 12 December 2007)

In a recent paper [B. Acharya, K. Bobkov, G. Kane, P. Kumar, and D. Vaman, Phys. Rev. Lett. **97**, 191601 (2006).] it was shown that in fluxless *M* theory vacua with at least two hidden sectors undergoing strong gauge dynamics and a particular form of the Kähler potential, all moduli are stabilized by the effective potential and a stable hierarchy is generated, consistent with standard gauge unification. This paper explains the results of [B. Acharya, K. Bobkov, G. Kane, P. Kumar, and D. Vaman, Phys. Rev. Lett. **97**, 191601 (2006).] in more detail and generalizes them, finding an essentially unique de Sitter vacuum under reasonable conditions. One of the main phenomenological consequences is a prediction which emerges from this entire class of vacua: namely, gaugino masses are significantly suppressed relative to the gravitino mass. We also present evidence that, for those vacua in which the vacuum energy is small, the gravitino mass, which sets all the superpartner masses, is automatically in the TeV–100 TeV range.

DOI: 10.1103/PhysRevD.76.126010 PACS numbers: 11.25.Mj, 04.65.+e, 12.60.Jv

I. INTRODUCTION AND SUMMARY

There are many good reasons why we study string theory as a theory of particle physics. One of these, discovered some 20 or so years ago [1], is that a simple question, ''what properties do four-dimensional heterotic string vacua generically have?'' has an extremely compelling answer: non-Abelian gauge symmetry, chiral fermions, hierarchical Yukawa couplings, and dynamical supersymmetry (SUSY) breaking. One can also add other important properties such as gauge coupling unification and doublet-triplet splitting. Furthermore, after the dust of the string duality revolution settled, a similar picture was discovered in other perturbative corners of the landscape, e.g. type IIA, type IIB, and *M* theory. The above four properties are the most important properties of the standard model (SM) . The fifth one—gauge coupling unification—is an important feature of the minimal supersymmetric standard model (MSSM) and low energy supersymmetry.

There is another crucial feature of the standard model: namely, its overall mass scale, which is of order M_W as opposed to some other scale such as M_P or M_{GUT}. This property of the standard model is much less well understood in string theory or otherwise, and will be the focus of this paper.

In string/*M* theory, masses and coupling constants, including M_W, are all functions of the moduli field vacuum expectation values (vevs). Thus the hierarchy problem in string theory is double edged: one has to both stabilize all the moduli *and* generate the hierarchy simultaneously. In recent years there has been progress in moduli stabilization via fluxes and other effects (for a recent review see [2]), and with the imminent arrival of the CERN LHC it is appropriate to address the hierarchy problem in this context. After all, any given string/*M* theory vacuum either will or will not be consistent with the LHC signal, but one cannot even begin to address this in a meaningful way if the hierarchy is not understood.

In type IIB vacua, moduli are stabilized via a combination of fluxes and quantum corrections [3,4]. In these vacua, hierarchies arise in three ways: warp factors [3,5] as in [6], the presence of nonperturbative effects [4], or by fine-tuning the large number of fluxes. However, flux vacua in type IIA [7], *M* theory [8], and heterotic string theory [9] have the property that the (currently known and understood) fluxes are roughly equal in number to the number of moduli. This leads to a large value of the superpotential, and consequently, if the volume of the extra dimensions is not huge, to a large gravitino mass. This tends to give a large mass to all scalars via the effective 4d supergravity (SUGRA) potential, which leads to either $M_W = 0$ or some other large value such as M_P or M_{GUT}. Therefore, for these vacua we require a good idea for generating and stabilizing the hierarchy.

Thus far, there has been essentially one good idea proposed to explain the relatively small value of the weak scale. This is that the weak scale might be identified with, or related to, the strong coupling scale of an asymptotically free theory which becomes strongly coupled at low energies and exhibits a mass gap at that strong coupling scale. Holographically dual to this is the idea of warped extra dimensions [6]. Strong dynamics (or its dual) can certainly generate a small scale in a natural manner, but can it also be compatible with the stabilization of all the moduli fields?

One context for this question, which we will see is particularly natural, is *M* theory compactification on manifolds *X* of G_2 holonomy without fluxes. In these vacua, the only moduli one has are zero modes of the metric on *X*, whose bosonic superpartners are axions. Thus each moduli

supermultiplet has a Peccei-Quinn shift symmetry (which originates from 3-form gauge transformations in the bulk 11d supergravity). Since such symmetries can only be broken by nonperturbative effects, the entire moduli superpotential W is nonperturbative. In general, W can depend on all the moduli. Therefore, in addition to the small scale generated by the strong dynamics, we might expect that all the moduli are actually stabilized. This paper will demonstrate in detail that this is indeed the case.

Having established that the basic idea works well, the next question we address is ''what are the phenomenological implications?'' Since string/M theory has many vacua, it would be extremely useful if we could obtain a general prediction from *all* vacua or at least some well-defined subset of vacua. Remarkably, we are able to give such a prediction for all fluxless M theory vacua within the supergravity approximation[1] with at least two hidden sectors undergoing strong gauge dynamics and a particular form of the Kähler potential as in (1): *gaugino masses are generically suppressed relative to the gravitino mass*.

A slightly more detailed elucidation of this result is that in all de Sitter (dS) vacua within this class, gaugino masses are always suppressed. In anti–de Sitter (AdS) vacua—which are obviously less interesting phenomenologically—the gaugino masses are suppressed in ''most'' of the vacua. This will be explained in more detail later.

The reason why we are able to draw such a generic conclusion is the following: any given nonperturbative contribution to the superpotential depends on various constants which are determined by a specific choice of G_2 manifold X. *These constants determine entirely the moduli potential*. They are given by the constants b_k which are related to the one-loop beta-function coefficients, the normalization of each term A_k, and the constants a_i [see (2)] which characterize the Kähler potential for the moduli. Finally, there is a dependence on the gauge kinetic function, and in M theory this is determined by a set of integers N_i which specify the homology class of the three-cycle on which the non-Abelian gauge group is localized. Rather than study a particular X which fixes a particular choice for these constants, we have studied the effective potential as a function of the (A_k, b_k, a_i, N_i). The result of gaugino mass suppression holds essentially for arbitrary values of the (A_k, b_k, a_i, N_i), at least in the supergravity regime where we have been able to calculate it. Thus, any G_2 manifold which has hidden sectors with strong gauge dynamics will lead to suppressed gaugino masses.

At a deeper level, however, the reason that this works is that the idea of strong gauge dynamics to solve the hierarchy problem is a good and simple idea which guides us to the answers directly. If one's theory does not provide a simple mechanism for how the hierarchy is generated, then it is difficult to see how one could obtain a reliable prediction for, say, the spectrum of beyond the standard model particles. In a particular subset of type IIB compactifications, Conlon and Quevedo have also discovered some general results [10]. In fact, they remarkably also find that gaugino masses are suppressed at tree level, though the nature of the suppression is not quite the same. Some heterotic compactifications also exhibit a suppression of tree-level gaugino masses [11].

The suppression of gaugino masses relative to $m_{3/2}$ applies for all vacua in the supergravity regime arising out of these compactifications, independent of the value of $m_{3/2}$. However, in a generic vacuum the cosmological constant is too large. If we therefore consider only those vacua in which the cosmological constant is acceptable at leading order, this constrains the scale of $m_{3/2}$ further. Remarkably, we find evidence that, for such vacua, $m_{3/2}$ is of order 1–100 TeV. This result certainly deserves much further investigation.

The fact that such general results emerge from these studies makes the task of predicting implications for various collider observables as well as distinguishing among different vacua with data from the LHC (or any other experiment) easier. A more detailed study of the collider physics and other phenomenology will appear in the future [12]. However, as we will see in Sec. VIII, it could be quite easy to distinguish type IIB and M theory vacua using the forthcoming LHC data.

This paper is the somewhat longer companion paper to [13]. Given its length we thought that it would be worthwhile to end this introduction with a guide to its contents. Much of the bulk of the paper is devoted to analyzing and explaining the details of why the potential generated by strong dynamics in the hidden sector has vacua in which all moduli are stabilized. At first we begin with the simplest nontrivial example, two hidden sectors, without any charged matter: only gauge bosons and gauginos. Section II calculates the moduli potential in this case. Section III analyzes its supersymmetric vacua: these are all isolated with a negative vacuum energy. Section IV describes explicit examples realizing the vacuum structure of Secs. III and V. Section V describes the vacua which spontaneously break supersymmetry. These also have negative vacuum energy and all moduli stabilized. Section VI goes on to consider more complicated hidden sectors, where it is argued that metastable de Sitter vacua can also occur under very reasonable conditions, and that the metastable de Sitter vacuum obtained for a given G_2 manifold is essentially *unique*. In Sec. VII we study the distribution of $m_{3/2}$. In particular, for the de Sitter vacua it is shown that requiring the absence of a large cosmological constant fixes the gravitino mass to be of $\mathcal{O}$(1–100) TeV. Section VIII discusses phenomenology. In particular, we explain the suppression of gaugino masses and discuss the other soft SUSY breaking couplings. We conclude in Sec. IX, followed by an appendix which discusses the Kähler metric for visible charged matter fields in M theory.

[1]To which we are restricted for calculability.

II. THE MODULI POTENTIAL

In this section we quickly summarize the basic relevant features of G_2 compactifications, setup the notation, and calculate the potential for the moduli generated by strong hidden sector gauge dynamics.

In M theory compactifications on a manifold X of G_2 holonomy, the moduli are in correspondence with the harmonic 3-forms. Since there are $N \equiv b_3(X)$ such independent 3-forms, there are N moduli $z_i = t_i + is_i$. The real parts of these moduli t_i are axion fields which originate from the 3-form field C in M theory, and the imaginary parts s_i are zero modes of the metric on X and characterize the size and shape of X. Roughly speaking, one can think of the s_i's as measuring the volumes of a basis of the N independent three-dimensional cycles in X.

Non-Abelian gauge fields are localized on three-dimensional submanifolds Q of X along which there is an orbifold singularity [14], while chiral fermions are localized at pointlike conical singularities [15–17]. Thus these provide M theory realizations of theories with localized matter. A particle localized at a point p will be charged under a gauge field supported on Q if $p \in Q$. Since generically, two three-dimensional submanifolds do not intersect in a seven-dimensional space, there will be no light matter fields charged under both the standard model gauge group and any hidden sector gauge group. *Supersymmetry breaking is therefore gravity mediated in these vacua*.[2]

In general, the Kähler potentials for the moduli are difficult to determine in these vacua. However, a set of Kähler potentials, consistent with G_2 holonomy and known to describe accurately some explicit examples of G_2 moduli dynamics, were given in [18]. These models are given by

$$K = -3\ln(4\pi^{1/3}V_X) \tag{1}$$

where the volume in 11-dimensional units as a function of s_i is

$$V_X = \prod_{i=1}^{N} s_i^{a_i}, \quad \text{with} \quad \sum_{i=1}^{N} a_i = 7/3. \tag{2}$$

We will assume that this N-parameter family of Kähler potentials represents well the moduli dynamics. More general Kähler potentials outside this class have the volume functional multiplied by a function invariant under rescaling of the metric. It would be extremely interesting to investigate the extension of our results to these cases.

[2]This is an example of the sort of general result one is aiming for in string/M theory. We can contrast this result with type IIA vacua. In type IIA the non-Abelian gauge fields are again localized on three-cycles, but since generically a pair of three-cycles intersect at points in six extra dimensions, *supersymmetry breaking will generically be gauge mediated*.

As motivated in the Introduction, we are interested in studying moduli stabilization induced via strong gauge dynamics. We will begin by considering hidden sector gauge groups with no chiral matter. Later sections will describe the cases with hidden sector chiral matter.

In this "no matter" case, a superpotential (in units of m_p^3) of the following form is generated,

$$W = \sum_{k=1}^{M} A_k e^{ib_k f_k} \tag{3}$$

where M is the number of hidden sectors undergoing gaugino condensation, $b_k = \frac{2\pi}{c_k}$ with c_k being the dual Coxeter numbers of the hidden sector gauge groups, and A_k are numerical constants. The A_k are renormalization group (RG)-scheme dependent and also depend upon the threshold corrections to the gauge couplings; the work of [19] shows that their ratios (which should be scheme independent) can in fact take a reasonably wide range of values in the space of M theory vacua. We will only consider the ratios to vary from $\mathcal{O}(0.1\text{–}10)$ in what follows.

The gauge coupling functions f_k for these singularities are integer linear combinations of the z_i, because a three-cycle Q along which a given non-Abelian gauge field is localized is a supersymmetric cycle, whose volume is linear in the moduli.

$$f_k = \sum_{i=1}^{N} N_i^k z_i. \tag{4}$$

Notice that, given a particular G_2 manifold X for the extra dimensions, the constants (a_i, b_k, A_k, N_i^k) are determined. Then, the Kähler potential and superpotential for that particular X are *completely determined* by the constants (a_i, b_k, A_k, N_i^k). This is as it should be, since M theory has no free dimensionless parameters.

We are ultimately aiming for an answer to the question, "do M theory vacua, in general, make a prediction for the beyond the standard model spectrum?" For this reason, since a fluxless M theory vacuum is completely specified by the constants (a_i, b_k, A_k, N_i^k), we will try as much as possible *not* to pick a particular value for the constants and try to first evaluate whether or not there is a prediction for *general values of the constants*. Our results will show that at least within the supergravity approximation there is indeed a general prediction: the suppression of gaugino masses relative to the gravitino mass.

At this point the simplest possibility would be to consider a single hidden sector gauge group. While this does in fact stabilize all the moduli, it (a) is nongeneric and (b) fixes the moduli in a place which is strictly beyond the supergravity approximation. Therefore we will begin, for simplicity, by considering two such hidden sectors, which is more representative of a typical G_2 compactification as well as being tractable enough to analyze. The superpotential therefore has the following form:

$$W^{np} = A_1 e^{ib_1 f_1} + A_2 e^{ib_2 f_2}. \tag{5}$$

The metric corresponding to the Kähler potential (1) is given by

$$K_{i\bar{j}} = \frac{3a_i}{4s_i^2}\delta_{i\bar{j}}. \tag{6}$$

The $\mathcal{N} = 1$ supergravity scalar potential given by

$$V = e^K (K^{i\bar{j}} F_i \bar{F}_{\bar{j}} - 3|W|^2), \tag{7}$$

where

$$F_i = \partial_i W + (\partial_i K) W, \tag{8}$$

can now be computed. The full expression for the scalar potential is given by

$$\begin{aligned} V = \frac{1}{48\pi V_X^3}\Bigg[& \sum_{k=1}^{2}\sum_{i=1}^{N} a_i \nu_i^k (\nu_i^k b_k + 3) b_k A_k^2 e^{-2b_k \vec{\nu}^k \cdot \vec{a}} \\ & + 3\sum_{k=1}^{2} A_k^2 e^{-2b_k \vec{\nu}^k \cdot \vec{a}} + 2\cos[(b_1 \vec{N}^1 - b_2 \vec{N}^2)\cdot \vec{t}] \\ & \times \sum_{i=1}^{N} a_i \prod_{k=1}^{2} \nu_i^k b_k A_k e^{-b_k \vec{\nu}^k \cdot \vec{a}} + 3\cos[(b_1 \vec{N}^1 - b_2 \vec{N}^2)\cdot \vec{t}] \\ & \times \Bigg(2 + \sum_{k=1}^{2} b_k \vec{\nu}^k \cdot \vec{a}\Bigg) \prod_{j=1}^{2} A_j e^{-b_j \vec{\nu}^j \cdot \vec{a}} \Bigg] \end{aligned} \tag{9}$$

where we introduced a variable

$$\nu_i^k \equiv \frac{N_i^k s_i}{a_i} \quad \text{(no sum)} \tag{10}$$

such that

$$\mathrm{Im}\, f_k = \vec{\nu}^k \cdot \vec{a}. \tag{11}$$

By extremizing (9) with respect to the axions t_i we obtain an equation

$$\sin[(b_1 \vec{N}^1 - b_2 \vec{N}^2)\cdot \vec{t}] = 0, \tag{12}$$

which fixes only one linear combination of the axions. In this case

$$\cos[(b_1 \vec{N}^1 - b_2 \vec{N}^2)\cdot \vec{t}] = \pm 1. \tag{13}$$

It turns out that, in order for the potential (9) to have minima, the axions must take on the values such that $\cos[(b_1 \vec{N}^1 - b_2 \vec{N}^2)\cdot \vec{t}] = -1$ for $A_1,\ A_2 > 0$. Otherwise the potential has a runaway behavior. After choosing the minus sign, the potential takes the form

$$\begin{aligned} V = \frac{1}{48\pi V_X^3}\Bigg[& \sum_{k=1}^{2}\sum_{i=1}^{N} a_i \nu_i^k (\nu_i^k b_k + 3) b_k A_k^2 e^{-2b_k \vec{\nu}^k \cdot \vec{a}} \\ & + 3\sum_{k=1}^{2} A_k^2 e^{-2b_k \vec{\nu}^k \cdot \vec{a}} - 2\sum_{i=1}^{N} a_i \prod_{k=1}^{2} \nu_i^k b_k A_k e^{-b_k \vec{\nu}^k \cdot \vec{a}} \\ & - 3\Bigg(2 + \sum_{k=1}^{2} b_k \vec{\nu}^k \cdot \vec{a}\Bigg) \prod_{j=1}^{2} A_j e^{-b_j \vec{\nu}^j \cdot \vec{a}} \Bigg]. \end{aligned} \tag{14}$$

In the next section we will go on to analyze the vacua of this potential with unbroken supersymmetry. The vacua in which supersymmetry is spontaneously broken are described in Secs. V and VI.

III. SUPERSYMMETRIC VACUA

In this section we will discuss the existence and properties of the supersymmetric vacua in our theory. This is comparatively easy to do since such vacua can be obtained by imposing the supersymmetry conditions instead of extremizing the full scalar potential (14). Therefore, we will study this case with the most detail. Experience has also taught us that potentials possessing rigid isolated supersymmetric vacua also typically have other nonsupersymmetric vacua with many qualitatively similar features.

The conditions for a supersymmetric vacuum are

$$F_i = 0,$$

which implies

$$\begin{aligned} & \left(b_1 N_i^1 + \frac{3a_i}{2s_i}\right) A_1 + \left(b_2 N_i^2 + \frac{3a_i}{2s_i}\right) A_2 [\cos[(b_1 \vec{N}^1 - b_2 \vec{N}^2)\cdot \vec{t}] \\ & \times e^{(b_1 \vec{N}^1 - b_2 \vec{N}^2)\cdot \vec{s}} + i \sin[(b_1 \vec{N}^1 - b_2 \vec{N}^2)\cdot \vec{t}] e^{(b_1 \vec{N}^1 - b_2 \vec{N}^2)\cdot \vec{s}}] = 0. \end{aligned} \tag{15}$$

Equating the imaginary part of (15) to zero, one finds that

$$\begin{aligned} & \sin[(b_1 \vec{N}^1 - b_2 \vec{N}^2)\cdot \vec{t}] = 0, \\ & \text{which implies } \cos[(b_1 \vec{N}^1 - b_2 \vec{N}^2)\cdot \vec{t}] = \pm 1. \end{aligned} \tag{16}$$

For $A_1,\ A_2 > 0$, a solution with positive values for the moduli (s_i) exists when the axions take on the values such that $\cos[(b_1 \vec{N}^1 - b_2 \vec{N}^2)\cdot \vec{t}] = -1$. Now, equating the real part of (15) to zero, one obtains

$$\left(b_1 N_i^1 + \frac{3a_i}{2s_i}\right) A_1 + \left(b_2 N_i^2 + \frac{3a_i}{2s_i}\right) A_2 e^{(b_1 \vec{N}^1 - b_2 \vec{N}^2)\cdot \vec{s}} = 0. \tag{17}$$

This is a system of N transcendental equations with N unknowns. As such, it can only be solved numerically, in which case, it is harder to get a good understanding of the nature of solutions obtained. Rather than doing a brute force numerical analysis of the system (17), it is very convenient to introduce a new auxiliary variable α to recast (17) into a system of *linear* equations with N unknowns

coupled to a single transcendental constraint as follows:

$$\alpha\left(b_1 N_i^1 + \frac{3a_i}{2s_i}\right) - \left(b_2 N_i^2 + \frac{3a_i}{2s_i}\right) = 0, \tag{18}$$

$$\frac{A_2}{A_1} = \frac{1}{\alpha} e^{-(b_1\vec{N}^1 - b_2\vec{N}^2)\cdot\vec{s}}. \tag{19}$$

The system of linear equations (18) can then be formally solved for s_i in terms of $\{b_1, b_2, N_i^1, N_i^2, a_i\}$ and α:

$$s_i = -\frac{3a_i(\alpha - 1)}{2(b_1 N_i^1 \alpha - b_2 N_i^2)}; \qquad i = 1, 2, \ldots, N. \tag{20}$$

One can then substitute the solutions for s_i into the constraint (19) and self-consistently solve for the parameter α in terms of the input quantities $\{A_1, A_2, b_1, b_2, N_i^1, N_i^2, a_i\}$. This, of course, has to be done numerically, but we have indeed verified that solutions exist. Thus, we have shown explicitly that the moduli can be stabilized. We now go on to discuss the solutions, in particular, those which lie within the supergravity approximation.

A. Solutions and the supergravity approximation

Not all choices of the constants $\{A_1, A_2, b_1, b_2, N_i^1, N_i^2, a_i\}$ lead to solutions consistent with the approximation that, in the bulk of spacetime, 11-dimensional supergravity is valid. Although this is not a precisely (in the numerical sense) defined approximation, a reasonable requirement would seem to be that the values of the stabilized moduli (s_i) obtained from (20) are greater than 1. It is an interesting question, certainly worthy of further study, whether or not this is the correct criterion. In any case, this is the criterion that we will use and discuss further.

From (19) and (20), and requiring the s_i to be greater than 1, we get the following two branches of conditions on parameter α:

$$\begin{aligned}
&a)\ \frac{A_2}{A_1} > 1; \quad \min\left\{\frac{b_2 N_i^2}{b_1 N_i^1}; i = \overline{1, N}\right\} \\
&\qquad > \alpha > \max\left\{\frac{b_2 N_i^2 + 3a_i/2}{b_1 N_i^1 + 3a_i/2}; i = \overline{1, N}\right\}, \\
&b)\ \frac{A_2}{A_1} < 1; \quad \max\left\{\frac{b_2 N_i^2}{b_1 N_i^1}; i = \overline{1, N}\right\} \\
&\qquad < \alpha < \max\left\{\frac{b_2 N_i^2 + 3a_i/2}{b_1 N_i^1 + 3a_i/2}; i = \overline{1, N}\right\}.
\end{aligned} \tag{21}$$

Notice that the solution for s_i (20) has a singularity at $\alpha = \frac{b_2 N_i^2}{b_1 N_i^1}$. This can be seen clearly from Fig. 1. We see that the modulus $s_1(>0)$ falls very rapidly as one moves away from the vertical asymptote representing the singularity and can become smaller than 1 very quickly, where the supergravity approximation fails to be valid.

The relative location of the singularities for different moduli will turn out to be very important as we will see shortly. From (21), we know that there are two branches for allowed values of α. Here we consider branch a) for concreteness; branch b) can be analyzed similarly.

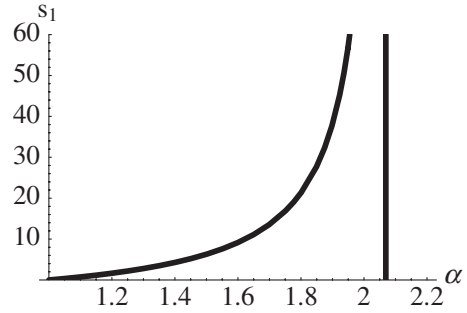

FIG. 1. Positive values of s_1 plotted as a function of α for a case with two condensates and three bulk moduli for the following choice of constants: $b_1 = \frac{2\pi}{30}$, $b_2 = \frac{2\pi}{29}$, $N_i^1 = \{1, 2, 2\}$, $N_i^2 = \{2, 3, 5\}$, $a_i = \{1, 1/7, 25/21\}$. The qualitative feature of this plot remains the same for different choices of constants as well as for different i. The vertical line is the locus for $\alpha = \frac{b_2 N_i^2}{b_1 N_i^1}$, where the denominator of (20) vanishes.

Figure 2 shows plots for A_2/A_1 and s_i as functions of α for a case with two condensates and three bulk moduli. The plots are for a given choice of the constants $\{b_1, b_2, N_i^1, N_i^2, a_i, i = 1, 2, 3\}$. The qualitative feature of the plots remains the same even if one has a different value for the constants.

Since the s_i fall very rapidly as one goes to the left of the vertical asymptotes, there is a small region of α between the origin and the leftmost vertical asymptote which yields allowed values for all $s_i > 1$. Thus, for a solution in the supergravity regime all (three) vertical lines representing the loci of singularities of the (three) moduli s_i should be (sufficiently) close to each other. This means that the positions of the vertical line for the ith modulus ($\alpha = \frac{b_2 N_i^2}{b_1 N_i^1}$) and the jth modulus ($\alpha = \frac{b_2 N_j^2}{b_1 N_j^1}$) cannot be too far apart. This in turn implies that the ratio of integer coefficients (N_i^1/N_i^2) and (N_j^1/N_j^2) for the ith and jth modulus cannot be too different from each other in order to remain within the approximation. Effectively, this means that the integer combinations in the gauge kinetic functions (4) of the two hidden sector gauge groups in (5) cannot be too linearly independent. We will give explicit examples of G_2 manifolds in which (N_i^1/N_i^2) and (N_j^1/N_j^2) are the same for all i and j, so the constraint of being within the supergravity approximation is satisfied.

We now turn to the effect of the other constants on the nature of solutions obtained. From the top right plot in Fig. 3, we see that increasing the ranks of the gauge groups while keeping them close to each other (with all other constants fixed) increases the size of the moduli in general. On the other hand, from the bottom left plot we see that introducing a large difference in the ranks leads to a decrease in the size of the moduli in general. Hence,

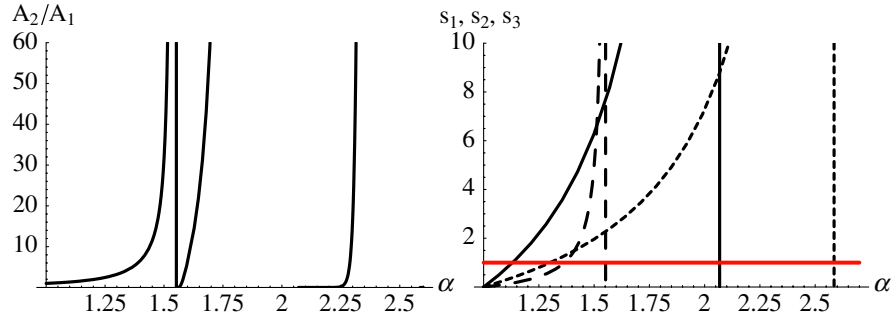

FIG. 2 (color online). Left panel—A_2/A_1 plotted as a function of α for a case with two condensates and three bulk moduli. The function diverges as it approaches the loci of singularities of (20), viz. $\alpha = \frac{b_2 N_i^2}{b_1 N_i^1}$. Right panel—Positive s_i, $i = 1, 2, 3$ for the same case plotted as functions of α. s_1 is represented by the solid curve, s_2 by the long-dashed curve, and s_3 by the short-dashed curve. The vertical lines again represent the loci of singularities of (20), which the respective moduli s_i asymptote to. The horizontal solid (red) line shows the value unity for the moduli, below which the supergravity approximation is not valid. Both plots are for $b_1 = \frac{2\pi}{30}$, $b_2 = \frac{2\pi}{29}$, $N_i^1 = \{1, 2, 2\}$, $N_i^2 = \{2, 3, 5\}$, $a_i = \{1, 1/7, 25/21\}$.

typically it is easier to find solutions with comparatively large rank gauge groups which are close to each other. The bottom right plot shows the sizes of the moduli as functions of A_2/A_1 while keeping the ranks of the gauge groups the same as in the top left plot but changing the integer coefficients. We typically find that if the integer coefficients are such that the two gauge kinetic functions are almost dependent, then it is easier to find solutions with values of moduli in the supergravity regime.

The above analysis performed for three moduli can be easily extended to include many more moduli. Typically, as the number of moduli grows, the values of a_i in (20) decrease because of (2). Therefore the ranks of the gauge groups should be increased in order to remain in the supergravity regime as one can see from the structure of (20). At the same time, for reasons described above, the integer combinations for the two gauge kinetic functions should not be too linearly independent. In addition, the integers N_i^k should not be too large, as they also decrease the moduli sizes in (20).

What happens if some of the integers N_i^1 or N_i^2 are zero. Figure 4 corresponds to this type of a situation when the integer combinations are given by $N_i^1 = \{1, 0, 1\}$, $N_i^1 = \{1, 1, 1\}$.

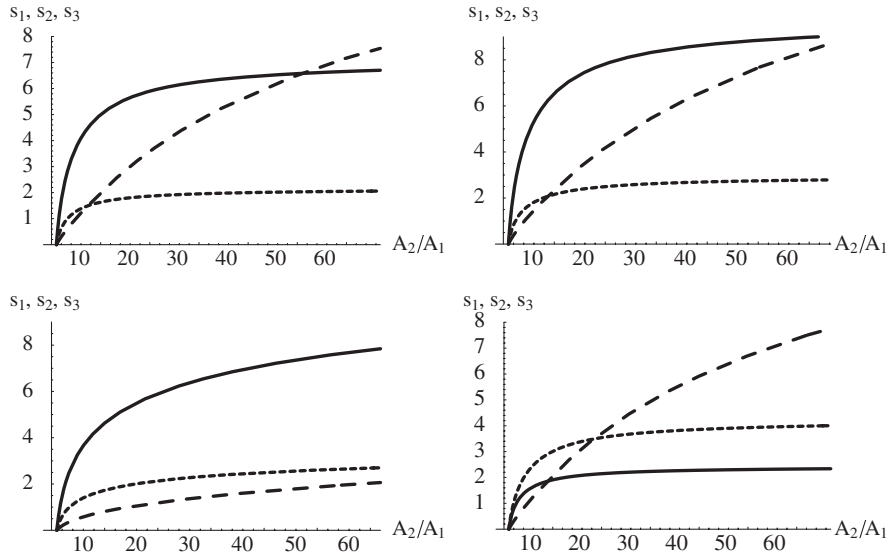

FIG. 3. Plots of positive s_i, $i = 1, 2, 3$ as functions of A_2/A_1. Top left panel: Same choice of constants as in Fig. 2, i.e. $b_1 = \frac{2\pi}{30}$, $b_2 = \frac{2\pi}{29}$, $N_i^1 = \{1, 2, 2\}$, $N_i^2 = \{2, 3, 5\}$, $a_i = \{1, 1/7, 25/21\}$. Top right panel: We increase the ranks of the gauge groups but keep them close (keeping everything else the same)—$b_1 = \frac{2\pi}{40}$, $b_2 = \frac{2\pi}{38}$. Bottom left panel: We introduce a large difference in the ranks of the gauge groups (with everything else the same)—$b_1 = \frac{2\pi}{40}$, $b_2 = \frac{2\pi}{30}$. Bottom right panel: We keep the ranks of the gauge groups as in the top left panel but change the integer coefficients to $N_i^1 = \{1, 2, 2\}$, $N_i^1 = \{3, 3, 4\}$.

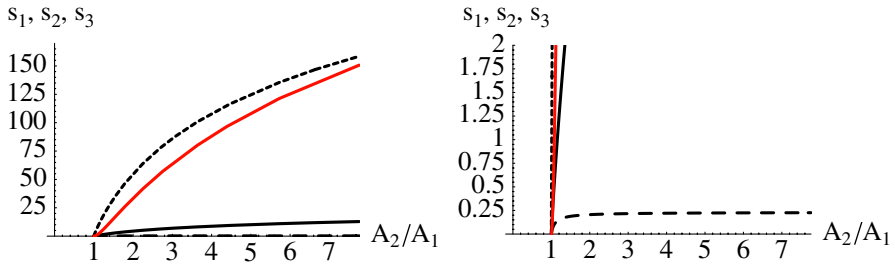

FIG. 4 (color online). Plots of positive s_i, $i = 1, 2, 3$ as functions of A_2/A_1. The constants are $b_1 = \frac{2\pi}{30}$, $b_2 = \frac{2\pi}{29}$, $N_i^1 = \{1, 0, 1\}$, $N_i^2 = \{1, 1, 1\}$, $a_i = \{1/10, 1, 37/30\}$. s_1 is represented by the solid curve, s_2 by the long-dashed curve, and s_3 by the short-dashed curve. The red curve represents the volume of the internal manifold as a function of A_2/A_1. Right panel—the same plot with the vertical plot range decreased.

As we can see from the plots, all the moduli can still be stabilized, although one of the moduli, namely s_2, is stabilized at values less than 1 in 11-dimensional Planck units. This gets us back to the previous discussion as to when the supergravity approximation can be valid. We will not have too much to say about this point, except to note that (a) the volume of X can still be large [(2) is large, greater than 1 in 11-dimensional Plank units], (b) the volumes of the associative three-cycles Q_k which appear in the gauge kinetic function (4), i.e. $\mathrm{Vol}(Q_k) = \sum_{i=1}^n N_i^k s_i$, can also be large, and (c) that the top Yukawa in these models comes from a small modulus vev [15]. From Fig. 4 we see that, although the modulus s_2 is always much smaller than 1, the overall volume of the manifold V_X represented by the solid red curve is much greater than 1. Likewise, the volumes of the associative three-cycles $\mathrm{Vol}(Q_1) = s_1 + s_3$ and $\mathrm{Vol}(Q_2) = s_1 + s_2 + s_3$ are also large. Therefore if one interprets the SUGRA approximation in this way, it seems possible to have zero entries in the gauge kinetic functions for some of the moduli and still stabilize all the moduli, as demonstrated by the explicit example given above. In general, however, there is no reason why any of the integers should vanish in the basis in which the Kähler metric is given by (6).

B. Special case

A very interesting special case arises when the gauge kinetic functions f_1 and f_2 in (5) are equal. Since in this case $N_i^1 = N_i^2$, the moduli vevs are larger in the supersymmetric vacuum; hence this case is representative of the vacua to be found within the supergravity approximation. Even though this is a special case, in Sec. IV, we will describe explicit examples of G_2 manifolds in which $N_i^1 = N_i^2$.

In the special case, we have

$$N_i^1 = N_i^2 \equiv N_i, \tag{22}$$

and therefore

$$\nu_i^1 = \nu_i^2 = \nu_i \equiv \frac{N_i s_i}{a_i}. \tag{23}$$

For this special case, the system of equations (17) can be simplified even further. We have

$$(b_1\nu_i + \tfrac{3}{2})A_1 - (b_2\nu_i + \tfrac{3}{2})A_2 e^{(b_1-b_2)\vec{\nu}\cdot\vec{a}} = 0 \tag{24}$$

with ν_i actually *independent* of i. Thus, we are left with just *one* simple algebraic equation and one transcendental constraint. The solution for ν_i is given by

$$\nu_i \equiv \nu = -\frac{3(\alpha - 1)}{2(\alpha b_1 - b_2)}, \tag{25}$$

with

$$\frac{A_2}{A_1} = \frac{1}{\alpha} e^{-(7/3)(b_1-b_2)\nu}. \tag{26}$$

Since ν_i is independent of i, it is also independent of the number of moduli N. In Fig. 5 we plotted ν as a function of A_2/A_1 when the hidden sector gauge groups are $SU(5)$ and $SU(4)$. Notice that here the ranks of the gauge groups do not have to be large for the moduli to be greater than 1. This is in contrast with the linearly independent cases plotted in Fig. 3. Once ν is determined in terms of A_2/A_1, the moduli are given by

$$s_i = \frac{a_i \nu}{N_i}. \tag{27}$$

Therefore, the hierarchy between the moduli sizes is com-

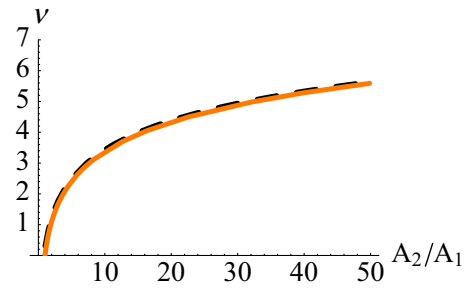

FIG. 5 (color online). Plot of ν as a function of A_2/A_1 for the choice $b_1 = \frac{2\pi}{5}$, $b_2 = \frac{2\pi}{4}$. The solid (red) curve represents the exact numerical solution, whereas the dashed (black) curve is the leading order approximation given by (29).

pletely determined by the ratios a_i/N_i for different values of i.

In addition, from Fig. 5 it can be seen that ν keeps increasing indefinitely if we keep increasing A_2/A_1 (though theoretically there may be a reasonable upper limit for A_2/A_1), which is not possible for the general case as there are N ν_i's. This implies that it is possible to have a wide range of the constants which yield a solution in the supergravity regime.

Although the numerical solutions to the system (25) and (26) described above are easy to generate, having an explicit analytic solution, even an approximate one, which could capture the dependence of ν on the constants A_2/A_1, b_1, and b_2, would be very useful.

Fortunately there exists a good approximation, namely, a large ν limit, which allows us to find an analytical solution for ν in a straightforward way. Expressing α from (25), in the leading order approximation when ν is large, we obtain

$$\alpha^{(0)} = \frac{b_2}{b_1}. \tag{28}$$

After substituting (28) into (26) we obtain the approximate solution for ν in the leading order:

$$\nu^{(0)} = \frac{3}{7}\frac{1}{b_2 - b_1}\ln\left(\frac{A_2 b_2}{A_1 b_1}\right) = \frac{3}{14\pi}\frac{PQ}{P-Q}\ln\left(\frac{A_2 P}{A_1 Q}\right), \tag{29}$$

where the last expression corresponds to $SU(P)$ and $SU(Q)$ hidden sector gauge groups. For the moduli to be positive, either of the two following conditions have to be satisfied:

$$a)\ A_1 Q < A_2 P; \quad P > Q, \qquad b)\ A_1 Q > A_2 P; \quad P < Q. \tag{30}$$

From the plots in Fig. 5 we notice that the above approximation is fairly accurate even when ν is $O(1)$. This is very helpful and can be seen once we compute the first subleading contribution. By substituting (29) back into (25) and solving for α we now have up to the first subleading order:

$$\alpha = \alpha^{(0)} + \alpha^{(1)} = \frac{P}{Q} - \frac{7}{2\ln(\frac{A_2 P}{A_1 Q})}\left(\frac{P-Q}{Q}\right)^2. \tag{31}$$

It is then straightforward to compute ν which includes the first subleading order contribution

$$\nu = \nu^{(0)} + \nu^{(1)} = \frac{3}{14\pi}\frac{PQ}{P-Q}\ln\left(\frac{A_2 P}{A_1 Q}\right) - \frac{3}{4\pi}\frac{P-Q}{\ln(\frac{A_2 P}{A_1 Q})}. \tag{32}$$

We can now examine the accuracy of the leading order approximation when ν is $O(1)$ by considering the region where the ratio A_2/A_1 is small. A quick check for the $SU(5)$ and $SU(4)$ hidden sector gauge groups chosen in the case presented in Fig. 5 yields for $A_2/A_1 = 4$

$$\alpha = \alpha^{(0)} + \alpha^{(1)} = 1.25 - 0.136, \tag{33}$$

$$\nu = \nu^{(0)} + \nu^{(1)} = 2.195 - 0.148, \tag{34}$$

which results in a 12% and 7% error for $\alpha^{(0)}$ and $\nu^{(0)}$, respectively. The errors get highly suppressed when ν becomes $O(10)$ and larger. Also, when the ranks of the gauge groups $SU(P)$ and $SU(Q)$ are $O(10)$ and $P - Q$ is small, the ratio A_2/A_1 can be $O(1)$ and still yield a large ν. The dependence of ν on the constants in (29) is very similar to the moduli dependence obtained for SUSY Minkowski vacua in the type IIB racetrack models [20].

We have demonstrated that there exist isolated supersymmetric vacua in M theory compactifications on G_2 manifolds with two strongly coupled hidden sectors which give nonperturbative contributions to the superpotential. Given the existence of supersymmetric vacua, it is very likely that the potential also contains nonsupersymmetric critical points. Previous examples have certainly illustrated this [18]. Before analyzing the nonsupersymmetric critical points, however, we will now present some examples of vacua which give rise to two strongly coupled hidden sectors.

IV. EXAMPLES OF G_2 MANIFOLDS

Having shown that the potential stabilizes all the moduli, it is of interest to construct explicit examples of G_2 manifolds realizing these vacua. To demonstrate the existence of a G_2-holonomy metric on a compact seven-manifold is a difficult problem in solving nonlinear equations [21]. There is no analogue of Yau's theorem for Calabi-Yau manifolds which allows an ''algebraic'' construction. However, Joyce and Kovalev have successfully constructed many smooth examples [21]. Furthermore, dualities with heterotic and type IIA string vacua also imply the existence of many singular examples. The vacua of interest to us here are those with two or more hidden sector gauge groups. These correspond to G_2 manifolds which have two three-dimensional submanifolds Q_1 and Q_2 along which there are orbifold singularities. In order to describe such examples we will (a) outline an extension of Kovalev's construction to include orbifold singularities and (b) use duality with the heterotic string.

Kovalev constructs G_2 manifolds which can be described as the total space of a fibration. The fibers are four-dimensional $K3$ surfaces, which vary over a three-dimensional sphere. Kovalev considers the case in which the $K3$ fibers are generically smooth, but it is reasonably straightforward to also consider cases in which the (generic) $K3$ fiber has orbifold singularities. This gives G_2 manifolds which also have orbifold singularities along the sphere and give rise to Yang-Mills fields in M theory. For example, if the generic fiber has both an $SU(4)$ and an $SU(5)$ singularity, then the G_2 manifold will have two such singularities, both parametrized by disjoint copies of the sphere. In this case N_i^1 and N_i^2 are equal because Q_1 and Q_2

are in the same homology class, which is precisely the special case that we consider both above and below.

We arrive at a very similar picture by considering the M theory dual of the heterotic string on a Calabi-Yau manifold at large complex structure. In this limit, the Calabi-Yau is T^3 fibered and the M theory dual is $K3$ fibered, again over a three-sphere (or a discrete quotient thereof). Then, if the hidden sector E_8 is broken by the background gauge field to, say, $SU(5) \times SU(2)$, the $K3$ fibers of the G_2 manifold generically have $SU(5)$ and $SU(2)$ singularities, again with $N_i^1 = N_i^2$. More generally, in $K3$ fibered examples, the homology class of Q_1 could be k times that of Q_2, and in this case $N_i^1 = kN_i^2$. As a particularly interesting example, the M theory dual of the heterotic vacua described in [22] includes a G_2 manifold whose singularities are such that they give rise to an observable sector with precisely the matter content of the MSSM, while the hidden sector has gauge group $G = E_8$.

Finally, we also note that Joyce's examples typically can have several sets of orbifold singularities which often fall into the special class [21]. We now go on to describe the vacua in which supersymmetry is spontaneously broken.

V. VACUA WITH SPONTANEOUSLY BROKEN SUPERSYMMETRY

The potential (9) also possesses vacua in which supersymmetry is spontaneously broken. Again these are isolated, so the moduli are all fixed. These all turn out to have a negative cosmological constant. We will see in Sec. VI that adding matter in the hidden sector can give a potential with de Sitter vacua.

Since the scalar potential (9) is extremely complicated, finding solutions is quite a nontrivial task. As for the supersymmetric solution, it is possible to simplify the system of N transcendental equations obtained. However, unlike the supersymmetric solution, we have only been able to do this so far for the special case as in Sec. III B. Therefore, for simplicity we analyze the special case in detail. As we described above, there are examples of vacua which fall into this special class. Moreover, as explained previously, we expect that typically vacua not in the special class are beyond the supergravity approximation.

By extremizing (14) with respect to s_k we obtain the following system of equations,

$$\begin{aligned} &2\nu_k^2(b_1\alpha - b_2)^2 - \nu_k\Big[2(b_1\alpha - b_2)(b_1^2\alpha - b_2^2)\sum_{i=1}^{N} a_i\nu_i^2 \\ &\quad + 3(\alpha - 1)(b_1^2\alpha - b_2^2)\vec{\nu}\cdot\vec{a} + 3(b_1\alpha - b_2)^2\vec{\nu}\cdot\vec{a} \\ &\quad + 3(\alpha - 1)(b_1\alpha - b_2)\Big] - 3\Big[(b_1\alpha - b_2)^2\sum_{i=1}^{N} a_i\nu_i^2 \\ &\quad + 3(\alpha - 1)(b_1\alpha - b_2)\vec{\nu}\cdot\vec{a} + 3(\alpha - 1)^2\Big] = 0, \end{aligned} \tag{35}$$

where we have again introduced an auxiliary variable α defined by

$$\frac{A_2}{A_1} \equiv \frac{1}{\alpha} e^{-(b_1 - b_2)\vec{\nu}\cdot\vec{a}}, \tag{36}$$

similar to that in Sec. III B. The definition (36) together with the system of polynomial equations (35) can be regarded as a coupled system of equations for α and ν_k. We introduce the following notation:

$$\begin{aligned} &x \equiv (\alpha - 1), \qquad y \equiv (b_1\alpha - b_2), \\ &z \equiv (b_1^2\alpha - b_2^2), \qquad w \equiv \frac{xz}{y^2}. \end{aligned} \tag{37}$$

In this notation, from (35) (divided by x^2) we obtain the following system of coupled equations:

$$\begin{aligned} &2\frac{y^2}{x^2}\nu_k^2 - \Big(2\frac{y^2}{x^2}w\sum_{i=1}^{N} a_i\nu_i^2 + 3\frac{y}{x}(w+1)\vec{\nu}\cdot\vec{a} + 3\Big)\frac{y}{x}\nu_k \\ &\quad - 3\Big(\frac{y^2}{x^2}\sum_{i=1}^{N} a_i\nu_i^2 + 3\frac{y}{x}\vec{\nu}\cdot\vec{a} + 3\Big) = 0. \end{aligned} \tag{38}$$

It is convenient to recast this system of N *cubic* equations into a system of N *quadratic* equations plus a constraint. Namely, by introducing a new variable T as

$$4T \equiv 2\frac{y^2}{x^2}w\sum_{i=1}^{N} a_i\nu_i^2 + 3\frac{y}{x}(w+1)\vec{\nu}\cdot\vec{a} + 3, \tag{39}$$

where the factor of 4 has been introduced for future convenience, the system in (38) can be expressed as

$$2\frac{y^2}{x^2}\nu_k^2 - 4T\frac{y}{x}\nu_k - 3\Big(\frac{y^2}{x^2}\sum_{i=1}^{N} a_i\nu_i^2 + 3\frac{y}{x}\vec{\nu}\cdot\vec{a} + 3\Big) = 0. \tag{40}$$

An important property of the system (40) is that *all of its equations are the same independent of the index* k. However, since the combination in the round brackets in (40) is not a constant with respect to $\vec{\nu}$, this system of quadratic equations does not decouple. Nevertheless, because both the first and the second monomials in (40) with respect to ν_k are *independent of* $\vec{\nu}$, the standard solution of a quadratic equation dictates that the solutions for ν_k of (40) have the form

$$\nu_k = \frac{x}{y}(T + m_k H), \quad \text{with} \quad m_k = \pm 1, \qquad k = \overline{1, N}, \tag{41}$$

where we introduced another variable H and pulled out the factor of x/y for future convenience.

We have now reduced the task of determining ν_k for each $k = \overline{1, N}$ to finding *only two* quantities—T and H. By substituting (41) into Eqs. (39) and (40) and using (2), we obtain a system of two coupled quadratic equations,

$$\frac{14w}{3}(T_A^2 + 2AT_AH_A + H_A^2) + 7(w+1)(T_A + AH_A) + 3 - 4T_A = 0,$$
$$9(T_A^2 + 2AT_AH_A + H_A^2) - 4H_A(H_A + AT_A) + 21(T_A + AH_A) + 9 = 0, \tag{42}$$

where parameter A, defined by

$$A \equiv \tfrac{3}{7}\vec{m}\cdot\vec{a}, \tag{43}$$

is now labeling each solution. Note that by factoring out x/y in (41), the system obtained in (42) is independent of either x or y. However, it does couple to the constraint (36) via w. In Sec. V C we will see that there exists a natural limit when the system (42) completely decouples from the constraint (36). Since T_A and H_A both depend on the parameter A, the solution in (41) is now written as

$$\nu_k^A = \frac{x}{y}(T_A + m_k H_A). \tag{44}$$

Since $k = \overline{1, N}$ and $m_k = \pm 1$, vector $\vec{m}$ represents one of 2^N possible combinations. Thus, parameter $\vec{m}\cdot\vec{a}$ can take on 2^N possible rational values within the range

$$-\tfrac{7}{3} \le \vec{m}\cdot\vec{a} \le \tfrac{7}{3}, \tag{45}$$

so that parameter A defined in (43) labeling each solution can take on 2^N rational values in the range

$$-1 \le A \le 1. \tag{46}$$

For example, when $N = 2$, there are four possible combinations for $\vec{m} = (m_1, m_2)$, namely,

$$(m_1, m_2) = \{(-1,-1), (1,-1), (-1,1), (1,1)\}. \tag{47}$$

These combinations result in the following four possible values for A:

$$A = \{-1, \tfrac{3}{7}(a_1 - a_2), \tfrac{3}{7}(-a_1 + a_2), 1\}, \tag{48}$$

where we used (2) for the first and last combinations.

In general, for an arbitrary value of A, system (42) has four solutions. However, with the exception of the case when $A = 1$, out of the four solutions only two are actually real, as we will see later in Sec. V C. The way to find those solutions is as follows.

Having found ν_k^A analytically in terms of α and the other constants, we can substitute it into the transcendental constraint (36) to determine α numerically for particular values of $\{A_1, A_2, b_1, b_2, N_k, a_k\}$. Again, in general, there will be more than one solution for α. We can then substitute those values back into the analytical solution for ν_k^A to find the corresponding extrema, having chosen only those α, obtained numerically from (36), which result in real values of ν_k^A. We thus have 2^{N+1} real extrema. However, after a closer look at the system of equations (42) we notice that, when $A \to -A$, equations remain invariant if in addition $H_{-A} \to -H_A$ and $T_{-A} \to T_A$. This simply exchanges the solutions $\nu^A_{(k,+)}$ where $m_k = 1$ with $\nu^A_{(k,-)}$ where $m_k = -1$,

$$\nu^{-A}_{(k,+)} = \nu^A_{(k,-)}, \tag{49}$$

This implies that the scalar potential (14), in general, has a total number of 2^N real independent extrema. However, as we will see later in Sec. V C, many of those vacua will be incompatible with the supergravity approximation.

For general values of A, Eqs. (42) have analytical solutions that are too complicated to be presented here. In addition to restricting to the case with the same gauge kinetic function f in both hidden sectors, we now further restrict to situations where A takes special values, so that the expressions are simple. However, it is important to understand that they still capture the main features of the general solution. In the following, we provide explicit solutions (in the restricted situation as mentioned above) for M theory compactifications on G_2 manifolds with one and two moduli, respectively. In Sec. V C we will generalize our results to the case with many moduli and give a complete classification of all possible solutions. We will then consider the limit when the volume of the associative cycle $\mathrm{Vol}(Q) = \vec{\nu}\cdot\vec{a}$ is large and obtain explicit analytic solutions for the moduli.

A. One modulus case

The first and the simplest case is to consider a manifold with only one modulus, i.e. $N = 1$, $a = \frac{7}{3}$. In this case, $A = \pm 1$. From the previous discussion we only need to consider the case $A = 1$. It turns out that this is a special case for which the system (42) degenerates to yield three solutions instead of four. All three are real; however, only two of them result in positive values of the modulus:

$$T_1^{(1)} = -\frac{15}{8}, \qquad H_1^{(1)} = \frac{3}{8} \tag{50}$$

and

$$T_1^{(2)} = \frac{3}{28(243 - 441w + 196w^2)}\Bigg(-13\,419 + \frac{3645}{w} + 15\,288w - 5488w^2 - 329\sqrt{729 - 1701w + 1323w^2 - 343w^3} + \frac{135}{w}\sqrt{729 - 1701w + 1323w^2 - 343w^3} + 196w\sqrt{729 - 1701w + 1323w^2 - 343w^3}\Bigg),$$
$$H_1^{(2)} = \frac{3}{28w}(-27 + 28w - \sqrt{729 - 1701w + 1323w^2 - 343w^3}), \tag{51}$$

which give the following two values for the modulus:

$$s^{(1)} = \frac{a}{N_1}\frac{x}{y}(T_1^{(1)} + H_1^{(1)}) = -\frac{7x}{2Ny},$$
$$s^{(2)} = \frac{a}{N_1}\frac{x}{y}(T_1^{(2)} + H_1^{(2)}) = -\frac{x}{Ny}\left(\frac{3+\sqrt{9-7w}}{w}\right). \tag{52}$$

In addition, each solution in (52) is a function of the auxiliary variable α defined in (36). By substituting (52) into (36) we obtain two equations for $\alpha^{(1)}$ and $\alpha^{(2)}$,

$$\frac{A_2}{A_1} = \frac{1}{\alpha^{(1)}} e^{-(b_1-b_2)s^{(1)}N_1}, \qquad \frac{A_2}{A_1} = \frac{1}{\alpha^{(2)}} e^{-(b_1-b_2)s^{(2)}N_1}. \tag{53}$$

The transcendental equations (53) can only be solved numerically. Here we will choose the following values for this simple toy model:

$$A_1 = 0.12, \qquad A_2 = 2, \qquad b_1 = \frac{2\pi}{8}, \qquad b_2 = \frac{2\pi}{7}, \qquad N_1 = 1. \tag{54}$$

By solving (53) numerically and keeping only those solutions that result in real positive values for the modulus s in (52), we get

$$s^{(1)} = 26.101, \qquad s^{(2)} = 27.185, \tag{55}$$

with

$$\alpha^{(1)} = 1.122, \qquad \alpha^{(2)} = 1.267. \tag{56}$$

In Fig. 6 we see that the two solutions in (55) correspond to an AdS minimum and a de Sitter maximum. In fact, the AdS minimum at $s^{(1)}$ is supersymmetric. The general solution for $s^{(1)}$ given in (52) can also be obtained by methods of Sec. III, imposing the SUSY condition on the corresponding F-term by setting it to zero, while introducing the same auxiliary constraint as in (36).

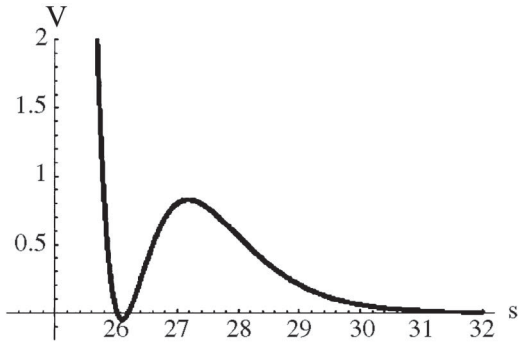

FIG. 6. Potential multiplied by 10^{32} plotted as a function of one modulus s. For our particular choice of constants in (54), the modulus is stabilized at the supersymmetric AdS minimum $s^{(1)} = 26.101$. The maximum is de Sitter, given by $s^{(2)} = 27.185$.

B. Two moduli case

While the previous example with one modulus is interesting, it does not capture some very important properties of the vacua which arise when two or more moduli are considered. In particular, in this subsection we will see that the supersymmetric AdS minimum, obtained in the one-dimensional case, actually turns into a saddle point, whereas the stable minima are AdS with spontaneously broken supersymmetry. Let us now consider a particularly simple example with two moduli. Here we will choose both moduli to appear on an equal footing in the Kähler potential (1) by choosing

$$a_1 = \tfrac{7}{6}, \qquad a_2 = \tfrac{7}{6}. \tag{57}$$

We now have four possible combinations for $\vec{m} = (m_1, m_2)$:

$$(1,1), \quad (1,-1), \quad (-1,1), \quad (-1,-1), \tag{58}$$

corresponding to the following possible values of A:

$$1, \quad 0, \quad 0, \quad -1, \tag{59}$$

where only two of the four actually produce independent solutions. The case when $A = 1$ has been solved in the previous subsection with $T_1^{(1)}$, $H_1^{(1)}$ and $T_1^{(2)}$, $H_1^{(2)}$ given by (50) and (51) with the moduli taking on the following values for the supersymmetric AdS extremum,

$$s_1^{(1)} = \frac{a_1 x}{N_1 y}\left(-\frac{3}{2}\right) = -\frac{7x}{4N_1 y},$$
$$s_2^{(1)} = \frac{a_2 x}{N_2 y}\left(-\frac{3}{2}\right) = -\frac{7x}{4N_2 y}, \tag{60}$$

and the de Sitter extremum,

$$s_1^{(2)} = \frac{a_1 x}{N_1 y}\left(-\frac{3}{7w}(3+\sqrt{9-7w})\right) = -\frac{x}{2N_1 y}\left(\frac{3+\sqrt{9-7w}}{w}\right),$$
$$s_2^{(2)} = \frac{a_2 x}{N_2 y}\left(-\frac{3}{7w}(3+\sqrt{9-7w})\right) = -\frac{x}{2N_2 y}\left(\frac{3+\sqrt{9-7w}}{w}\right). \tag{61}$$

As mentioned earlier, the supersymmetric solution can also be obtained by the methods of Sec. III. Now, we also have a new case when $A = 0$. The corresponding two real solutions for T_0 and H_0 are

$$T_0^{(1)} = \frac{3}{112w}(15 - 63w - D),$$
$$H_0^{(1)} = \frac{1}{4\sqrt{5}}\sqrt{-\frac{585}{8} - \frac{18225}{392w^2} + \frac{3915}{28w} + \frac{1215}{392w^2}D - \frac{225}{56w}D} \tag{62}$$

and

$$T_0^{(2)} = \frac{3}{112w}(15 - 63w - D),$$
$$H_0^{(2)} = -\frac{1}{4\sqrt{5}} \times \sqrt{-\frac{585}{8} - \frac{18\,225}{392w^2} + \frac{3915}{28w} + \frac{1215}{392w^2}D - \frac{225}{56w}D}, \tag{63}$$

where we defined

$$D \equiv \sqrt{225 - 770w + 833w^2}. \tag{64}$$

The moduli are then extremized at the values given by

$$s_1^{(3)} = \frac{a_1 x}{N_1 y}(T_0^{(1)} + H_0^{(1)}), \qquad s_2^{(3)} = \frac{a_2 x}{N_2 y}(T_0^{(1)} - H_0^{(1)}) \tag{65}$$

and

$$s_1^{(4)} = \frac{a_1 x}{N_1 y}(T_0^{(2)} + H_0^{(2)}), \qquad s_2^{(4)} = \frac{a_2 x}{N_2 y}(T_0^{(2)} - H_0^{(2)}). \tag{66}$$

To completely determine the extrema we again need to substitute the solutions given above into the constraint equation (36) and choose a particular set of values for A_1, A_2, b_1, and b_2 to find numerical solutions that result in real positive values for the moduli s_1 and s_2. Here we again use the same values as we chose in the previous case given by

$$A_1 = 0.12, \qquad A_2 = 2, \qquad b_1 = \frac{2\pi}{8}, \qquad b_2 = \frac{2\pi}{7}, \qquad N_1 = 1, \qquad N_2 = 1. \tag{67}$$

For the SUSY extremum we have

$$s_1^{(1)} = 13.05, \qquad s_2^{(1)} = 13.05. \tag{68}$$

The de Sitter extremum is given by

$$s_2^{(2)} = 13.59, \qquad s_2^{(2)} = 13.59. \tag{69}$$

The other two extrema are at the values

$$s_1^{(3)} = 2.61, \qquad s_2^{(3)} = 23.55 \quad \text{and} \quad s_1^{(4)} = 23.55, \qquad s_2^{(4)} = 2.61. \tag{70}$$

It is interesting to note that the supersymmetric extremum in (68) is no longer a stable minimum but, instead, a saddle point. The two symmetrically located stable minima seen in Fig. 7 are nonsupersymmetric. Thus we have an explicit illustration of a potential where spontaneous breaking of supersymmetry can be realized. The stable minima appear symmetrically since both moduli were chosen to be on an equal footing in the scalar potential.

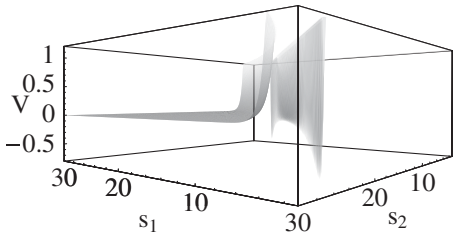

FIG. 7. Potential multiplied by 10^{32} plotted as a function of two moduli, s_1 and s_2, for the values in (67). The SUSY AdS extremum given by (68) is a saddle point, located between the nonsupersymmetric AdS minima given by (70).

With a slight deviation where $a_1 \neq a_2$ and/or $N_1 \neq N_2$, one of the minima will be deeper than the other. It is important to note that, at both minima, the volume given by (2) is stabilized at the value $V_X = 122.28$ which is large enough for the supergravity analysis presented here to be valid.

C. Generalization to many moduli

In the previous section we demonstrated the existence of stable vacua with broken SUSY for the special case with two moduli. Here we will extend the analysis to include cases with an arbitrary number of moduli for any value of the parameter A. It was demonstrated in Sec. III B that the SUSY extremum has an approximate analytical solution given by (29). Therefore, it would be highly desirable to obtain approximate analytical solutions for the other extrema in a similar way. We will start with the observation that, for the SUSY extremum (60) obtained for the special case when $A = 1$, both $T_1^{(1)}$ and $H_1^{(1)}$ given by (50) are independent of w. On the other hand, if in the leading order parameter α is given by (28), from the definitions in (37) it follows that in this case

$$y \to 0 \quad \text{and} \quad w \to -\infty. \tag{71}$$

Thus, if we consider the system (42) in the limit when $w \to -\infty$, we should still be able to obtain the SUSY extremum exactly. In addition, one might also expect that the solutions for the vacua with broken SUSY may also be located near the loci where $y \to 0$. With this in mind we will take the limit (71) which results in the following somewhat simplified system of equations for T_A and H_A:

$$2(T_A^2 + 2AT_AH_A + H_A^2) + 3(T_A + AH_A) = 0,$$
$$9(T_A^2 + 2AT_AH_A + H_A^2) - 4H_A(H_A + AT_A) + 21(T_A + AH_A) + 9 = 0. \tag{72}$$

Because system (72) is completely decoupled from the constraint (36) and hence the microscopic constants, we can perform a completely general analysis of the vacua valid for arbitrary values of the microscopic constants, at least when the limit (71) is a good approximation. It is straightforward to see that (50) is an exact solution to the

above system when $A = 1$. Moreover, unlike the general case when w is finite, where the system had three real solutions, two of which resulted in positive moduli, system (72) above completely degenerates when $A = 1$, yielding only one solution corresponding to the SUSY extremum. On the other hand, for an arbitrary $0 \leq A < 1$ the system has four solutions. One can check that at every point A in the range $0 \leq A < 1$ exactly two out of these four solutions are real. The corresponding plots are presented in Fig. 8. Before we discuss the plots we would like to introduce some new notation:

$$L^{(c)}_{A,k} = T^{(c)}_A + m_k H^{(c)}_A, \tag{73}$$

where $c = \overline{1,2}$ corresponding to the two real solutions. In this notation (44) can be reexpressed as

$$\nu^{(c)}_{A,k} = \frac{x}{y} L^{(c)}_{A,k}. \tag{74}$$

The volume of the associative three-cycle Q for these vacua is then

$$\mathcal{T}^{(c)}_A \equiv \mathrm{Vol}(Q)^{(c)}_A = \mathrm{Im}(f^{(c)}_A) = \sum_{i=1}^{N} N_i s^{(c)}_{A,i} = \sum_{i=1}^{N} a_i \nu^{(c)}_{A,i} = \frac{x}{y} \vec{a} \cdot \vec{L}^{(c)}_A. \tag{75}$$

For future convenience we will also introduce

$$B^{(c)}_A \equiv \vec{a} \cdot \vec{L}^{(c)}_A = \tfrac{7}{3}(T^{(c)}_A + A H^{(c)}_A). \tag{76}$$

Constraint (36) is then given by

$$\alpha^{(c)}_A = \frac{A_1}{A_2} e^{-(b_1 - b_2)\mathcal{T}^{(c)}_A}, \tag{77}$$

which is coupled to

$$\frac{x}{y} = \frac{\alpha^{(c)}_A - 1}{b_1 \alpha^{(c)}_A - b_2} = \frac{\mathcal{T}^{(c)}_A}{B^{(c)}_A}, \tag{78}$$

where definitions (37) were used to substitute for x and y. Both $L^{(c)}_{A,k}$ and $B^{(c)}_A$ are completely determined by the system (72), whereas $\mathcal{T}^{(c)}_A$ is determined from (77) and (78). Then solution (74) can be conveniently expressed as

$$\nu^{(c)}_{A,k} = \frac{\mathcal{T}^{(c)}_A}{B^{(c)}_A} L^{(c)}_{A,k}. \tag{79}$$

Recall that $m_k = \pm 1$. Thus the only two possibilities for $L^{(c)}_{A,k}$ for any $k = \overline{1,N}$ are

$$L^{(c)}_{A,\pm} = T^{(c)}_A \pm H^{(c)}_A. \tag{80}$$

As we vary parameter A over the range $0 \leq A < 1$ point by point, system (72) always has exactly two real solutions. In Fig. 8 we present plots of $L^{(c)}_{A,+}$, $L^{(c)}_{A,-}$, and $B^{(c)}_A$, where $c = \overline{1,2}$ as functions of A.

We only need to consider the positive range $0 \leq A < 1$ because of the symmetry (49).

What happens to these solutions when $A = 1$? We already know from the previous discussion that the system (72) obtained in the limit $w \to -\infty$ degenerates for $A = 1$, and one obtains the solution that corresponds to the SUSY extremum explicitly. The solutions plotted in Fig. 8 were obtained assuming $A \neq 1$ and therefore have an apparent singularity when $A = 1$. Thus they cannot capture either the SUSY or the de Sitter extrema that arise in this special case. To explain what happens to the de Sitter extremum we need to examine the exact solution in (51), in the same limit. Indeed, bearing in mind that w is negative, from (51) we have

$$L^{(2)}_{A,+} = T^{(2)}_1 + H^{(2)}_1 = -\frac{3}{7}\left(\frac{3 + \sqrt{9 - 7w}}{w}\right). \tag{81}$$

Here we see immediately that in the limit $w \to -\infty$ for the solution above $L^{(2)}_{A,+} \to 0$. Therefore we conclude that the de Sitter extremum cannot be obtained from (72) which correlates with the previous observation that for $A = 1$ (72) has only one solution—the SUSY extremum. Nevertheless, as we will see in the next subsection the real solutions plotted in Fig. 8 are a very good approxima-

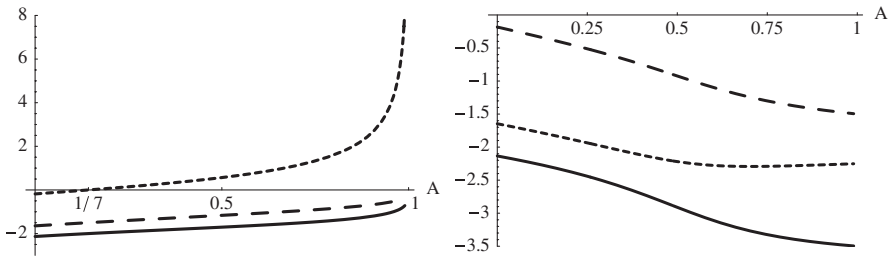

FIG. 8. Plots of $L^{(c)}_{A,+}$, $L^{(c)}_{A,-}$, and $B^{(c)}_A$, where $c = \overline{1,2}$, corresponding to the two real solutions of the system (72) as functions of parameter A in the range $0 \leq A < 1$. Both the left and right graphs have $L^{(c)}_{A,+}$ (long-dashed line), $L^{(c)}_{A,-}$ (short-dashed line), and $B^{(c)}_A$ (solid line). Left panel: Plots of $L^{(1)}_{A,+}$, $L^{(1)}_{A,-}$, and $B^{(1)}_A$ corresponding to the first real solution at each A. There is a critical value $A = 1/7$ where $L^{(1)}_{A,-} = 0$ and becomes positive for $A > 1/7$. Right panel: Plots of $L^{(2)}_{A,+}$, $L^{(2)}_{A,-}$, and $B^{(2)}_A$ corresponding to the second real solution at each A.

tion to the exact numerical solutions corresponding to the AdS vacua with spontaneously broken supersymmetry.

Now we would like to classify which of these AdS vacua have all the moduli stabilized at positive values. Indeed if some of the moduli are fixed at negative values we can automatically exclude such vacua from further consideration since the supergravity approximation assumes that all the moduli are positive. Since the volume $\mathcal{T}_A^{(c)}$ is always positive by definition, from (79) we see immediately that, for all moduli to be stabilized in the positive range, all three quantities $L_{A,+}^{(c)}$, $L_{A,-}^{(c)}$, and $B_A^{(c)}$ must have the same sign. In Fig. 8 the plots on the right satisfy this requirement for the entire range $0 \le A < 1$. On the other hand, the short-dashed curve corresponding to $L_{A,-}^{(1)}$ on the left plot is negative when $0 \le A < 1/7$, features a zero at $A = 1/7$, and becomes positive for $1/7 < A < 1$. Yet, both $L_{A,+}^{(1)}$ and $B_A^{(1)}$ remain negative throughout the entire range. Moreover, it is easy to verify that the solution with $T_{1/7}^{(1)} = -3/4$ and $H_{1/7}^{(1)} = -3/4$, such that $L_{1/7,-}^{(1)} = 0$, is also an exact solution for the general case (42) when w is finite. Therefore, all solutions compatible with the SUGRA approximation can be classified as follows.

Given a set of $\{a_i\}$ with $i = \overline{1, N}$, there are 2^N possible values of A, including the negative ones. From the symmetry in (49), only half of those give independent solutions. This narrows the possibilities to 2^{N-1} positive combinations that fall in the range $0 \le A \le 1$. For each A in the range $0 \le A < 1/7$ there exist exactly two solutions describing AdS vacua with broken SUSY with all the moduli fixed at positive values.

For each A in the range $1/7 \le A < 1$ there exists exactly one solution describing an AdS vacuum with broken SUSY with all the moduli stabilized in the positive range of values. For $A = 1$ there are exactly two solutions with all the moduli stabilized in the positive range—de Sitter extremum in (51) and the SUSY AdS extremum in (50). These two solutions are always present for any set of $\{a_i\}$.

D. Explicit approximate solutions

In this section we will complete our analysis of the AdS vacua and obtain explicit analytic solutions for the moduli. We will take an approach similar to the one we employed in Sec. III B when we obtained an approximate formula (29). Expressing $\alpha^{(c)}$ from (78) we obtain

$$\alpha_A^{(c)} = \frac{b_2 \mathcal{T}_A^{(c)} - B_A^{(c)}}{b_1 \mathcal{T}_A^{(c)} - B_A^{(c)}}. \tag{82}$$

There exists a natural limit when the volume of the associative cycle $\mathcal{T}_A^{(c)}$ is large. Just like in the approximate SUSY case in (28), the leading order solution to (82) in this limit is given by

$$\alpha_A^{(c)} = \frac{b_2}{b_1}, \tag{83}$$

independent of A and c. Plugging this into (77) and solving for $\mathcal{T}_A^{(c)}$ we have in the leading order

$$\mathcal{T}_A^{(c)} = \frac{1}{b_2 - b_1} \ln\left(\frac{A_2 b_2}{A_1 b_1}\right) = \frac{1}{2\pi} \frac{PQ}{P - Q} \ln\left(\frac{A_2 P}{A_1 Q}\right), \tag{84}$$

where we again assumed the hidden sector gauge groups to be $SU(P)$ and $SU(Q)$. Notice that this approximation automatically results in the limit $w \to -\infty$, and therefore, $L_{A,+}^{(c)}$, $L_{A,-}^{(c)}$, and $B_A^{(c)}$ computed by solving (72) and plotted in Fig. 8 are consistent with this approximation. Thus, combining (84) with (23) and (79) we have the following approximate analytic solution for the moduli in the leading order:

$$s_{A,k}^{(c)} = \frac{1}{2\pi} \left(\frac{a_k}{N_k}\right) \left(\frac{L_{A,k}^{(c)}}{B_A^{(c)}}\right) \frac{PQ}{P - Q} \ln\left(\frac{A_2 P}{A_1 Q}\right). \tag{85}$$

To verify the approximation we can check it for the previously considered special case with two moduli when $a_1 = a_2 = 7/6$, i.e. the case when $A = 0$. By solving (72) we obtain

$$\begin{aligned} L_{0,+}^{(1)} &= L_{0,-}^{(2)} = \frac{3}{16}(-9 + \sqrt{17} + \sqrt{-26 + 10\sqrt{17}}), \\ L_{0,-}^{(1)} &= L_{0,+}^{(2)} = \frac{3}{16}(-9 + \sqrt{17} - \sqrt{-26 + 10\sqrt{17}}), \\ B_0^{(1)} &= B_0^{(2)} = \frac{7}{16}(-9 + \sqrt{17}). \end{aligned} \tag{86}$$

Thus, we have the following two solutions for the moduli for the AdS vacua with broken SUSY:

$$\begin{aligned} s_{0,1}^{(1)} &= \left(1 - \frac{\sqrt{-26 + 10\sqrt{17}}}{9 - \sqrt{17}}\right) \frac{1}{4\pi N_1} \frac{PQ}{P - Q} \ln\left(\frac{A_2 P}{A_1 Q}\right) \\ &\sim \frac{0.016}{N_1} \frac{PQ}{P - Q} \ln\left(\frac{A_2 P}{A_1 Q}\right), \\ s_{0,2}^{(1)} &= \left(1 + \frac{\sqrt{-26 + 10\sqrt{17}}}{9 - \sqrt{17}}\right) \frac{1}{4\pi N_2} \frac{PQ}{P - Q} \ln\left(\frac{A_2 P}{A_1 Q}\right) \\ &\sim \frac{0.143}{N_2} \frac{PQ}{P - Q} \ln\left(\frac{A_2 P}{A_1 Q}\right) \end{aligned} \tag{87}$$

and

$$s_{0,1}^{(2)} = \left(1 + \frac{\sqrt{-26 + 10\sqrt{17}}}{9 - \sqrt{17}}\right)\frac{1}{4\pi N_1}\frac{PQ}{P-Q}\ln\left(\frac{A_2 P}{A_1 Q}\right) \sim \frac{0.143}{N_2}\frac{PQ}{P-Q}\ln\left(\frac{A_2 P}{A_1 Q}\right),$$

$$s_{0,2}^{(2)} = \left(1 - \frac{\sqrt{-26 + 10\sqrt{17}}}{9 - \sqrt{17}}\right)\frac{1}{4\pi N_2}\frac{PQ}{P-Q}\ln\left(\frac{A_2 P}{A_1 Q}\right) \sim \frac{0.016}{N_1}\frac{PQ}{P-Q}\ln\left(\frac{A_2 P}{A_1 Q}\right). \quad (88)$$

The choice of the constants given in (67) results in the following values:

$$s_{0,1}^{(1)} = s_{0,2}^{(2)} = 2.62, \qquad s_{0,2}^{(1)} = s_{0,1}^{(2)} = 23.64. \quad (89)$$

A quick comparison with the exact values in (70) obtained numerically leads us to believe that the approximate analytical solutions presented here are highly accurate. This is especially true when the volume of the associative cycle $\mathcal{T}_A^{(c)}$ is large. For the particular choice above, the approximate value is

$$\mathcal{T}_0^{(1)} = \mathcal{T}_0^{(2)} = 26.16, \quad (90)$$

which is indeed fairly large. To complete the picture, we also would like to include the first subleading order contributions to the approximate solutions presented here. After a straightforward computation we have the following:

$$\alpha_A^{(c)} = \frac{P}{Q} + \frac{B_A^{(c)}}{\ln(\frac{A_2 P}{A_1 Q})}\left(\frac{P-Q}{Q}\right)^2 \quad (91)$$

and

$$\mathcal{T}_A^{(c)} = \frac{1}{2\pi}\frac{PQ}{P-Q}\ln\left(\frac{A_2 P}{A_1 Q}\right) + \frac{B_A^{(c)}}{2\pi}\left(\frac{P-Q}{\ln(\frac{A_2 P}{A_1 Q})}\right). \quad (92)$$

By combining (92) with (23) and (79) it is easy to obtain the corresponding expressions for the moduli that include the first subleading order correction:

$$s_{A,k}^{(c)} = \frac{1}{2\pi}\left(\frac{a_k}{N_k}\right)\left(\frac{L_{A,k}^{(c)}}{B_A^{(c)}}\right)\frac{PQ}{P-Q}\ln\left(\frac{A_2 P}{A_1 Q}\right) + \frac{L_{A,k}^{(c)}}{2\pi}\left(\frac{a_k}{N_k}\right)\left(\frac{P-Q}{\ln(\frac{A_2 P}{A_1 Q})}\right). \quad (93)$$

VI. VACUA WITH CHARGED MATTER IN THE HIDDEN SECTOR

Thus far, we have studied, in reasonable detail, the vacuum structure in the cases when the hidden sector has two strongly coupled gauge groups without any charged matter. It is of interest to study how the addition of matter charged under the hidden sector gauge group changes the conclusions. We argue that the addition of charged matter can give rise to Minkowski or metastable dS vacua due to additional F-terms for the hidden sector matter fields. Hence, dS vacua are obtained without adding any antibranes which explicitly break supersymmetry. This possibility was first studied in [23]. Moreover, we explain why it is reasonable to expect that, for a given choice of G_2 manifold, the dS vacuum obtained is *unique*.

A. Scalar potential

Generically we would expect that a hidden sector gauge theory can possess a fairly rich particle spectrum which, like the visible sector, may include chiral matter. For example, an $SU(N_c)$ gauge theory apart from the "pure glue" may also include massless quark states Q and $\tilde{Q}$ transforming in N_c and $\bar{N}_c$ of $SU(N_c)$. When embedded into M theory the effective superpotential due to gaugino condensation for such a hidden sector with N_f ($N_f < N_c$) quark flavors has the following form [24]:

$$W = A_1 e^{i(2\pi/N_c - N_f)\sum_{i=1}^{N} N_i^{(1)} z_i} \det(Q\tilde{Q})^{-(1/N_c - N_f)}. \quad (94)$$

We can introduce an effective meson field ϕ to replace the quark bilinear,

$$\phi \equiv (2Q\tilde{Q})^{1/2} = \phi_0 e^{i\theta}, \quad (95)$$

and for notational brevity we define

$$b_1 \equiv \frac{2\pi}{N_c - N_f}, \qquad a \equiv -\frac{2}{N_c - N_f}. \quad (96)$$

Here we will consider the case when the hidden sector gauge groups are $SU(N_c)$ and $SU(Q)$ with N_f flavors of the quarks Q ($\tilde{Q}$) transforming as N_c ($\bar{N}_c$) under $SU(N_c)$ and as singlets under $SU(Q)$. In this case, when $N_f = 1$, the effective nonperturbative superpotential has the following form:

$$W = A_1 \phi^a e^{ib_1 f} + A_2 e^{ib_2 f}. \quad (97)$$

One serious drawback of considering hidden sector matter is that we cannot explicitly calculate the moduli dependence of the matter Kähler potential. Therefore we will have to make some (albeit reasonable) assumptions, unlike the cases studied in the previous sections. In what follows we will assume that we work in a particular region of the moduli space where the Kähler metric for the matter fields in the hidden sector is a very slowly varying function of the moduli, essentially a constant. This assumption is based on the fact that the chiral fermions are localized at pointlike conical singularities so that the bulk moduli s_i should have very little effect on the local physics. In general, a singularity supporting a chiral fermion has no local moduli, since there are no flat directions constructed from a single chiral matter representation. Our assumption is further justified by the M theory lift of some calculable type IIA matter metrics as described in the Appendix. It is an

interesting and extremely important problem to properly derive the matter Kähler potential in M theory and test our assumptions.

Thus we will consider the case when the hidden sector chiral fermions have "modular weight zero" and assume a canonically normalized Kähler potential. The scalar potential is invariant under $Q \leftrightarrow \tilde{Q}$ and $Q = \tilde{Q}$ along the D-flat direction. For the sake of simplicity, we will first study the case $N_f = 1$, but later it will be shown that all the results also hold true for $N_f > 1$. The meson field $\phi \equiv (2Q\tilde{Q})^{1/2}$ along the D-flat direction is such that the corresponding Kähler potential for ϕ is canonical. The total Kähler potential, i.e. moduli plus matter, thus takes the form

$$\begin{aligned} K &= -3\ln(4\pi^{1/3}V_X) + Q^\dagger Q + \tilde{Q}^\dagger \tilde{Q} \\ &= -3\ln(4\pi^{1/3}V_X) + \phi\bar{\phi}. \end{aligned} \tag{98}$$

The moduli F-terms are then given by

$$\begin{aligned} F_k = ie^{ib_2\vec{N}\cdot\vec{t}}\Big[& N_k(b_1A_1\phi_0^a e^{-b_1\vec{N}\cdot\vec{s}+i(b_1-b_2)\vec{N}\cdot\vec{t}+ia\theta} \\ & + b_2A_2e^{-b_2\vec{N}\cdot\vec{s}}) + \frac{3a_k}{2s_k}(A_1\phi_0^a e^{-b_1\vec{N}\cdot\vec{s}+i(b_1-b_2)\vec{N}\cdot\vec{t}+ia\theta} \\ & + A_2e^{-b_2\vec{N}\cdot\vec{s}})\Big]. \end{aligned} \tag{99}$$

In addition, an F-term due to the meson field is also generated,

$$\begin{aligned} F_\phi = \phi_0 e^{-i\theta+ib_2\vec{N}\cdot\vec{t}}\Big[& \left(\frac{a}{\phi_0^2}+1\right)A_1\phi_0^a e^{-b_1\vec{N}\cdot\vec{s}+i(b_1-b_2)\vec{N}\cdot\vec{t}+ia\theta} \\ & + A_2e^{-b_2\vec{N}\cdot\vec{s}}\Big]. \end{aligned} \tag{100}$$

The supergravity scalar potential is then given by

$$\begin{aligned} V = \frac{e^{\phi_0^2}}{48\pi V_X^3}\Big[& (b_1^2A_1^2\phi_0^{2a}e^{-2b_1\vec{\nu}\cdot\vec{a}} + b_2^2A_2^2e^{-2b_2\vec{\nu}\cdot\vec{a}} + 2b_1b_2A_1A_2\phi_0^a e^{-(b_1+b_2)\vec{\nu}\cdot\vec{a}}\cos((b_1-b_2)\vec{N}\cdot\vec{t}+a\theta))\sum_{i=1}^N a_i(\nu_i)^2 \\ & + 3(\vec{\nu}\cdot\vec{a})(b_1A_1^2\phi_0^{2\alpha}e^{-2b_1\vec{\nu}\cdot\vec{a}} + b_2A_2^2e^{-2b_2\vec{\nu}\cdot\vec{a}} + (b_1+b_2)A_1A_2\phi_0^a e^{-(b_1+b_2)\vec{\nu}\cdot\vec{a}}\cos((b_1-b_2)\vec{N}\cdot\vec{t}+a\theta)) \\ & + 3(A_1^2\phi_0^{2a}e^{-2b_1\vec{\nu}\cdot\vec{a}} + A_2^2e^{-2b_2\vec{\nu}\cdot\vec{a}} + 2A_1A_2\phi_0^a e^{-(b_1+b_2)\vec{\nu}\cdot\vec{a}}\cos((b_1-b_2)\vec{N}\cdot\vec{t}+a\theta)) \\ & + \frac{3}{4}\phi_0^2(A_1^2\phi_0^{2\alpha}\left(\frac{a}{\phi_0^2}+1\right)^2e^{-2b_1\vec{\nu}\cdot\vec{a}} + A_2^2e^{-2b_2\vec{\nu}\cdot\vec{a}} + 2A_1A_2\phi_0^a\left(\frac{a}{\phi_0^2}+1\right)e^{-(b_1+b_2)\vec{\nu}\cdot\vec{a}}\cos((b_1-b_2)\vec{N}\cdot\vec{t}+a\theta))\Big]. \end{aligned} \tag{101}$$

Minimizing this potential with respect to the axions and θ, we obtain the following condition:

$$\sin((b_1-b_2)\vec{N}\cdot\vec{t}+a\theta) = 0. \tag{102}$$

The potential has local minima with respect to the moduli s_i when

$$\cos((b_1-b_2)\vec{N}\cdot\vec{t}+a\theta) = -1. \tag{103}$$

In this case (101) reduces to

$$\begin{aligned} V = \frac{e^{\phi_0^2}}{48\pi V_X^3}\Big[& (b_1A_1\phi_0^a e^{-b_1\vec{\nu}\cdot\vec{a}} - b_2A_2e^{-b_2\vec{\nu}\cdot\vec{a}})^2\sum_{i=1}^N a_i(\nu_i)^2 \\ & + 3(\vec{\nu}\cdot\vec{a})(A_1\phi_0^a e^{-b_1\vec{\nu}\cdot\vec{a}} - A_2e^{-b_2\vec{\nu}\cdot\vec{a}}) \\ & \times (b_1A_1\phi_0^a e^{-b_1\vec{\nu}\cdot\vec{a}} - b_2A_2e^{-b_2\vec{\nu}\cdot\vec{a}}) \\ & + 3(A_1\phi_0^a e^{-b_1\vec{\nu}\cdot\vec{a}} - A_2e^{-b_2\vec{\nu}\cdot\vec{a}})^2 \\ & + \frac{3}{4}\left(A_1\phi_0^a\left(\frac{a}{\phi}+\phi_0\right)e^{-b_1\vec{\nu}\cdot\vec{a}} - A_2\phi_0e^{-b_2\vec{\nu}\cdot\vec{a}}\right)^2\Big]. \end{aligned} \tag{104}$$

B. Supersymmetric extrema

Here we consider a case when the scalar potential (104) possesses SUSY extrema and find approximate solutions for the moduli and the meson field vevs. Taking into account (103) and setting the moduli F-terms (99) to zero, we obtain

$$\nu_k = \nu = -\frac{3}{2}\frac{\tilde{\alpha}-1}{b_1\tilde{\alpha}-b_2}, \tag{105}$$

together with the constraint

$$\tilde{\alpha} \equiv \frac{A_1}{A_2}\phi_0^a e^{-(7/3)(b_1-b_2)\nu}. \tag{106}$$

At the same time, setting the matter F-term (100) to zero results in the following condition:

$$\left(\frac{a}{\phi_0^2}+1\right)\tilde{\alpha} - 1 = 0. \tag{107}$$

Expressing $\tilde{\alpha}$ from (105) and substituting it into (107) we obtain the following solution for the meson vev at the SUSY extremum:

$$\phi_0^2 = a\frac{b_2+3/(2\nu)}{b_1-b_2}. \tag{108}$$

Recall that in our analysis we are considering the case when $P \equiv N_c - N_f > 0$, which implies that parameter a defined in (96) is negative. Thus, since the left-hand side of (108) is positive, for the SUSY solution to exist, it is

necessary to satisfy

$$b_2 > b_1 \Rightarrow P > Q. \tag{109}$$

Recall that for the moduli to be positive, the constants have to satisfy certain conditions resulting in two possible branches (30). Therefore, condition (109) implies that the SUSY AdS extremum exists only for branch a) in (30). In the limit, when ν is large, the approximate solution is given by

$$\begin{aligned} \tilde{\alpha} &= \frac{P}{Q}, \\ s_i &= \frac{a_i \nu}{N_i}, \quad \text{with} \quad \nu = \frac{3}{14\pi}\frac{PQ}{P-Q}\ln\left(\frac{A_2 P}{A_1 Q}\right), \\ \phi_0^2 &= \frac{2}{P-Q} + \frac{7}{P\ln(\frac{A_2 P}{A_1 Q})}, \end{aligned} \tag{110}$$

where we also assumed that $P \sim \mathcal{O}(10)$, such that $\phi_0^a \approx 1$. For the case with two moduli where $a_1 = a_2 = 7/6$ and the choice

$$\begin{aligned} A_1 &= 4.1, \qquad A_2 = 30, \qquad b_1 = \frac{2\pi}{30}, \\ b_2 &= \frac{2\pi}{27}, \qquad N_1 = 1, \qquad N_2 = 1, \end{aligned} \tag{111}$$

the numerical solution for the SUSY extremum obtained by minimizing the scalar potential (104) gives

$$s_1 \approx 44.5, \qquad s_2 \approx 44.5, \qquad \phi_0 \approx 0.883, \tag{112}$$

whereas the approximate analytic solution obtained in (110) yields

$$s_1 \approx 45.0, \qquad s_2 \approx 45.0, \qquad \phi_0 \approx 0.882. \tag{113}$$

This vacuum is very similar to the SUSY AdS extremum obtained previously for the potential arising from the "pure glue" super Yang-Mills (SYM) hidden sector gauge theory. Thus, we will not discuss it any further and instead move to the more interesting case, for which condition (109) is not satisfied.

C. Metastable dS minima

Below we will use the same approach and notation we used in Sec. V, to describe AdS vacua with broken SUSY. Again, for brevity we denote

$$\begin{aligned} \tilde{x} &\equiv (\tilde{\alpha} - 1), \qquad \tilde{y} \equiv (b_1\tilde{\alpha} - b_2), \\ \tilde{z} &\equiv (b_1^2\tilde{\alpha} - b_2^2), \qquad \tilde{w} \equiv \frac{\tilde{x}\,\tilde{z}}{\tilde{y}^2}. \end{aligned} \tag{114}$$

Extremizing (104) with respect to the moduli s_i and dividing by $\tilde{x}^2$ we obtain the following system of coupled equations,

$$\begin{aligned} &2\frac{\tilde{y}^2}{\tilde{x}^2}\nu_k^2 - \left(2\frac{\tilde{y}^2}{\tilde{x}^2}\tilde{w}\sum_{i=1}^{N} a_i\nu_i^2 + 3\frac{\tilde{y}}{\tilde{x}}(\tilde{w}+1)\vec{\nu}\cdot\vec{a} + 3\right. \\ &\quad \left. + \frac{3}{2}\phi_0^2\left(\frac{a\tilde{\alpha}}{\phi_0^2\tilde{x}} + 1\right)\left(\frac{a\tilde{\alpha}b_1}{\phi_0^2\tilde{y}} + 1\right)\right)\frac{\tilde{y}}{\tilde{x}}\nu_k - 3\left(\frac{\tilde{y}^2}{\tilde{x}^2}\sum_{i=1}^{N} a_i\nu_i^2\right. \\ &\quad \left. + 3\frac{\tilde{y}}{\tilde{x}}\vec{\nu}\cdot\vec{a} + 3 + \frac{3}{4}\phi_0^2\left(\frac{a\tilde{\alpha}}{\phi_0^2\tilde{x}} + 1\right)^2\right) = 0, \end{aligned} \tag{115}$$

plus the constraint (106). Next, we extremize (104) with respect to ϕ_0 and divide it by $2\phi_0\tilde{x}^2$ to obtain

$$\begin{aligned} &\frac{\tilde{y}^2}{\tilde{x}^2}\sum_{i=1}^{N} a_i\nu_i^2 + \frac{3}{2}\frac{\tilde{y}}{\tilde{x}}\vec{\nu}\cdot\vec{a} + \frac{3}{4}\left(2\frac{\tilde{y}}{\tilde{x}}\vec{\nu}\cdot\vec{a} + \frac{a\tilde{\alpha}}{\tilde{x}}\left(\frac{a-1}{\phi_0^2} + 2\right)\right. \\ &\quad \left. + 5 + \phi_0^2\right)\left(\frac{a\tilde{\alpha}}{\phi_0^2\tilde{x}} + 1\right) + \frac{a\tilde{\alpha}b_1}{\phi_0^2\tilde{x}}\left(\frac{\tilde{y}}{\tilde{x}}\sum_{i=1}^{N} a_i\nu_i^2 + \frac{3}{2}\vec{\nu}\cdot\vec{a}\right) = 0. \end{aligned} \tag{116}$$

To solve the system of N cubic equations (115), we introduce a quadratic constraint

$$\begin{aligned} 4\tilde{T} \equiv\ & 2\frac{\tilde{y}^2}{\tilde{x}^2}\tilde{w}\sum_{i=1}^{N} a_i\nu_i^2 + 3\frac{\tilde{y}}{\tilde{x}}(\tilde{w}+1)\vec{\nu}\cdot\vec{a} + 3 \\ &+ \frac{3}{2}\phi_0^2\left(\frac{a\tilde{\alpha}}{\phi_0^2\tilde{x}} + 1\right)\left(\frac{a\tilde{\alpha}b_1}{\phi_0^2\tilde{y}} + 1\right), \end{aligned} \tag{117}$$

such that (115) turns into a system of N coupled quadratic equations:

$$\begin{aligned} &2\frac{\tilde{y}^2}{\tilde{x}^2}\nu_k^2 - 4\tilde{T}\frac{\tilde{y}}{\tilde{x}}\nu_k - 3\left(\frac{\tilde{y}^2}{\tilde{x}^2}\sum_{i=1}^{N} a_i\nu_i^2 + 3\frac{\tilde{y}}{\tilde{x}}\vec{\nu}\cdot\vec{a}\right. \\ &\quad \left. + 3 + \frac{3}{4}\phi_0^2\left(\frac{a\tilde{\alpha}}{\phi_0^2\tilde{x}} + 1\right)^2\right) = 0. \end{aligned} \tag{118}$$

Again, the standard solution of a quadratic equation dictates that the solutions for ν_k of (118) have the form

$$\nu_k = \frac{\tilde{x}}{\tilde{y}}(\tilde{T} + m_k\tilde{H}), \quad \text{with} \quad m_k = \pm 1, \qquad k = \overline{1, N}. \tag{119}$$

We have now reduced the task of determining ν_k for each $k = \overline{1, N}$ to finding *only two* quantities—$\tilde{T}$ and $\tilde{H}$. By substituting (119) into Eqs. (116)–(118) and using (2), we obtain a system of three coupled equations,

$$\frac{7}{3}(\tilde{T}_A^2 + 2A\tilde{T}_A\tilde{H}_A + \tilde{H}_A^2) + \frac{7}{2}(\tilde{T}_A + A\tilde{H}_A) + \frac{3}{4}\left(\frac{14}{3}(\tilde{T}_A + A\tilde{H}_A) + \frac{a\tilde{\alpha}}{x}\left(\frac{a-1}{\phi_0^2} + 2\right) + 5 + \phi_0^2\right)\left(\frac{a\tilde{\alpha}}{\phi_0^2\tilde{x}} + 1\right)$$
$$+ \frac{a\tilde{\alpha}b_1}{\phi_0^2}\frac{7}{3\tilde{y}}\left((\tilde{T}_A^2 + 2A\tilde{T}_A\tilde{H}_A + \tilde{H}_A^2) + \frac{3}{2}(\tilde{T}_A + A\tilde{H}_A)\right) = 0,$$
$$\frac{14w}{3}(\tilde{T}_A^2 + 2A\tilde{T}_A\tilde{H}_A + \tilde{H}_A^2) + 7(w+1)(\tilde{T}_A + A\tilde{H}_A) + 3 + \frac{3}{2}\phi_0^2\left(\frac{a\tilde{\alpha}}{\phi_0^2\tilde{x}} + 1\right)\left(\frac{a\tilde{\alpha}b_1}{\phi_0^2\tilde{y}} + 1\right) - 4\tilde{T}_A = 0,$$
$$9(\tilde{T}_A^2 + 2A\tilde{T}_A\tilde{H}_A + \tilde{H}_A^2) - 4\tilde{H}_A(\tilde{H}_A + A\tilde{T}_A) + 21(\tilde{T}_A + A\tilde{H}_A) + 9 + \frac{9}{4}\phi_0^2\left(\frac{a\tilde{\alpha}}{\phi_0^2\tilde{x}} + 1\right)^2 = 0, \quad (120)$$

plus the constraint (106). Note that each solution is again labeled by parameter A so that (119) becomes

$$\nu_k^A = \frac{\tilde{x}}{\tilde{y}}(\tilde{T}_A + m_k\tilde{H}_A). \quad (121)$$

Let us consider the case when $A = 1$. In this case, the solution is given by

$$\nu_k^1 = \nu = \frac{\tilde{x}}{\tilde{y}}(\tilde{T}_1 + \tilde{H}_1) = \frac{\tilde{x}}{\tilde{y}}\tilde{L}_{1,+}, \quad (122)$$

and (120) is reduced to

$$\frac{7}{3}(\tilde{T}_1 + \tilde{H}_1)^2 + \frac{7}{2}(\tilde{T}_1 + \tilde{H}_1) + \frac{3}{4}\left(\frac{14}{3}(\tilde{T}_1 + \tilde{H}_1) + \frac{a\tilde{\alpha}}{x}\left(\frac{a-1}{\phi_0^2} + 2\right) + \phi_0^2 + 5\right)\left(\frac{a\tilde{\alpha}}{\phi_0^2\tilde{x}} + 1\right)$$
$$+ \frac{a\tilde{\alpha}b_1}{\phi_0^2}\frac{7}{3\tilde{y}}\left((\tilde{T}_1 + \tilde{H}_1)^2 + \frac{3}{2}(\tilde{T}_1 + \tilde{H}_1)\right) = 0,$$
$$\frac{14w}{3}(\tilde{T}_1 + \tilde{H}_1)^2 + 7(w+1)(\tilde{T}_1 + \tilde{H}_1) + 3 + \frac{3}{2}\phi_0^2\left(\frac{a\tilde{\alpha}}{\phi_0^2\tilde{x}} + 1\right)\left(\frac{a\tilde{\alpha}b_1}{\phi_0^2\tilde{y}} + 1\right) - 4\tilde{T}_1 = 0,$$
$$9(\tilde{T}_1 + \tilde{H}_1)^2 - 4\tilde{H}_1(\tilde{H}_1 + \tilde{T}_1) + 21(\tilde{T}_1 + \tilde{H}_1) + 9 + \frac{9}{4}\phi_0^2\left(\frac{a\tilde{\alpha}}{\phi_0^2\tilde{x}} + 1\right)^2 = 0. \quad (123)$$

In the notation introduced in (114), the SUSY condition (107) can be written as

$$\frac{a\tilde{\alpha}}{\phi_0^2} + \tilde{x} = 0. \quad (124)$$

It is then straightforward to check that, in the SUSY case, the system (123) yields

$$\tilde{T}_1 = -\frac{15}{8}, \qquad \tilde{H}_1 = \frac{3}{8}, \qquad \tilde{L}_{1,+} = -\frac{3}{2}, \quad (125)$$

as expected. We will now consider branch b) in (30) for which (124) is not satisfied. Moreover, in order to obtain analytical solutions for the moduli and the meson vev ϕ_0 we will again consider the large three-cycle volume approximation. Recall that in this case we take the $\tilde{y} \to 0$ and $\tilde{w} \to -\infty$ limit to obtain the following reduced system of equations when $A = 1$ for $\tilde{L}_{1,+}$ and ϕ_0:

$$\frac{7}{3}(\tilde{L}_{1,+})^2 + \frac{7}{2}\tilde{L}_{1,+} + \frac{3}{4}\left(\frac{14}{3}\tilde{L}_{1,+} + \frac{a\tilde{\alpha}}{x}\left(\frac{a-1}{\phi_0^2} + 2\right)\right.$$
$$\left. + \phi_0^2 + 5\right)\left(\frac{a\tilde{\alpha}}{\phi_0^2\tilde{x}} + 1\right) + \frac{a\tilde{\alpha}b_1}{\phi_0^2}\frac{7}{3\tilde{y}}\left((\tilde{L}_{1,+})^2 + \frac{3}{2}\tilde{L}_{1,+}\right) = 0,$$
$$\frac{2}{3}(\tilde{L}_{1,+})^2 + \tilde{L}_{1,+} + \frac{3a\tilde{\alpha}b_1\tilde{y}}{14\tilde{x}\,\tilde{z}}\left(\frac{a\tilde{\alpha}}{\phi_0^2\tilde{x}} + 1\right) = 0. \quad (126)$$

Note that in (126), we have dropped the third equation since for $A = 1$ we only need to know $\tilde{L}_{1,+}$ and the third equation in (123) determines $\tilde{H}_{1,+}$ in terms of $\tilde{L}_{1,+}$. We also kept the first subleading term in the second equation. Note that the term in the second line of the first equation proportional to $\sim 1/\tilde{y}$ appears to blow up as $\tilde{y} \to 0$. However, from the second equation one can see that the combination $(\tilde{L}_{1,+})^2 + \frac{3}{2}\tilde{L}_{1,+}$ is proportional to $\tilde{y}$ which makes the corresponding term finite. By keeping the subleading term in the second equation, we can express

$$(\tilde{L}_{1,+})^2 = -\frac{3}{2}\tilde{L}_{1,+} - \frac{9a\tilde{\alpha}b_1\tilde{y}}{28\tilde{x}\,\tilde{z}}\left(\frac{a\tilde{\alpha}}{\phi_0^2\tilde{x}} + 1\right) \quad (127)$$

from the second equation to substitute into the first equation to obtain in the leading order

$$\left(\frac{14}{3}\tilde{L}_{1,+} + 5 + \phi_0^2 + \frac{a\tilde{\alpha}}{x}\left(\frac{a-1}{\phi_0^2} + 2\right)\right.$$
$$\left. - \frac{1}{\tilde{z}\,\tilde{x}}\left(\frac{a\tilde{\alpha}b_1}{\phi_0}\right)^2\right)\left(\frac{a\tilde{\alpha}}{\phi_0^2\tilde{x}} + 1\right) = 0. \quad (128)$$

Since we are now considering branch b) in (30), the second factor in (128) is automatically nonzero. Therefore, the first factor in (128) must be zero. Thus, after substituting

$$\tilde{L}_{1,+} \approx -\frac{3}{2} + \frac{3a\tilde{\alpha}b_1\tilde{y}}{14\tilde{x}\,\tilde{z}}\left(\frac{a\tilde{\alpha}}{\phi_0^2\tilde{x}} + 1\right), \quad (129)$$

obtained from (127), we have the following equation for ϕ_0:

$$\phi_0^2 - 2 + \frac{a\tilde{\alpha} b_1 \tilde{y}}{\tilde{x}\,\tilde{z}}\left(\frac{a\tilde{\alpha}}{\phi_0^2 \tilde{x}} + 1\right) + \frac{a\tilde{\alpha}}{x}\left(\frac{a-1}{\phi_0^2} + 2\right) - \frac{1}{\tilde{z}\,\tilde{x}}\left(\frac{a\tilde{\alpha} b_1}{\phi_0}\right)^2 = 0. \quad (130)$$

Also, since in the leading order $\tilde{L}_{1,+} = -3/2$, using the definitions in (114) we can express $\tilde{\alpha}$ from (122) in the limit when ν is large, including the first subleading term,

$$\tilde{\alpha} \approx \frac{b_2}{b_1} + \frac{3(b_1 - b_2)}{2 b_1^2 \nu}. \quad (131)$$

By combining (106) with the leading term in (131) and taking into account that $\phi_0^a \sim 1$ we again obtain

$$s_i = \frac{a_i \nu}{N_i}, \quad \text{with} \quad \nu \approx \frac{3}{14\pi}\frac{PQ}{Q-P}\ln\left(\frac{A_1 Q}{A_2 P}\right). \quad (132)$$

Thus, from (131) we have

$$\tilde{\alpha} \approx \frac{P}{Q} + \frac{7(Q-P)^2}{2Q^2 \ln(\frac{A_1 Q}{A_2 P})}. \quad (133)$$

Finally, using (133) along with the definitions of $\tilde{x}$, $\tilde{y}$, and $\tilde{z}$ in (114) in terms of $\tilde{\alpha}$, we can solve for ϕ_0^2 from (130) and assuming that $Q - P \sim \mathcal{O}(1)$, in the limit when P is large, we obtain

$$\phi_0^2 \approx 1 - \frac{2}{Q-P} + \sqrt{1 - \frac{2}{Q-P}} - \frac{7}{P \ln(\frac{A_1 Q}{A_2 P})}\left(\frac{3}{2} + \sqrt{1 - \frac{2}{Q-P}}\right). \quad (134)$$

We notice immediately that since ϕ_0^2 is real and positive it is necessary that

$$Q - P > 2. \quad (135)$$

We will show shortly that the extremum we found above corresponds to a metastable minimum. Also, for a simple case with two moduli, via an explicit numerical check we have confirmed that if $Q - P \leq 2$ the local minimum is completely destabilized yielding a runaway potential. Also note that for (134) to be accurate, it is not only P which has to be large but also the product $P \ln(\frac{A_1 Q}{A_2 P})$ has to stay large to keep the subleading terms suppressed. To check the accuracy of the solution we again consider a manifold with two moduli where the values of the microscopic constants are

$$a_1 = a_2 = 7/6, \quad P = 20, \quad Q = 23, \quad A_1 = 27, \quad A_2 = 2, \quad N_1 = N_2 = 1. \quad (136)$$

The exact values obtained numerically are

$$s_1 \approx 33.470, \quad s_2 \approx 33.470, \quad \phi_0 \approx 0.810. \quad (137)$$

The approximate equations above yield the following values:

$$s_1 \approx 33.463, \quad s_2 \approx 33.463, \quad \phi_0 \approx 0.803. \quad (138)$$

Note the high accuracy of the leading order approximation for the moduli s_i.

It is now straightforward to compute the vacuum energy using the approximate solution obtained above. First, we compute

$$K^{i\bar{j}} F_i \bar{F}_{\bar{j}} - 3|W|^2 = 4(A_2\tilde{x})^2\left(\frac{7}{9}(L_{1,+})^2 + \frac{7}{3}L_{1,+} + 1\right) \times \left(\frac{A_1 Q}{A_2 P}\right)^{-(2P/(Q-P))} \quad (139)$$

and

$$K^{\phi\bar{\phi}} F_\phi \bar{F}_{\bar{\phi}} = (A_2 \tilde{x}\phi_0)^2\left(\frac{a\tilde{\alpha}}{\phi_0^2\tilde{x}} + 1\right)^2\left(\frac{A_1 Q}{A_2 P}\right)^{-(2P/(Q-P))}. \quad (140)$$

Using (129), (139), and (140) we obtain the following expression for the potential at the extremum with respect to the moduli s_i as a function of ϕ_0,

$$V_0 = \frac{(A_2\tilde{x})^2}{64\pi V_X^3}\left[\phi_0^4 + \left(\frac{2a\tilde{\alpha}}{\tilde{x}} - 3\right)\phi_0^2 + \left(\frac{a\tilde{\alpha}}{\tilde{x}}\right)^2\right]\frac{e^{\phi_0^2}}{\phi_0^2} \times \left(\frac{A_1 Q}{A_2 P}\right)^{-(2P/(Q-P))}, \quad (141)$$

where the terms linear in $\tilde{y}$ canceled and the quadratic terms were dropped. A quick look at the structure of the potential (141) as a function of ϕ_0^2, where $\phi_0^2 > 0$, is enough to see that there is a single extremum with respect to ϕ_0^2 which is, indeed, a minimum. The polynomial in the square brackets is quadratic with respect to ϕ_0^2. Moreover, the coefficient of the ϕ_0^4 monomial is equal to unity and therefore is always positive. This implies that for the minimum of such a biquadratic polynomial to be positive, it is necessary for the corresponding discriminant to be negative, which results in the following condition:

$$3 - 4\frac{a\tilde{\alpha}}{\tilde{x}} < 0. \quad (142)$$

Again, since in the leading order $\tilde{L}_{1,+} = -3/2$, using the definitions in (132), we can express $\tilde{\alpha}$ from (122) in terms of ν to get

$$\frac{\tilde{\alpha}}{\tilde{x}} = \frac{\tilde{\alpha}}{\tilde{\alpha} - 1} = \frac{P}{P-Q} + \frac{3PQ}{4\pi\nu(P-Q)}. \quad (143)$$

We then substitute ν from (132) into (143) and use it together with $a = -2/P$ to obtain from (142) the following condition:

$$3 - \frac{8}{Q-P} - \frac{28}{P\ln(\frac{A_1 Q}{A_2 P})} < 0. \quad (144)$$

The above equation is the leading order requirement for the energy density at the minimum to be positive. It is also clear that the minimum is *metastable*; as in the decompactification limit ($V_X \to \infty$), the scalar potential vanishes from above, leading to an absolute Minkowski minimum. Figure 9 shows the scalar potential for a manifold with two moduli along the slice $s_1 = s_2$ with the meson field ϕ equal to its value at the minimum of the potential (134). The microscopic constants are the same as in (136).

D. The uniqueness of the dS vacuum

In the previous subsection we found a particular solution of the system in (120) corresponding to $A = 1$. Here we would like to investigate if solutions for $0 \leq A < 1$ are possible when the vacuum for $A = 1$ is de Sitter. Just like for the pure SYM case, we can recast (121) as

$$\nu_k^A = \frac{\mathcal{T}_A}{\tilde{B}_A} \tilde{L}_{A,k}, \tag{145}$$

where the volume of the associative three-cycle Q is again

$$\mathcal{T}_A \equiv \mathrm{Vol}(Q)_A = \vec{a} \cdot \vec{\nu}^A = \frac{\tilde{x}}{\tilde{y}} \tilde{B}_A, \tag{146}$$

and we have introduced

$$\tilde{B}_A \equiv \vec{a} \cdot \vec{\tilde{L}}_A = \tfrac{7}{3}(\tilde{T}_A + A\tilde{H}_A). \tag{147}$$

Just like we did in Eq. (82) for the pure SYM case, we can also express $\tilde{\alpha}_A$ as

$$\tilde{\alpha}_A = \frac{b_2 \mathcal{T}_A - \tilde{B}_A}{b_1 \mathcal{T}_A - \tilde{B}_A}. \tag{148}$$

If we again consider the large associative cycle volume limit and take $\tilde{y} \to 0$ and $\tilde{w} \to -\infty$, the second and third equations in (120) in the leading order reduce to

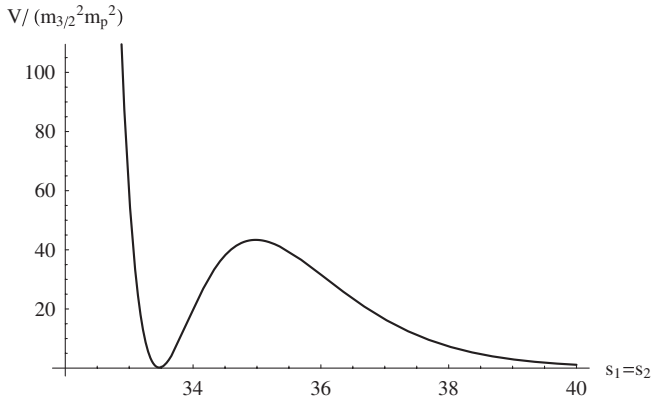

FIG. 9. Potential in units of $m_{3/2}^2 m_p^2$ along the slice $s_1 = s_2$ for a manifold with two moduli with the meson field equal to its value at the minimum of the potential (134). The microscopic constants are as in (136). Although hard to see from the graph, the value of the potential at the minimum (i.e. the cosmological constant) is $0.194 m_{3/2}^2 m_p^2$.

$$2(\tilde{T}_A^2 + 2A\tilde{T}_A\tilde{H}_A + \tilde{H}_A^2) + 3(\tilde{T}_A + A\tilde{H}_A) = 0,$$
$$9(\tilde{T}_A^2 + 2A\tilde{T}_A\tilde{H}_A + \tilde{H}_A^2) - 4\tilde{H}_A(\tilde{H}_A + A\tilde{T}_A)$$
$$+21(\tilde{T}_A + A\tilde{H}_A) + 9 + \frac{9}{4}\phi_0^2\left(\frac{a\tilde{\alpha}}{\phi_0^2\tilde{x}} + 1\right)^2 = 0. \tag{149}$$

Note that the only difference between (72) and (149) is the presence of the term

$$\delta \equiv \frac{9}{4}\phi_0^2\left(\frac{a\tilde{\alpha}}{\phi_0^2\tilde{x}} + 1\right)^2, \tag{150}$$

which couples the system (149) to the first equation in (120) which determines ϕ_0. Instead of solving the full system to determine $\tilde{T}_A$, $\tilde{H}_A$, and ϕ_0 and analyzing the solutions, we choose a quicker strategy for our further analysis. Namely, we can solve the system of two equations in (149) and regard δ as a continuous deformation parameter. One may object to this proposition because $\tilde{\alpha}$ and therefore $\tilde{x} = \tilde{\alpha} - 1$ are not independent of parameter A. However, in the limit when $\mathcal{T}_A$ is large, we notice from (148) that, in the leading order, $\tilde{\alpha}_A$ is indeed *independent* of A.

Recall that in the pure SYM case the system (72) corresponding to the case when $\delta = 0$ has two *real* solutions for all $0 \leq A \leq 1$. Thus, one may expect that the system may still yield real solutions for $A < 1$, as we continuously dial δ. Let us first determine the range of possible values of parameter δ. A quick calculation yields that the combination in (150) is the smallest with respect to ϕ_0 when $\phi_0^2 = \frac{a\tilde{\alpha}}{\tilde{x}}$. In this case

$$\delta = 9\frac{a\tilde{\alpha}}{\tilde{x}}. \tag{151}$$

Now, recall from the previous subsection that, for the solution corresponding to $A = 1$ to have a positive vacuum energy, condition (142) must hold. Since $\tilde{\alpha}$ and $\tilde{x}$ are independent of A in the leading order, condition (142) implies that

$$\delta > \frac{27}{4}. \tag{152}$$

Again, since the volume $\mathcal{T}_A$ is always positive, from (145) we see that, for all moduli to be stabilized in the positive range, all three quantities $\tilde{L}_{A,+}$, $\tilde{L}_{A,-}$, and $\tilde{B}_A$ must have the same sign. For $\delta = 27/4$, the system (149) has two real solutions when $0.877\,781 < A < 1$.

However, from the left plot in Fig. 10, corresponding to the minimum value $\delta = 27/4$, we see that neither of the two solutions satisfies the above requirement since both short-dashed curves corresponding to $\tilde{L}_{A,-}$ for the two solutions are *always* positive for the entire range $0.877\,781 < A < 1$, whereas both $\tilde{L}_{A,+}$ and $\tilde{B}_A$ remain negative. Therefore for $\delta = 27/4$ and $A < 1$ there are no solutions for which all the moduli are stabilized at positive values. Moreover, as parameter δ is further increased, the

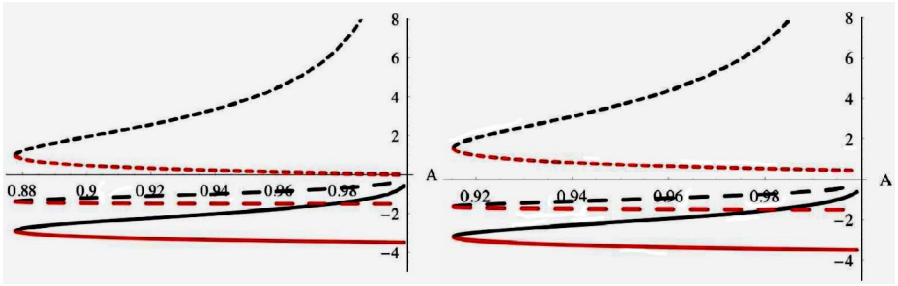

FIG. 10 (color online). Plots of $\tilde{L}^{(c)}_{A,+}$, $\tilde{L}^{(c)}_{A,-}$, and $\tilde{B}^{(c)}_{A}$, where $c = \overline{1,2}$, corresponding to the two real solutions of the system (149) as functions of parameter A. $\tilde{L}^{(c)}_{A,+}$ is represented by the long-dashed curve, $\tilde{L}^{(c)}_{A,-}$ by the short-dashed curve, $\tilde{B}^{(c)}_{A}$ by the solid curve. Black lines: $\tilde{L}^{(1)}_{A,+}$, $\tilde{L}^{(1)}_{A,-}$, and $\tilde{B}^{(1)}_{A}$ corresponding to the first real solution. Red (gray) lines: $\tilde{L}^{(2)}_{A,+}$, $\tilde{L}^{(2)}_{A,-}$, and $\tilde{B}^{(2)}_{A}$ corresponding to the second real solution. Left panel: when $\delta = 27/4$ the real solutions exist in the range $0.877\,781 < A < 1$. Right panel: when $\delta = 8$ the real solutions exist in the range $0.915\,342 < A < 1$.

range of possible values of A for which the system has two real solutions gets smaller, and, more importantly, the values of $\tilde{L}_{A,-}$ remain positive and only increase while both $\tilde{L}_{A,+}$ and $\tilde{B}_{A}$ remain negative, which can be seen from the right plot in Fig. 10, where $\delta = 8$. This trend continues as we increase δ.

Thus, we can make the following general claim: If the solution for $A = 1$ has a positive vacuum energy, condition (152) must hold. When this condition is satisfied the system (149) has no solutions in the range $0 \leq A < 1$ for which all the moduli are stabilized at positive values. Therefore, if the vacuum found for $A = 1$ is de Sitter it is the only possible vacuum where all the moduli are stabilized at positive values. Although the above analysis was done in the limit when $\mathcal{T}_A$ is large, we have run a number of explicit numerical checks for a manifold with two moduli and various values of the constants confirming the above claim. In addition, although we have not proved it, it seems plausible from many numerical checks we carried out that it is also not possible to have a metastable dS minimum for values of A different from unity, even if the dS condition on the $A = 1$ vacuum is *not* imposed.

Finally, it should be noted that the situation with a "unique" dS vacuum is in sharp contrast to that when one obtains anti-de Sitter vacua, where there are between 2^{N-1} and 2^N solutions for N moduli depending on the value of A (see Sec. V). Let us explain this in a bit more detail. Since the dS solution found for $A = 1$ is located right in the vicinity of the "would-be AdS SUSY extremum,[3]" where the moduli F-terms are nearly zero, it is the large contribution from the matter F-term (140) which cancels the $-3|W|^2$ term in the scalar potential resulting in a positive vacuum energy. Recall that in the leading order all the AdS vacua with the moduli vevs $s^{(c)}_{A,i}$ are located within the hyperplane[4]

$$\sum_{i=1}^{N} s^{(c)}_{A,i} N_i = \frac{1}{2\pi} \frac{PQ}{P-Q} \ln\left(\frac{A_2 P}{A_1 Q}\right) = \text{constant}. \qquad (153)$$

The matter F-term contribution to the scalar potential $K^{\phi\bar{\phi}} F_{\phi} \bar{F}_{\bar{\phi}}$ evaluated at the same $s^{(c)}_{A,i}$ but arbitrary ϕ_0 is therefore also *constant* along the hyperplane (153). Thus, while the matter F-term contribution stays constant, as we move along the hyperplane (153) away from the dS minimum, where the moduli F-terms are the smallest, the moduli F-term contributions can only get larger so that the scalar potential becomes even more positive. This implies that the AdS minima with broken SUSY found in Sec. V completely disappear, as the AdS SUSY extremum becomes a dS minimum.

VII. RELEVANT SCALES

We have demonstrated above that in fluxless M theory vacua, strong gauge dynamics can generate a potential which stabilizes all the moduli. Since the entire potential is generated by this dynamics, and the strong coupling scale is below the Planck scale, we also have a hierarchy of scales. In this section we calculate some of the basic scales in detail. In particular, the gravitino mass, which typically controls the scale of supersymmetry breaking, is calculated. By uniformly scanning over the constants (N, P, Q, A_k) with N_i order 1, we demonstrate in Sec. VII C that a reasonable fraction of choices of constants have a TeV scale gravitino mass. We do not know if the space of G_2 manifolds uniformly scans the (P, Q, A_k, N_i) or not, and more importantly, the scale of variation of the A_k's in the space of manifolds is not clear. The variation of the A_k's is the most important issue here, since one can certainly vary P and Q over an order of magnitude. We begin with a discussion of the basic scales in the problem. We will begin with the AdS vacua, then go on to discuss the de Sitter case. In particular, in the dS case, requiring a small vacuum energy seems to lead to superpartners at around the TeV scale. It will also be shown that including more than one flavor of quarks in the hidden

[3]This can be seen by comparing the leading order expression for the moduli vevs in the dS case (132) with the corresponding formula for the SUSY AdS extremum (31).

[4]$c = 1, 2$ labels the two real solutions of the system (72).

sector or including matter in both hidden sectors does not change this result. The section will end with an estimation of the height of the potential barrier in these vacua.

A. Scales: AdS vacua

As an example, we consider one of the non-SUSY minima in our toy model given by (70) and compute some of the quantities relevant for phenomenology. Namely, the vacuum energy

$$\Lambda_0 = -(5.1 \times 10^{10}\ \text{GeV})^4, \tag{154}$$

the gravitino mass

$$M_{3/2} = m_p e^{K/2}|W| \approx 2.081\ \text{TeV}, \tag{155}$$

the 11-dimensional Planck scale

$$M_{11} = \frac{\sqrt{\pi} m_p}{V_X^{1/2}} \approx 3.9 \times 10^{17}\ \text{GeV}, \tag{156}$$

and the scale of gaugino condensation in the hidden sectors

$$\Lambda_g^{(1)} = m_p e^{-(b_1/3)\Sigma_i N_i s^i} \approx 2.6 \times 10^{15}\ \text{GeV}, \tag{157}$$

$$\Lambda_g^{(2)} \approx 9.7 \times 10^{14}\ \text{GeV}, \tag{158}$$

where $m_p = (8\pi G_N)^{-1/2} = 2.43 \times 10^{18}$ GeV is the reduced four-dimensional Planck mass.

From (155) and (156), we see that it is possible to have a TeV scale gravitino mass together with $M_{11} \geq M_{\text{unif}}(2 \times 10^{16}\ \text{GeV})$. This feature survives in more general cases as well, *implying that standard gauge unification is compatible with low scale SUSY in these vacua*.

B. Gravitino mass

By definition, the gravitino mass is given by

$$m_{3/2} = m_p e^{K/2}|W|. \tag{159}$$

For the particular M theory vacua with Kähler potential given by (1) and the nonperturbative superpotential as in (5) with $SU(P)$ and $SU(Q)$ hidden sector gauge groups, we have

$$m_{3/2} = \frac{m_p}{8\sqrt{\pi} V_X^{3/2}} |A_1 e^{-(2\pi/P)\text{Im}f} - A_2 e^{-(2\pi/Q)\text{Im}f}|, \tag{160}$$

where the relative minus sign inside the superpotential is due to the axions. Before we get to the gravitino mass we first compute the volume of the compactified manifold V_X for the AdS vacua with broken SUSY. By plugging the approximate leading order solution for the moduli (85) into the definition (2) of V_X, we obtain

$$(V_X)_A^{(c)} = \left[\frac{1}{2\pi} \frac{PQ}{P-Q} \ln\left(\frac{A_2 P}{A_1 Q}\right)\right]^{7/3} \prod_{i=1}^{N} \left(\frac{a_i L_{A,i}^{(c)}}{N_i B_A^{(c)}}\right)^{a_i}. \tag{161}$$

Recalling the definition (75) of $\mathcal{T}_A^{(c)}$ and using (84) together with (161) to plug into (160), the gravitino mass for these vacua in the leading order approximation is given by

$$(m_{3/2})_A^{(c)} = \sqrt{2}\pi^3 A_2 P \left|\frac{P-Q}{PQ}\right| \left[\frac{PQ}{P-Q} \ln\left(\frac{A_2 P}{A_1 Q}\right)\right]^{-(7/2)} \times \left[\frac{A_2 P}{A_1 Q}\right]^{-(P/(P-Q))} \prod_{i=1}^{N} \left(\frac{N_i B_A^{(c)}}{a_i L_{A,i}^{(c)}}\right)^{3a_i/2}. \tag{162}$$

For the special case with two moduli when $a_1 = a_2 = 7/6$, considered in the previous sections, we obtain the following:

$$\begin{aligned}(m_{3/2})_0^{(1,2)} &= m_p 2^{1/2} \pi^3 (7+\sqrt{17})^{7/4} \\ &\quad \times (N_1 N_2)^{7/4} A_2 P \left|\frac{P-Q}{PQ}\right| \left(\frac{A_2 P}{A_1 Q}\right)^{-(P/(P-Q))} \\ &\quad \times \left(\frac{PQ}{P-Q} \ln\frac{A_2 P}{A_1 Q}\right)^{-(7/2)} \\ &\sim m_p 2.97 \times 10^3 (N_1 N_2)^{7/4} A_2 P \left|\frac{P-Q}{PQ}\right| \\ &\quad \times \left(\frac{A_2 P}{A_1 Q}\right)^{-(P/(P-Q))} \left(\frac{PQ}{P-Q} \ln\frac{A_2 P}{A_1 Q}\right)^{-(7/2)}.\end{aligned} \tag{163}$$

For the choice of constants as in (67) the leading order approximation (163) yields

$$(m_{3/2})_0^{(1,2)} = 2061\ \text{GeV}, \tag{164}$$

whereas the exact value computed numerically for the same choice of constants is

$$m_{3/2} = 2081\ \text{GeV}. \tag{165}$$

Again, we see a good agreement between the leading order approximation and the exact values.

C. Scanning the gravitino mass

In previous sections we found explicit solutions describing vacua with spontaneously broken supersymmetry. Moreover, we also demonstrated that for a particular set of the constants these solutions can result in $m_{3/2} \sim O(1)$ TeV. It would be extremely interesting and worthwhile to estimate (even roughly) the fraction of all possible solutions which exhibit spontaneously broken SUSY at the scales of $O(1)$–$O(10)$ TeV. We would first like to do this for generic AdS/dS vacua with a large magnitude of the cosmological constant ($\sim m_{3/2}^2 m_p^2$). The analysis for the AdS vacua is given below but, as we will see, the results obtained for the fraction of vacua are quite similar for the dS case as well. In Sec. VII D, we impose the requirement of a small cosmological constant as a constraint and try to understand its repercussions for the gravitino mass.

We do not yet know the range that the constants (N, P, Q, A_1, A_2) take in the space of all G_2 manifolds. Nevertheless, we do have a rough idea about some of

them. For example, we expect that the quantity given by the ratio

$$\rho \equiv \frac{A_2 P}{A_1 Q}, \tag{166}$$

which appears in several equations, does deviate from unity. One reason for this may be due to the threshold corrections [19] which in turn depend on the properties of a particular G_2-holonomy manifold. For concreteness, we take an upper bound $\rho \leq 10$. Also, based on the duality with the heterotic string we can get some idea on the possible range of integers P and Q corresponding to the dual Coxeter numbers of the hidden sector gauge groups. Namely, since for both $SO(32)$ and E_8 gauge groups appearing in the heterotic string theories the dual Coxeter numbers are $h^v = 30$, we can tentatively assume that both P and Q can be at least as large as 30. Of course, we do not rule out any values higher than 30, but in this section we will assume an upper bound $P, Q \leq 30$.

We now turn our attention to Eq. (162) which will be used to estimate the gravitino mass scale. It is clear from the structure of the formula that $m_{3/2}$ is extremely sensitive to P, Q as well as the ratio ρ, given by (166). On the other hand, it is less sensitive to the other constants appearing in the equation such as N_i, a_i and the ratios $B_A^{(c)}/L_{A,i}^{(c)}$. This is because for each term under the product, the exponents $3a_i/2$ become much less than 1 as the number of moduli increases due to the constraint on a_i in (2). This will smooth any differences between the contributions coming from the individual factors inside the product. Since for $0 \leq A \leq 1$ [A is defined in (44)], the ratios $B_A^{(c)}/L_{A,i}^{(c)}$ vary only in the range $O(1)$–$O(10)$, for our purposes it will be sufficient to simply consider (162) for the case when $A = 1$ corresponding to the SUSY extremum so that $B_1^{(1)}/L_{1,i}^{(1)} = 7/3$ for all i. This is certainly good enough for the order of magnitude estimates we are interested in. It also seems reasonable to assume that the integers N_i are all of $O(1)$. Yet, even if some N_i are unnaturally large, their individual contributions are generically washed out since they are raised to the powers that are much less than 1. Thus, for simplicity we will take $N_i = 1$ for all $i = \overline{1, N}$. Finally, from field theory computations [25], $A_2 = Q$ (in a particular RG scheme) up to threshold corrections. We therefore take $A_2 \sim Q$ for simplicity, allowing A_1 to vary.

Thus, the gravitino mass in our analysis is given by

$$m_{3/2} \sim \sqrt{2}\pi^3 PQ\left(\frac{P-Q}{PQ}\right)^{9/2}[\ln\rho]^{-(7/2)}(\rho)^{-(P/(P-Q))} \times \prod_{i=1}^{N}\left(\frac{7}{3a_i}\right)^{3a_i/2}. \tag{167}$$

Finally, with regard to the constants a_i which are constrained by

$$\sum_{i=1}^{N} a_i = \frac{7}{3}, \tag{168}$$

we will narrow our analysis to two opposite cases. For the first case we make the following choice:

$$1)\ a_1 = 2 \quad \text{and} \quad a_i = \frac{1}{3(N-1)} \quad \text{for } i = \overline{2, N}, \tag{169}$$

such that one modulus is generically large and all the other moduli are much smaller. This is a highly anisotropic G_2 manifold. The second case is

$$2)\ a_i = \frac{7}{3N}, \quad \text{for all } i = \overline{1, N}, \tag{170}$$

with all the moduli being on an equal footing. Therefore, by considering these opposite cases we expect that most other possible sets of a_i will give similar results that are somewhere in between. For each set of a_i above, Eq. (167) gives

$$1)\ m_{3/2}^{(1)} \sim \frac{343\sqrt{14}\pi^3}{216} PQ\left(\frac{P-Q}{PQ}\right)^{9/2} \times [\ln\rho]^{-(7/2)}(\rho)^{-(P/(P-Q))}(N-1)^{1/2}, \tag{171}$$

$$2)\ m_{3/2}^{(2)} \sim \sqrt{2}\pi^3 PQ\left(\frac{P-Q}{PQ}\right)^{9/2} \times [\ln\rho]^{-(7/2)}(\rho)^{-(P/(P-Q))}(N)^{7/2}. \tag{172}$$

For a typical compactification we expect $N \sim O(100)$; therefore the variation of $m_{3/2}$ due to an $O(1)$ change in the number of moduli for the first case is $O(1)$, whereas in the second case it can be as large as $O(10)$. Thus, if we choose $N = 100$, we expect that our order of magnitude analysis will be fairly robust for case 1). For case 2), however, we will perform the same analysis for $N = 100$ and $N = 50$ to see how different the results will be. Before we proceed further we need to impose a restriction on the possible solutions to remain within the SUGRA framework. Using (161), the condition that V_X must remain greater than 1 for the two cases under consideration translates into the following two conditions:

$$1)\ \frac{3}{7}\left(\frac{64}{3(N-1)}\right)^{1/7}\frac{1}{2\pi}\frac{PQ}{P-Q}\ln\rho > 1, \tag{173}$$

$$2)\ \frac{1}{2\pi N}\frac{PQ}{P-Q}\ln\rho > 1. \tag{174}$$

Then, as long as conditions (173) and (174) hold, the volume of the associative cycle $\mathcal{T}$ being greater than 1 is satisfied automatically—a necessary condition for the validity of supergravity. This is obvious from comparing the right-hand side (R.H.S.) of (84) with each condition above. From (173) and (174) we can find a critical value of $\rho = \rho_{\text{crit}}$ for both cases at which $V_X = 1$:

$$1)\ \rho_{\rm crit}^{(1)} \equiv \exp\left[\frac{14\pi}{3}\left(\frac{3(N-1)}{64}\right)^{1/7}\frac{P-Q}{PQ}\right], \quad (175)$$

$$2)\ \rho_{\rm crit}^{(2)} \equiv \exp\left[2\pi N\left(\frac{P-Q}{PQ}\right)\right]. \quad (176)$$

By substituting (175) and (176) into (171) and (172) we can find the corresponding upper limits on $m_{3/2}$ as functions of P and Q, below which our solutions are going to be consistent with the SUGRA approximation.

In Fig. 11 we present plots of $\log_{10}(m_{3/2})$ for both cases as a function of P in the range where $\rho_{\rm crit} \le \rho \le 10$ for different values of $P - Q$.

On all the plots the light gray area represents possible values of $\log_{10}(m_{3/2})$ consistent with the supergravity framework. For the sake of completeness we have also included the formal plot of $\log_{10}(m_{3/2})$ corresponding to $\rho = 1.01$ represented by the dashed curve. From the plots it is clear that as the difference $P - Q$ is increased from 1 to 3 (top) and from 1 to 2 (bottom), both the light gray area representing all possible values of $\log_{10}(m_{3/2})$ consistent with the SUGRA approximation and the dark area corresponding to $-16 \le \log_{10}(m_{3/2}) \le -14$ get significantly smaller. If we further increase $P - Q$, the light gray region shrinks even more for case 1) and does not exist for case 2), while the dark region completely disappears in both cases. Therefore, for case 2) the plots on the bottom of Fig. 11 are the only possibilities where solutions for $P \le 30$ and $N = 100$ consistent with the SUGRA approximation are possible, implying an upper bound $(P - Q)_{\rm max} = 2$. It turns out that for case 1) the upper bound on $(P - Q)$ where such solutions are possible is much higher, $(P - Q)_{\rm max} = 23$.

Assuming that all values of the constants such as P, Q, and ρ are equally likely to occur in the ranges chosen above, we can perform a crude estimate of the number of solutions with $-16 \le \log_{10}(m_{3/2}) \le -14$ relative to the total number of possible solutions consistent with the SUGRA approximation. In doing so we will use the following approach. For each value of $(P - Q)$ in the range $1 \le (P - Q) \le (P - Q)_{\rm max}$ we compute the area of the gray region for each plot and then add all of them to find the total volume corresponding to all possible values of $\log_{10}(m_{3/2})$ consistent with the supergravity approximation.

$$\Omega_{\rm tot} = \sum_{(P-Q)=1}^{(P-Q)_{\rm max}} \int_{P_{\rm min}}^{30} dP \log_{10}(m_{3/2})_{|_{\{\rho_{\rm crit} \le \rho \le 10\}}}. \quad (177)$$

Likewise, we add all the dark areas for each plot to find the volume corresponding to the region where $-16 \le \log_{10}(m_{3/2}) \le -14$,

$$\Omega_0 = \sum_{(P-Q)=1}^{(P-Q)^*_{\rm max}} \int dP \log_{10}(m_{3/2})_{|_{\{-16 \le \log_{10}(m_{3/2}) \le -14\}}^{\rho_{\rm crit} \le \rho \le 10}}, \quad (178)$$

where $(P - Q)^*_{\rm max}$ is an upper bound before the dark region completely disappears. From the previous discussion we have the following: for case 1), $(P - Q)^*_{\rm max} = 3$; for case 2), $(P - Q)^*_{\rm max} = 2$. Then, the fraction of the volume where 240 GeV $\le m_{3/2} \le$ 24 TeV is given by the ratio

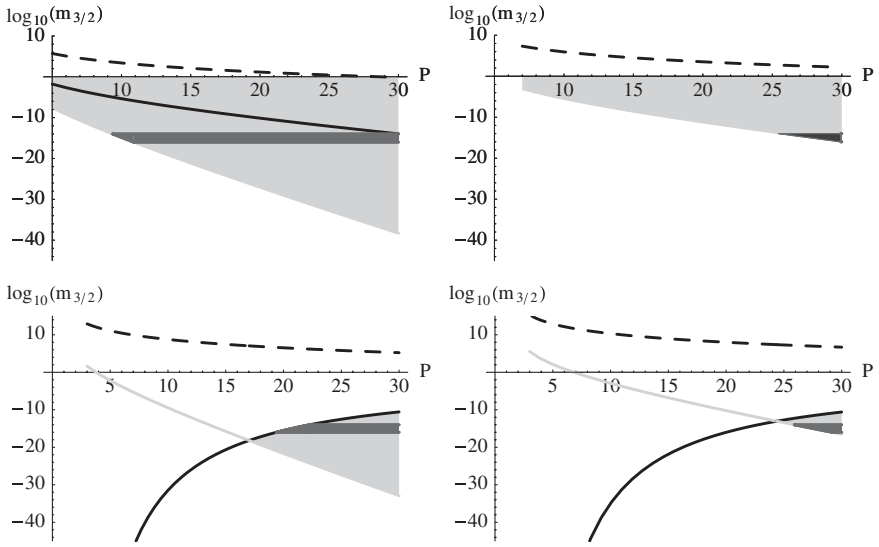

FIG. 11. $\log_{10}(m_{3/2})$ as a function of P for case 1) (top panels) and case 2) (bottom panels). The light gray area represents possible values of $\log_{10}(m_{3/2})$ in the range where $\rho_{\rm crit} \le \rho \le 10$, consistent with the SUGRA approximation. The dark area indicates the region of interest where $-16 \le \log_{10}(m_{3/2}) \le -14$ such that 240 GeV $\le m_{3/2} \le$ 24 TeV. The dark solid curve corresponds to $\log_{10}(m_{3/2})$ when $\rho = \rho_{\rm crit}$. The lower boundary of the light gray area represents the $\log_{10}(m_{3/2})$ curve when $\rho = 10$. The dashed curve corresponds to $\rho = 1.01$. Top left panel: Case 1) when $P - Q = 1$. Top right panel: Case 1) when $P - Q = 3$. Bottom left panel: Case 2) when $P - Q = 1$. Bottom right panel: Case 2) when $P - Q = 2$.

$$\Delta = \frac{\Omega_0}{\Omega_{\rm tot}}. \tag{179}$$

Numerical computations yield the following values for the two cases when $N = 100$:

$$1)\ \Delta_1 = 3.5\%, \tag{180}$$

$$2)\ \Delta_2 = 13.6\%. \tag{181}$$

Because of the significant difference in the dependence of $\rho_{\rm crit}$ on the number of moduli N in (175) versus (176), the number of solutions consistent with the SUGRA approximation is cut down dramatically in case 2) compared to case 1). This also occurs because of the different dependence of $m_{3/2}$ in (171) and (172) on N. Namely, for $N \sim O(100)$, the values of $m_{3/2}$ for case 2) in (172) are $\sim O(10^6)$ greater than those for case 1). Furthermore, for the same reasons, it turns out that if we keep increasing the number of moduli N, for case 2) there is an upper bound $N \leq 157$ for the solutions with 240 GeV $\leq m_{3/2} \leq$ 24 TeV compatible with the SUGRA approximation. Of course, this upper bound can be higher if we allow P to be greater than 30.

By performing the same analysis for $N = 50$ we get the following estimates:

$$1)\ \Delta_1 = 3.4\%, \tag{182}$$

$$2)\ \Delta_2 = 10.7\%. \tag{183}$$

As expected, decreasing the number of moduli by half has produced little effect on Δ_1 while decreasing Δ_2 by a few percent. These numbers coming from our somewhat crude analysis already demonstrate that a comparatively large fraction of vacua in M theory generate the desired hierarchy between the Planck and the electroweak scale physics. Also, one can easily check that all the solutions consistent with the SUGRA framework for which 240 GeV $\leq m_{3/2} \leq$ 24 TeV for any number of moduli N satisfy the following bound on the 11-dimensional scale:

$$3.6 \times 10^{16}\ \text{GeV} \leq m_{11} \leq 4.3 \times 10^{18}\ \text{GeV}, \tag{184}$$

which makes them compatible with the standard unification at $M_{\rm GUT} \sim 2 \times 10^{16}$ GeV. This is also a nice feature. Of course, apart from determining the upper and lower bounds on the constants, it would be desirable to know their distribution for all possible manifolds of G_2 holonomy. In this case, instead of using the flat statistical measure as we did here, each solution would be assigned a certain weight, making the sampling analysis more accurate. However, this is an extremely challenging task which goes beyond the scope of this work.

The simple analysis presented in this section clearly points to a very restrictive nature of the solutions. Namely, the requirement of consistency with the supergravity regime results in very strict bounds on the properties of the compactification manifold. A further requirement coming from the SUSY breaking scale to be in the range required for supersymmetry to solve the hierarchy problem narrows down the class of possible G_2 holonomy manifolds even more. It would be extremely interesting to know to what extent these results extend into the small volume, ''stringy'' regime, about which we have nothing to say here.

1. Results for dS vacua

We will now show that the results obtained in the previous subsection also hold true for dS vacua with Kähler potential given by (98) and the nonperturbative superpotential as in (97) with $SU(N_c)$ and $SU(Q)$ hidden sector gauge groups. For this case, we have

$$m_{3/2} = m_p \frac{e^{\phi_0^2/2}}{8\sqrt{\pi} V_X^{3/2}} |A_1 \phi_0^a e^{-(2\pi/P){\rm Im}f} - A_2 e^{-(2\pi/Q){\rm Im}f}|, \tag{185}$$

where the relative minus sign inside the superpotential is due to the axions and $P \equiv N_c - 1$. Before we get to the gravitino mass we first compute the volume of the compactified manifold V_X for the metastable dS vacuum with broken SUSY. By substituting the approximate leading order solution for the moduli (132) into the definition (2) of V_X, we obtain

$$V_X = \left(\frac{1}{2\pi}\right)^{7/3} \left[\frac{PQ}{Q-P} \ln\left(\frac{A_1 Q}{A_2 P}\right)\right]^{7/3} \prod_{i=1}^{N} \left(\frac{3a_i}{7N_i}\right)^{a_i}. \tag{186}$$

Recalling the definition of ${\rm Im}(f)$ in terms of ν and using the solution for ν [Eq. (132)] together with (186), the gravitino mass for the dS vacuum in the leading order approximation is given by

$$\begin{aligned} m_{3/2} = m_p \sqrt{2}\pi^3 A_2 & \left| \frac{P}{Q} \phi_0^{-(2/P)} - 1 \right| \\ & \times \left(\frac{PQ}{Q-P} \ln\left(\frac{A_1 Q}{A_2 P}\right)\right)^{-(7/2)} \left(\frac{A_1 Q}{A_2 P}\right)^{-(P/(Q-P))} \\ & \times \prod_{i=1}^{N} \left(\frac{7N_i}{3a_i}\right)^{3a_i/2} e^{\phi_0^2/2}, \end{aligned} \tag{187}$$

where ϕ_0^2 is given by (134). Since $\phi_0^{-2/P} \sim 1$ from Sec. VI and $A_2 \sim Q$, we see that the expression for the gravitino mass for dS vacua is almost the same as that for the AdS vacua [Eq. (167)], provided we replace ρ in (167) by $\tilde{\rho} = A_1 Q / A_2 P$ in (187) and $P - Q$ in (167) by $Q - P$ in (187).

For the de Sitter vacua, we use a less restrictive upper bound $\tilde{\rho} \equiv \frac{A_1 Q}{A_2 P} \leq 100$. For a manifold with $N = 100$ moduli we obtain

$$1)\ \Delta_1 = 3\%, \tag{188}$$

$$2)\ \Delta_2 = 31\%. \tag{189}$$

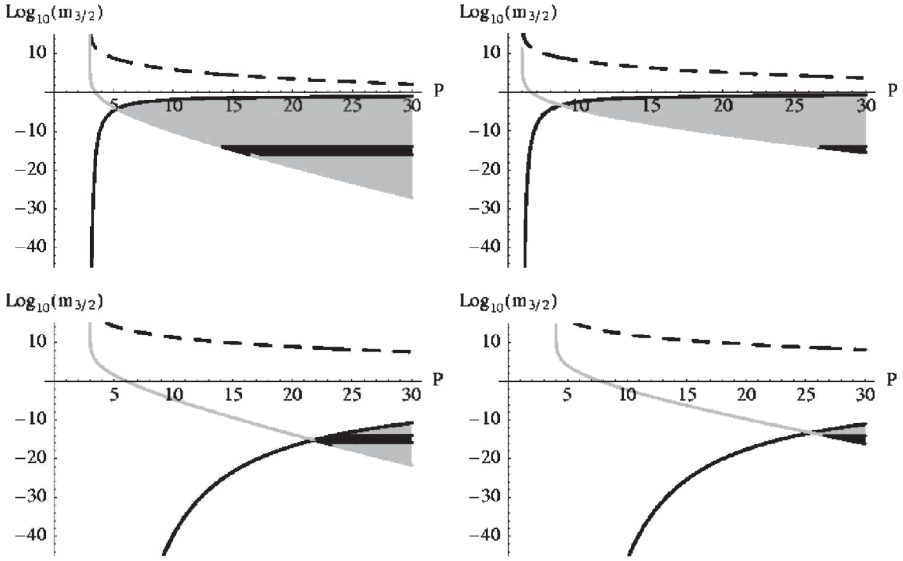

FIG. 12. $\log_{10}(m_{3/2})$ as a function of P for case 1) (top panels) and case 2) (bottom panels). The light gray area represents possible values of $\log_{10}(m_{3/2})$ in the range where $\tilde{\rho}_{\text{crit}} \leq \tilde{\rho} \leq 100$, consistent with the SUGRA approximation. The dark area indicates the region of interest where $-16 \leq \log_{10}(m_{3/2}) \leq -14$ such that 240 GeV $\leq m_{3/2} \leq 24$ TeV. The dark solid curve corresponds to $\log_{10}(m_{3/2})$ when $\tilde{\rho} = \tilde{\rho}_{\text{crit}}$. The lower boundary of the light gray area represents the $\log_{10}(m_{3/2})$ curve when $\tilde{\rho} = 100$. The dashed curve corresponds to $\tilde{\rho} = 1.01$. Top left panel: Case 1) when $Q - P = 3$. Top right panel: Case 1) when $Q - P = 6$. Bottom left panel: Case 2) when $Q - P = 3$. Bottom right panel: Case 2) when $Q - P = 4$.

In Fig. 12 we present plots of $\log_{10}(m_{3/2})$ for both cases as a function of P in the range where $\tilde{\rho}_{\text{crit}} \leq \tilde{\rho} \leq 100$ for different values of $Q - P$.

Recall that the smallest possible value of $Q - P$ for de Sitter vacua is $(Q - P)_{\text{min}} = 3$. In this case the region where 240 GeV $\leq m_{3/2} \leq 24$ TeV exists for $3 \leq Q - P \leq 6$ for the anisotropic case in (188), and for $3 \leq Q - P \leq 4$ for the "democratic" case in (189).

D. Small cosmological constant implies low scale supersymmetry in dS vacua

In this subsection we will study the distribution of SUSY breaking scales in the de Sitter vacua which, as we showed earlier, can arise when the hidden sector has chiral matter. In particular, we will see that the requirement of a small cosmological constant leads to a scale of SUSY breaking of $\mathcal{O}(1\text{–}100)$ TeV.

In Sec. VI, we saw that the minimum obtained is de Sitter if the discriminant of the quadratic polynomial with respect to ϕ_0^2 in Eq. (141) is negative, while it is anti-de Sitter if the discriminant in (141) is positive. For $m_{3/2} \sim \mathcal{O}(1\text{–}10$ TeV) the magnitude of the vacuum energy in both cases can be estimated to be

$$|V_0| \sim m_p^2 m_{3/2}^2 \sim (10^{10}\ \text{GeV})^4\text{–}(10^{11}\ \text{GeV})^4. \qquad (190)$$

On the other hand, if the discriminant in (141) vanishes, one obtains a vanishing cosmological constant (to leading order in the approximation). At present it is not known if there is a physical principle which imposes this condition. However, one can still use it as an observational constraint since the observed value of the cosmological constant is known to be extremely small. For instance, it could happen that the space of G_2 manifolds scans the constants (A_i, P, Q, N) finely enough such that there exist vacua for which the vacuum energy is acceptably low. In particular, the constants A_i, $i = 1, 2$ which are determined by the threshold corrections have been shown to depend on integers[5] [19]. In this work, we will assume that to be the case. A detailed computation to show this in a convincing manner is currently being attempted and will be reported in the future. It should also be kept in mind that a different mechanism for solving the cosmological constant, completely decoupled with particle physics, could exist. Such a mechanism, if present, would not affect any predictions for low energy particle physics.

By setting the left-hand side in (144) to zero, we can then express

$$P \ln\left(\frac{A_1 Q}{A_2 P}\right) = \frac{28(Q - P)}{3(Q - P) - 8}. \qquad (191)$$

Of course, since the above constraint was obtained in the leading order, the vacuum energy is only zero in the leading order in our analytic expansion. The subleading contributions we neglected in (225), although smaller than the leading contributions, are still much larger than the observed value of the cosmological constant. However, one

[5]This is because the threshold corrections can be related to certain topological invariants of the associative three-cycle.

can *in principle* take into account all the subleading corrections and tune the ratio A_1Q/A_2P inside the logarithm to set the vacuum energy to a very small value compatible with the observations. As will be seen later, since the expression in the R.H.S. of (191) turns out to be large, the subleading corrections which affect the value of the cosmological constant will have little effect on the phenomenological quantities calculated by imposing the constraint to leading order.

We would now like to analyze in detail the phenomenological implications of the solutions obtained by imposing (191) as a constraint. The most important phenomenological quantity in this regard is the gravitino mass, as it sets the scale of all soft supersymmetry breaking parameters. We focus on the gravitino mass in this section. The soft supersymmetry breaking parameters will be discussed in Sec. VIII.

1. Gravitino mass with a small positive cosmological constant

By substituting the constraint (191) into the gravitino mass formula (187), we obtain

$$m_{3/2} = m_p\sqrt{2}\pi^3 A_2 \left|\frac{P}{Q}\phi_0^{-(2/P)} - 1\right| \left(\frac{28Q}{3(Q-P)-8}\right)^{-(7/2)} \times e^{-\{28/[3(Q-P)-8]\}} \prod_{i=1}^{N}\left(\frac{7N_i}{3a_i}\right)^{3a_i/2} e^{\phi_0^2/2}, \tag{192}$$

where the meson vev is now given by

$$\phi_0^2 \approx -\frac{1}{8} + \frac{1}{Q-P} + \frac{1}{4}\sqrt{1-\frac{2}{Q-P}} + \frac{2}{Q-P}\sqrt{1-\frac{2}{Q-P}}. \tag{193}$$

In this case, the moduli vevs are given by

$$s_i = \frac{a_i\nu}{N_i}, \quad \text{with} \quad \nu \approx \frac{6Q}{\pi(3(Q-P)-8)}. \tag{194}$$

From (192), one notes that the gravitino mass (when the cosmological constant is made tiny) is completely determined by the dual Coxeter numbers of the hidden sector gauge groups N_c and Q, the rational numbers a_i [see (2)] characterizing the volume of the G_2 manifold and the integers N_i.[6]

The rationals a_i are subject to the constraint $\sum_{i=1}^{N} a_i = 7/3$. It is reasonable to consider a democratic choice for a_i, $a_i = 7/(3N)$ for all $i = \overline{1, N}$ and also to take for simplicity all the integers $N_i = 1$. The integers N_i will generically be of $\mathcal{O}(1)$; even if some of the N_i are unnaturally large, their individual contributions will be typically washed out, as they are raised to powers that are much less than unity [see (187) and the expression for a_i for the democratic choice]. In this case, after setting $A_2 = QC_2$, the gravitino mass formula is given by

$$m_{3/2} = m_p\sqrt{2}\pi^3 C_2 |P\phi_0^{-(2/P)} - Q| \left(\frac{N(3(Q-P)-8)}{28Q}\right)^{7/2} e^{-\{28/[3(Q-P)-8]\}} e^{\phi_0^2/2}, \tag{195}$$

and the moduli vevs are

$$s_i = \frac{14Q}{\pi N(3(Q-P)-8)}. \tag{196}$$

From (195), the gravitino mass depends on just four constants—C_2, P, Q, and N (the total number of moduli), determined by the topology of the manifold. It should be kept in mind that, for the solution to exist, it is necessary that $Q - P > 2$ [see (135)]. For the smallest possible value $(Q-P)_{\min} = 3$, the expression for $m_{3/2}$ simplifies even further,

$$m_{3/2} = m_p\sqrt{2}\pi^3 C_2 |P(\phi_0^{-(2/P)} - 1) - 3| \times \left(\frac{N}{28(P+3)}\right)^{7/2} e^{-28} e^{\phi_0^2/2} \approx m_p 3\sqrt{2}\pi^3 C_2 \left(\frac{N}{28(P+3)}\right)^{7/2} e^{-28} e^{\phi_0^2/2}, \tag{197}$$

together with

$$\phi_0^2 \approx \frac{1}{72}(15 + 22\sqrt{3}) \approx 0.7376, \qquad s_i = \frac{14(P+3)}{\pi N}.$$

Note that the dependence on N and P in (197) is due solely to the volume V_X dependence on those parameters. The expression for the gravitino mass has a more transparent form if we do not substitute the expression for the volume (186) into (185). For $Q - P = 3$ we obtain

$$m_{3/2} \approx m_p \frac{3e^{\phi_0^2/2}}{8\sqrt{\pi}V_X^{3/2}} e^{-28} C_2 \approx 514 \text{ TeV} \frac{C_2}{V_X^{3/2}}, \tag{198}$$

where the detailed dependence on a_i, N_i, P, and the number of moduli N is completely encoded inside the seven-dimensional volume V_X which appears to be the more relevant physical quantity. Furthermore, in the supergravity approximation the volume $V_X > 1$, which translates into an upper bound on the gravitino mass when $Q - P = 3$,

$$m_{3/2} < \mathcal{O}(100 \text{ TeV}). \tag{199}$$

[6] From field theory computations [25], $A_1 = N_c - N_f = P$ and $A_2 = Q$ (in a particular RG scheme), up to threshold corrections. We can therefore express A_1, A_2 as $A_1 = PC_1$ and $A_2 = QC_2$, where coefficients C_1 and C_2 depend *only* on the threshold corrections and are constant with respect to the moduli [19]. In this case, the quantity $\ln(A_1Q/A_2P) = \ln(C_1/C_2)$ is fixed by imposing (191).

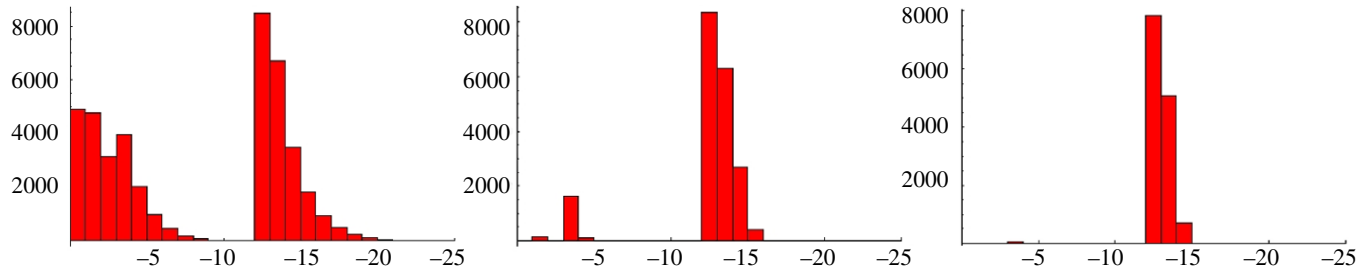

FIG. 13 (color online). The gravitino mass distribution with the x axis denoting the logarithm of the gravitino mass (to base 10). Left panel: Distribution corresponding to scan 1 in (200). Middle panel: Distribution corresponding to scan 2 in (201), for which manifolds with the number of moduli $N < 50$ were excluded from the scan. Right panel: Distribution corresponding to scan 3 in (202), for which manifolds with the number of moduli $N < 100$ were excluded from the scan.

2. The gravitino mass distribution and its consequences

The gravitino mass (195) depends on three integers: the two gauge group dual Coxeter numbers N_c, Q and the number of moduli N.[7] This will give us an idea about the distribution of the gravitino mass (which sets the superpartner masses) obtained after imposing the constraint (191) that the vacuum energy is acceptable. Aside from only considering the vacua within the supergravity approximation (i.e. $s_i > 1$), we expect an upper bound on the dual Coxeter numbers of the hidden sector gauge groups P and Q. Based on duality with the heterotic string, it seems reasonable to assume that they can be at least as large as 30—the dual Coxeter number of E_8. Of course, values of P, Q larger than 30 cannot be ruled out, and here we assume an upper bound $P \leq 100$. Notice that from the constraint in (191), the ratio $(A_1 Q)/(A_2 P)$ can get exponentially large when $Q - P = 3$ and the values of P are small. Here we are going to completely relax the requirement on the upper bound of the ratio because, as we will see, for generic manifolds with a large number of moduli, P has to be large for the supergravity approximation to hold. The distribution can be constructed as follows. The three integers, P, $Q - P$, and N, are varied subject to (135) and the supergravity constraint $s_i > 1$. For each point in the resulting two-dimensional subspace, $\log_{10}(m_{3/2})$ can be computed and rounded off to the closest integer value. One can then count how many times each integer value is encountered in the entire scan and plot the corresponding distribution.

In the first three scans we cover a broad range of values by choosing $P_{\max} = 100$. Taking into account the SUGRA constraint ($s_i > 1$), we have the following ranges of integers for the first scan:

$$3 \leq P \leq 100; \qquad 3 \leq (Q - P) \leq 100 - P; \qquad 2 \leq N < \frac{14(P + (Q - P))}{\pi(3(Q - P) - 8)}. \tag{200}$$

[7]We can set $C_2 = 1$ for the order of magnitude estimates we are doing here.

In the second scan we have excluded the small N region and considered only the manifolds with $N \geq 50$. Thus we have the following ranges of constants for the second scan:

$$3 \leq P \leq 100; \qquad 3 \leq (Q - P) \leq 100 - P; \qquad 50 \leq N < \frac{14(P + (Q - P))}{\pi(3(Q - P) - 8)}. \tag{201}$$

In the third scan we have only considered manifolds with $N \geq 100$. Thus we have the following ranges of integers for the second scan:

$$3 \leq P \leq 100; \qquad 3 \leq (Q - P) \leq 100 - P; \qquad 100 \leq N < \frac{14(P + (Q - P))}{\pi(3(Q - P) - 8)}. \tag{202}$$

The first two distributions in Fig. 13 clearly have several prominent peaks. Amazingly, in all three plots one of the peaks landed right in the $m_{3/2} \sim \mathcal{O}(1\text{–}100)$ TeV range. The high scale peaks on the left plot appear to be around $m_{3/2} \sim 10^{14}$ GeV and the grand unified theory (GUT) scales. However, for the middle plot the GUT scale peak almost disappears. Recall that the middle plot corresponds to scan 2 in (201) where we excluded all the manifolds for which the number of moduli N is less than 50. Therefore, the high scale peaks are largely dominated by contributions from the G_2 manifolds with a small number of moduli $N < 50$. As seen from the right plot, when G_2 manifolds with $N < 100$ are excluded from the scan, the peak at the $m_{3/2} \sim 10^{14}$ GeV scale has all but disappeared, whereas the peak at $m_{3/2} \sim \mathcal{O}(1\text{–}100)$ TeV remains virtually unchanged.

In Fig. 14 we included three more scans for which the upper bound on P was reduced to $P_{\max} = 30$. The fourth scan has the following ranges:

$$3 \leq P \leq 30; \qquad 3 \leq (Q - P) \leq 30 - P; \qquad 2 \leq N < \frac{14(P + (Q - P))}{\pi(3(Q - P) - 8)}. \tag{203}$$

In the fifth scan we again excluded the small N region and

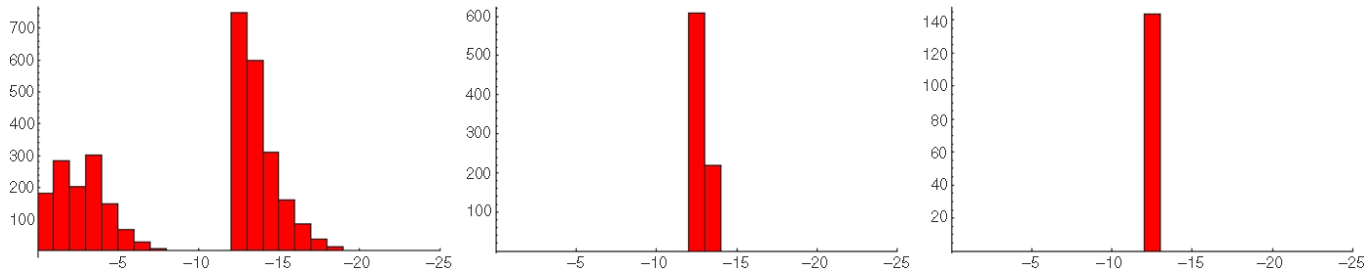

FIG. 14 (color online). The gravitino mass distribution with the x axis denoting the logarithm of the gravitino mass (to base 10). Left panel: Distribution corresponding to scan 4 in (203). Middle panel: Distribution corresponding to scan 5 in (204), for which manifolds with the number of moduli $N < 50$ were excluded from the scan. Right panel: Distribution corresponding to scan 6 in (205), for which manifolds with the number of moduli $N < 100$ were excluded from the scan.

considered only the manifolds with $N \geq 50$ and $P_{\max} = 30$:

$$3 \leq P \leq 30; \qquad 3 \leq (Q-P) \leq 30-P;$$
$$50 \leq N < \frac{14(P+(Q-P))}{\pi(3(Q-P)-8)}. \tag{204}$$

In the sixth scan we considered only the manifolds with $N \geq 100$ and $P_{\max} = 30$:

$$3 \leq P \leq 30; \qquad 3 \leq (Q-P) \leq 30-P;$$
$$100 \leq N < \frac{14(P+(Q-P))}{\pi(3(Q-P)-8)}. \tag{205}$$

Again, in Fig. 14 we notice that the $\mathcal{O}$(1–100) TeV peak narrows around $m_{3/2} \sim \mathcal{O}(100)$ TeV, as we exclude manifolds with a small number of moduli. At the same time, the peaks at the high scale completely disappear for G_2 manifolds with $N > 50$. Finally, in Fig. 15 we chose the smallest possible value $Q - P = 3$ and scanned integers P and N in the following ranges:

$$3 \leq P \leq 200; \qquad 50 \leq N < \frac{14(P+3)}{\pi},$$
$$3 \leq P \leq 100; \qquad 50 \leq N < \frac{14(P+3)}{\pi}, \tag{206}$$
$$3 \leq P \leq 30; \qquad 50 \leq N < \frac{14(P+3)}{\pi}.$$

In all three plots in Fig. 15 we see the same peak at $m_{3/2} \sim \mathcal{O}$(1–100) TeV, which narrows around $m_{3/2} \sim \mathcal{O}(100)$ TeV as $P_{\max}$ is decreased.

Therefore, from the above distributions we conclude that the peak corresponding to $m_{3/2} \sim$ (1–100) TeV is entirely due to the smallest possible value $(Q-P)_{\min} = 3$. This can be explained if we examine the gravitino mass formula in (197). In particular, the constant factor $e^{-28} \sim 10^{-12}$ is most crucial in lowering the gravitino mass to the TeV scale. It is easy to trace the origin of this factor to the constraint (191), imposed by the requirement to have a zero cosmological constant (to leading order). When (191) is used along with the requirement $Q - P = 3$ we simply get

$$P \ln\left(\frac{A_1 Q}{A_2 P}\right) = 84. \tag{207}$$

When this is substituted into the gravitino mass (187), the corresponding suppression factor turns into the constant

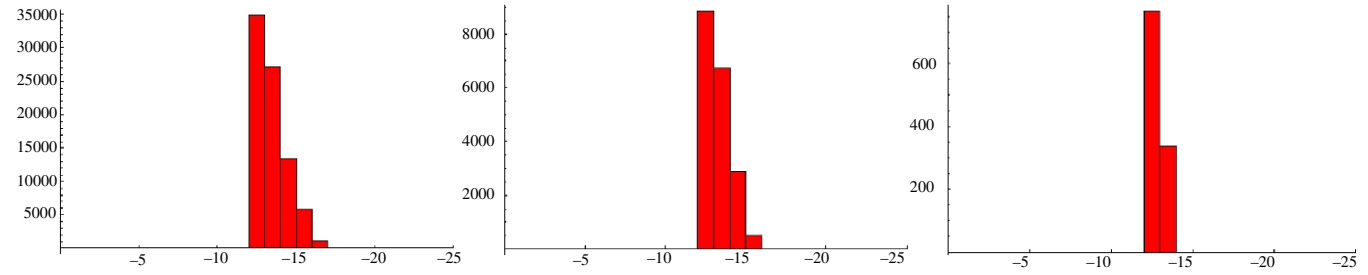

FIG. 15 (color online). The gravitino mass distribution with the x axis denoting the logarithm of the gravitino mass (to base 10). Scans for the smallest possible choice $(Q-P)_{\min} = 3$. Left panel: Distribution corresponding to the scan with $P_{\max} = 200$. Middle panel: Distribution corresponding to the scan with $P_{\max} = 100$. Right panel: Distribution corresponding to the scan with $P_{\max} = 30$.

$$\left(\frac{A_1 Q}{A_2 P}\right)^{-(P/(Q-P))} = e^{-28}. \tag{208}$$

Physically, this suppression factor corresponds to the hidden sector gaugino condensation scale (cubed). Recall that, for an $SU(Q)$ hidden sector gauge group, the scale of gaugino condensation is given by

$$\Lambda_g = m_p e^{-(8\pi^2/3Qg^2)} = m_p e^{-(2\pi/3Q)\mathrm{Im}f}. \tag{209}$$

The moduli vevs in (194) completely determine the gauge kinetic function. Taking $Q - P = 3$ we obtain

$$\mathrm{Im}\, f = \sum_{i=1}^{N} N_i s_i = \frac{14Q}{\pi}. \tag{210}$$

Substituting (210) into (209) we obtain the following scale of gaugino condensation:

$$\Lambda_g = m_p e^{-28/3} \approx 2.15 \times 10^{14}\ \mathrm{GeV}. \tag{211}$$

It is important to note that the expression in the R.H.S. of (191) is quite large ($= 84$, when $Q - P = 3$) in the leading order, and the quantity $(A_1 Q/A_2 P)$ which is fixed by imposing the vacuum energy constraint is inside a logarithm. Therefore, even when one incorporates all the higher order corrections and tunes the ratio $A_1 Q/A_2 P$ inside the logarithm to set the cosmological constant equal to the observed value, the constant on the R.H.S. ($= 84$), crucial in obtaining the $\mathcal{O}(100)$ TeV scale peak, is hardly affected.

The dominance of the $\mathcal{O}(1$–$100)$ TeV range also becomes clear from Fig. 16, where $\log_{10}(m_{3/2})$ as a function of P for $Q - P = 3$ is plotted for a manifold with $N = 50$ moduli (short-dashed curve) and a manifold with $N = 500$ moduli (long-dashed curve).

Indeed, even when we do not impose the SUGRA constraint, from the above plot we can see that the $\mathcal{O}(1$–$100)$ TeV range is covered by a large swath on the graph and it is not so surprising that the corresponding distribution peaks at that scale. This essentially follows from the formula for the gravitino mass in (197).

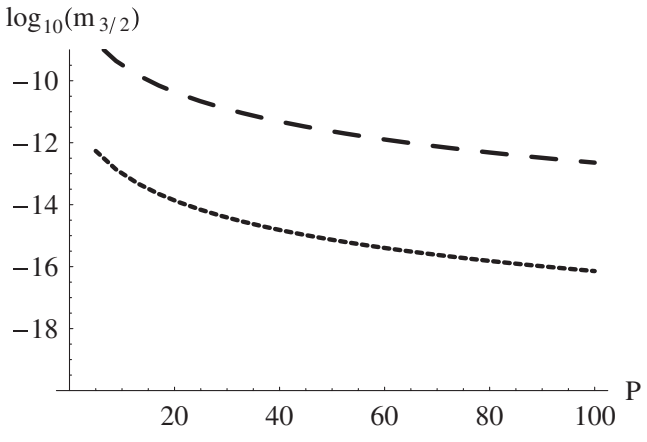

FIG. 16. Plot of $\log_{10}(m_{3/2})$ as a function of P for $Q - P = 3$. The short-dashed curve corresponds to $N = 50$. The long-dashed curve corresponds to $N = 500$.

An important point which should be emphasized is that, for $Q - P = 3$, the gravitino mass dependence on P and N appears *only* through the volume V_X, as can be seen from (198). Thus, the distribution in Fig. 15 directly correlates with the corresponding distribution of the stabilized volume of the seven-dimensional manifold V_X as a function of P and N. Therefore, it is the dominance of the vacua with a relatively small volume which results in the peak at $\mathcal{O}(100)$ TeV.

Also note that in the above analysis we simply set the constant coefficient due to the threshold corrections C_2 to unity. It would be interesting to get a handle on this quantity and include its variation into the gravitino mass distribution study.

One could argue that, even though $Q - P = (Q - P)_{\mathrm{min}} = 3$ gives a peak for the gravitino mass distribution at around the $\mathcal{O}(100)$ TeV scale, it seems plausible from a theoretical point of view to have many examples of gauge singularities in G_2 manifolds such that $Q - P > 3$. However, by imposing the supergravity constraint that all moduli s_i are larger than unity (which is the regime in which the entire analysis is valid), one sees that having $Q - P > 3$ drastically reduces the upper bound on N compared to that for $Q - P = 3$ [see Eq. (194)]. Therefore, the peaks in the gravitino mass distribution obtained for $-2 \leq \log_{10}(m_{3/2}) \leq -5$ in Figs. 13 and 14 come from vacua with a *small* number of moduli as well as $Q - P > 3$, compatible with the analysis in the supergravity regime. Since it is presumably true that the number of G_2 manifolds with the required gauge singularities which have a large number of moduli is much larger than those with a small number of moduli, it seems reasonable to expect that the peak of the gravitino mass distribution obtained at around the $\mathcal{O}(100)$ TeV scale is quite robust and is representative of the most generic class of G_2 manifolds with the appropriate gauge singularities. Notice also that in the case of manifolds with a large number of moduli $N \geq 100$, because of the constraint from the supergravity approximation, the actual minimal value of P in the scans (202) and (205) is quite large, i.e. $P_{\mathrm{min}} = 20$. Hence, if $P \geq 20$, from (191) the value of the ratio when $Q - P = 3$ is bounded from above,

$$\frac{A_1 Q}{A_2 P} \lesssim 67.7. \tag{212}$$

On the other hand, for less generic manifolds with a small number of moduli the supergravity constraint allows P to be small. In this case, in order to satisfy (191), $(A_1 Q)/(A_2 P)$ has to be exponentially large. Whether this is possible remains to be seen. However, because for the more generic case when $N \geq 100$ the upper bound in (212) is quite reasonable, our analysis remains robust.

One could also contrast the results obtained above with those obtained for the type IIB flux vacua. In type IIB flux vacua, one has to *independently* tune both the gravitino mass to a TeV scale (if one requires low scale supersymmetry to solve the hierarchy problem) as well as the cosmological constant to its observed value. This is quite different than what we are finding here. Finally, we should emphasize that imposing the supergravity approximation was crucial in obtaining low scale SUSY breaking. Plausibly, the vacua which exist in the M theoretic, small volume regime will have a much higher SUSY breaking scale. However, such vacua presumably also have the incorrect electroweak scale (either zero or M_{11}).

E. Including more than one flavor of quarks in the hidden sector

In the previous analysis we assumed a single flavor for the quarks in the hidden sector, i.e. $N_f = 1$. In order to check that the way we obtain a dS metastable minimum is robust and not dependent on a particular choice of chiral hidden sector matter spectrum, we would like to extend our analysis to include more than one flavor (but still with $N_f < N_c$) so that the meson fields are given by

$$\phi^{\sigma}_{\bar{\sigma}} \equiv (2Q^{\sigma}\tilde{Q}_{\bar{\sigma}})^{1/2}, \tag{213}$$

where σ, $\bar{\sigma} = \overline{1, N_f}$. In the absence of a perturbative superpotential (which is guaranteed in the absence of fluxes), one has, along the D-flat direction,

$$Q = \tilde{Q} = \frac{1}{\sqrt{2}}\begin{pmatrix} \phi^1_1 & & & \\ & \phi^2_2 & & \\ & & \ddots & \\ & & & \phi^{N_f}_{N_f} \end{pmatrix}. \tag{214}$$

Thus, the determinant appearing in (94) becomes

$$\det(\phi^{\sigma}_{\bar{\sigma}}) = \prod_{\sigma=1}^{N_f} \phi_{\sigma}, \quad \text{where } \phi_{\sigma} \equiv \phi^{\sigma}_{\sigma}. \tag{215}$$

The nonperturbative superpotential and the Kähler potential are then given by

$$\begin{aligned} W &= A_1 \prod_{\sigma=1}^{N_f} \phi_{\sigma}{}^{a} e^{ib_1 f} + A_2 e^{ib_2 f}, \\ K &= -3\ln(4\pi^{1/3}V_X) + \sum_{\sigma=1}^{N_f} \phi_{\sigma}\bar{\phi}_{\sigma}, \end{aligned} \tag{216}$$

where we again denoted $b_1 \equiv 2\pi/P$, $b_2 \equiv 2\pi/Q$, $P \equiv N_c - N_f$, and $a \equiv -2/P$. After minimizing with respect to the axions, the scalar potential is given by

$$\begin{aligned} V = \frac{e^{\sum_{\sigma=1}^{N_f}(\phi_0)^2_{\sigma}}}{48\pi V_X^3}\Bigg[& \Bigg(b_1 A_1 \prod_{\sigma=1}^{N_f}(\phi_0)^a_{\sigma} e^{-b_1\vec{\nu}\cdot\vec{a}} - b_2 A_2 e^{-b_2\vec{\nu}\cdot\vec{a}}\Bigg)^2 \sum_{i=1}^{N} a_i(\nu_i)^2 + 3\Bigg(A_1 \prod_{\sigma=1}^{N_f}(\phi_0)^a_{\sigma} e^{-b_1\vec{\nu}\cdot\vec{a}} - A_2 e^{-b_2\vec{\nu}\cdot\vec{a}}\Bigg)^2 \\ & + 3(\vec{\nu}\cdot\vec{a})\Bigg(A_1 \prod_{\sigma=1}^{N_f}(\phi_0)^a_{\sigma} e^{-b_1\vec{\nu}\cdot\vec{a}} - A_2 e^{-b_2\vec{\nu}\cdot\vec{a}}\Bigg)\Bigg(b_1 A_1 \prod_{\sigma=1}^{N_f}(\phi_0)^a_{\sigma} e^{-b_1\vec{\nu}\cdot\vec{a}} - b_2 A_2 e^{-b_2\vec{\nu}\cdot\vec{a}}\Bigg) \\ & + \sum_{\gamma=1}^{N_f}\frac{3}{4}(\phi_0)^2_{\gamma}\Bigg(\Bigg(\frac{a}{(\phi_0)^2_{\gamma}} + 1\Bigg)A_1 \prod_{\sigma=1}^{N_f}(\phi_0)^a_{\sigma} e^{-b_1\vec{\nu}\cdot\vec{a}} - A_2 e^{-b_2\vec{\nu}\cdot\vec{a}}\Bigg)^2\Bigg]. \end{aligned} \tag{217}$$

Instead of presenting a full analysis of this more general case we would simply like to check that we have a metastable dS vacuum, and that the main feature of the dS vacuum, namely, the emergence of the TeV scale when the tree-level cosmological constant is set to zero, survives when $N_f > 1$. For this purpose we need to compute the scalar potential at the minimum with respect to the moduli s_i as a function of the meson fields ϕ_{σ}.

The generalization of the equations minimizing the scalar potential is fairly straightforward. In particular, in the limit when the size of the associative cycle $\mathrm{Im} f = \vec{\nu}\cdot\vec{a}$ is large, for $A = 1$ the generalization of the second equation in (126), which determines $\tilde{L}_{1,+}$, takes on the following form:

$$\frac{2}{3}(\tilde{L}_{1,+})^2 + \tilde{L}_{1,+} + \sum_{\sigma=1}^{N_f}\frac{3a\beta b_1\hat{y}}{14\hat{x}\,\hat{z}}\Bigg(\frac{a\beta}{(\phi_0)^2_{\sigma}\hat{x}} + 1\Bigg) = 0$$

where we again defined $\beta \equiv \frac{A_1}{A_2}\prod_{\sigma=1}^{N_f}(\phi_0)^a_{\sigma} e^{-(b_1-b_2)\vec{\nu}\cdot\vec{a}}$, $\hat{x} \equiv \beta - 1$, $\hat{y} \equiv b_1\beta - b_2$, and $\hat{z} \equiv b_1^2\beta - b_2^2$. Thus, in the large three-cycle limit we again have $\beta \approx b_2/b_1 = P/Q$ so that $\hat{y} \to 0$, and the leading order solution for $\tilde{L}_{1,+}$ is again given by

$$\tilde{L}_{1,+} \approx -\tfrac{3}{2}. \tag{218}$$

In this case the moduli are stabilized at the same values given by (132). Since both the superpotential and the Kähler potential are completely symmetric with respect to the meson fields, it seems reasonable to expect that there is a vacuum where all ϕ_{σ} are stabilized at the same value, i.e. $(\phi_0)_{\sigma} = \tilde{\phi}_0$ for all $\sigma = \overline{1, N_f}$. Using the solution for the moduli vevs (132) and the above assumption, we obtain the following expression for the potential at the extremum with respect to the moduli s_i as a function of $\tilde{\phi}_0$:

$$V_0 = N_f \frac{(A_2\hat{x})^2}{64\pi V_X^3}\left[\tilde{\phi}_0^4 + \left(\frac{2a\beta}{\hat{x}} - \frac{3}{N_f}\right)\tilde{\phi}_0^2 + \left(\frac{a\beta}{\hat{x}}\right)^2\right]\frac{e^{N_f\tilde{\phi}_0^2}}{\tilde{\phi}_0^2} \times \left(\frac{A_1 Q}{A_2 P}\right)^{-(2P/(Q-P))}. \quad (219)$$

By setting the discriminant of the biquadratic polynomial in the square brackets to zero, we again obtain the condition on the tree-level cosmological constant to vanish in the leading order:

$$\frac{3}{N_f} - \frac{8}{Q-P} - \frac{28}{P\ln(\frac{A_1 Q}{A_2 P})} = 0. \quad (220)$$

Since the solutions for the moduli in the dS case correspond to branch b) where $Q > P$ and $A_1 Q > A_2 P$, the zero vacuum energy condition (220) can be satisfied only when

$$\frac{3}{N_f} > \frac{8}{Q-P} \Rightarrow (Q-P) > \frac{8}{3}N_f. \quad (221)$$

Therefore, a vanishing tree-level cosmological constant in the leading order results in the following set of conditions:

$$P\ln\left(\frac{A_1 Q}{A_2 P}\right) = \frac{28(Q-P)N_f}{3(Q-P) - 8N_f} \quad \text{and} \quad (Q-P) > \frac{8}{3}N_f. \quad (222)$$

Recall that the key to obtaining the TeV scale gravitino mass was the exponential suppression factor e^{-28} when $Q - P = (Q-P)_{\min} = 3$, related to the scale of gaugino condensation. In the present case, up to a factor of order 1, we have

$$m_{3/2} \sim \frac{m_p}{V_X^{3/2}}\left(\frac{A_1 Q}{A_2 P}\right)^{-(P/(Q-P))} = \frac{m_p}{V_X^{3/2}} e^{-\{28N_f/[3(Q-P)-8N_f]\}}. \quad (223)$$

Consider a few examples where $N_f > 1$. From (222) we have the following set:

$$\begin{aligned} &N_f = 2, \quad (Q-P)_{\min} = 6, \quad P\ln\left(\frac{A_1 Q}{A_2 P}\right) = 168, \quad m_{3/2} \sim \frac{m_p}{V_X^{3/2}} e^{-\{28N_f/[3(Q-P)-8N_f]\}} = \frac{m_p}{V_X^{3/2}} e^{-28}, \\ &N_f = 3, \quad (Q-P)_{\min} = 9, \quad P\ln\left(\frac{A_1 Q}{A_2 P}\right) = 252, \quad m_{3/2} \sim \frac{m_p}{V_X^{3/2}} e^{-\{28N_f/[3(Q-P)-8N_f]\}} = \frac{m_p}{V_X^{3/2}} e^{-28}, \\ &N_f = 4, (Q-P)_{\min} = 11, \quad P\ln\left(\frac{A_1 Q}{A_2 P}\right) = 1232, \quad m_{3/2} \sim \frac{m_p}{V_X^{3/2}} e^{-\{28N_f/[3(Q-P)-8N_f]\}} = \frac{m_p}{V_X^{3/2}} e^{-112}, \\ &N_f = 4, \quad Q-P = 12, \quad P\ln\left(\frac{A_1 Q}{A_2 P}\right) = 336, \quad m_{3/2} \sim \frac{m_p}{V_X^{3/2}} e^{-\{28N_f/[3(Q-P)-8N_f]\}} = \frac{m_p}{V_X^{3/2}} e^{-28}. \end{aligned} \quad (224)$$

Remarkably, in all but one case listed above we obtain *the same* suppression factor $e^{-28} \approx 7 \times 10^{-13}$ which was the reason for the peak at $m_{3/2} \sim \mathcal{O}(1\text{–}100)$ TeV. Note that the only example which did not fall into this range was the third case for which the condition on the cosmological constant to vanish was $P\ln(\frac{A_1 Q}{A_2 P}) = 1232$, which is too unrealistic anyway, as it requires either extremely large dual Coxeter numbers for the gauge groups N_c, $Q \sim \mathcal{O}(1000)$, or an exponentially large ratio inside the logarithm. On a similar note, as can be seen from the third entry in each line in (224), increasing the number of flavors N_f even further would again require either P, $Q > 300$ or an extremely large ratio $(\frac{A_1 Q}{A_2 P})$, which appears inside the logarithm. Therefore, limiting our analysis to the cases with $N_f < 5$ seems quite reasonable.

Recall that for $N_f = 1$ the TeV scale appeared for the minimum value $(Q-P)_{\min} = 3$, whereas the vacua corresponding to the higher values of $Q - P$ generally failed to satisfy the SUGRA constraint for more generic G_2 manifolds with a large number of moduli. For this reason, considering larger values of $Q - P$ for the examples listed above is probably unnecessary. Hence, for more than one flavor of quarks, we only need to take

$$Q - P = 3N_f. \quad (225)$$

Thus, given that the assumptions we made in the beginning of this subsection are reasonable, it appears that the connection of the TeV scale SUSY breaking to the requirement that the tree-level vacuum energy is very small is a fairly robust feature of these vacua, independent of the number of flavors.

F. Including matter in both hidden sectors

In the previous analysis we tried to be minimalistic and included chiral matter in only one of the hidden sectors. Because of this asymmetry, we obtained two types of solutions—a supersymmetric AdS extremum when $P > Q$, corresponding to branch a); and a dS minimum when $Q > P$ [when condition (144) holds], corresponding to branch b). Using this result it is then fairly straightforward to figure out what happens when both hidden sectors produce F-terms due to chiral matter. For the sake of simplicity, we will again consider the case when $N_f = 1$ in both hidden sectors. In this case, the Kähler potential is

given by

$$K = -3\ln(4\pi^{1/3}V_X) + \phi\bar{\phi} + \psi\bar{\psi}. \tag{226}$$

After minimizing with respect to the axions, the nonperturbative superpotential (up to a phase) is given by

$$W = -A_1\phi^{a_1}e^{-(2\pi/P)\mathrm{Im}f} + A_2\psi^{a_2}e^{-(2\pi/Q)\mathrm{Im}f}, \tag{227}$$

where $a_1 \equiv -2/P$ and $a_2 \equiv -2/Q$. We will now check to see if it is still possible to obtain SUSY extrema when both hidden sectors have chiral matter. Setting the moduli F-terms to zero we obtain

$$\nu_k = \nu = -\frac{3PQ}{4\pi}\frac{\tilde{\beta}-1}{Q\tilde{\beta}-P}, \tag{228}$$

where $\tilde{\beta} \equiv \frac{A_1\phi^{a_1}}{A_2\psi^{a_2}}e^{-((2\pi/P)-(2\pi/Q))\mathrm{Im}f}$. At the same time, setting the matter F-terms to zero results in the following conditions:

$$\left(\frac{a_1}{\phi_0^2}+1\right)\tilde{\beta}-1=0, \tag{229}$$

$$-\frac{a_2}{\psi_0^2}+\tilde{\beta}-1=0. \tag{230}$$

Expressing $\tilde{\beta}$ from (228) and substituting it into (229) and (230) and using the definitions for a_1 and a_2, we obtain the following expressions for the meson field vevs:

$$\phi_0^2 = \frac{2+3Q/(2\pi\nu)}{P-Q}, \tag{231}$$

$$\psi_0^2 = \frac{2+3P/(2\pi\nu)}{Q-P}. \tag{232}$$

Since ν as well as both ϕ_0^2 and ψ_0^2 are positive definite, we have the following two possibilities:

$$\begin{aligned} &a)\ P>Q:\ \Rightarrow F_\phi = 0 \quad \text{and} \quad F_\psi \neq 0,\\ &b)\ P<Q:\ \Rightarrow F_\phi \neq 0 \quad \text{and} \quad F_\psi = 0. \end{aligned} \tag{233}$$

Thus, when both hidden sectors have chiral matter, supersymmetric extrema are absent. Instead, when condition (144) holds [for branch a) we simply swap P and Q, A_1 and A_2 in (144)], for each branch we obtain a dS vacuum where only one of the matter F-terms is nonzero. Keep in mind that, although in the above analysis we used condition (228) obtained by setting the moduli F-terms to zero, even in the dS case when the moduli F-terms are nonzero, one of the two mesons will be stabilized at a value such that the corresponding matter F-term is zero. The zero F-term has no effect on the analysis of the dS solution and, apart from replacing $\tilde{\alpha}$ with $\tilde{\beta}$ defined above, the same solution obtained previously for the dS vacuum applies. In this case, the only difference will be in the meson field vevs:

$$\begin{aligned} a)\ \phi_0^2 &\approx \frac{2}{P-Q}+\frac{7}{P\ln(\frac{A_2P}{A_1Q})},\\ \psi_0^2 &\approx 1-\frac{2}{P-Q}+\sqrt{1-\frac{2}{P-Q}}\\ &\quad -\frac{7}{Q\ln(\frac{A_2P}{A_1Q})}\left(\frac{3}{2}+\sqrt{1-\frac{2}{P-Q}}\right),\\ b)\ \psi_0^2 &\approx \frac{2}{Q-P}+\frac{7}{Q\ln(\frac{A_1Q}{A_2P})},\\ \phi_0^2 &\approx 1-\frac{2}{Q-P}+\sqrt{1-\frac{2}{Q-P}}\\ &\quad -\frac{7}{P\ln(\frac{A_1Q}{A_2P})}\left(\frac{3}{2}+\sqrt{1-\frac{2}{Q-P}}\right). \end{aligned} \tag{234}$$

Therefore, the dS solution obtained for the minimal case when only one of the hidden sectors has chiral matter does not change even when we include chiral matter in both hidden sectors.

G. Height of the potential barrier

For simplicity, we first compute the height of the potential barrier for the case with a pure SYM hidden sector. The two solutions for $A = 1$ in Eqs. (50) and (51) exist for any number of moduli, and therefore the analysis below extends to the general case with an arbitrary number of moduli. The solution in Eq. (51) corresponds to the dS maximum which determines the height of the barrier. Using Eq. (44), from Eq. (51) we have

$$\nu_k^1 = \nu = -\frac{3}{7}\frac{x}{y}\left(\frac{3+\sqrt{9-7w}}{w}\right). \tag{235}$$

Therefore, we can express the volume of the associative cycle $\mathrm{Vol}(Q) \equiv \vec{\nu}\cdot\vec{a}$ as

$$\vec{\nu}\cdot\vec{a} = -\frac{x}{y}\left(\frac{3+\sqrt{9-7w}}{w}\right), \tag{236}$$

where we used the fact that $\nu_k^1 = \nu$ in (235) is independent of k and $\sum_{i=1}^N a_i = \frac{7}{3}$. Using the definitions of x, y, z, and w in Eq. (37) in terms of α, from (236) we can solve for α:

$$\alpha = \frac{P^2(7Q^2+12\pi Q\vec{\nu}\cdot\vec{a}+4\pi^2(\vec{\nu}\cdot\vec{a})^2)}{Q^2(7P^2+12\pi P\vec{\nu}\cdot\vec{a}+4\pi^2(\vec{\nu}\cdot\vec{a})^2)}. \tag{237}$$

From Eq. (36) we can express $\vec{\nu}\cdot\vec{a}$ as

$$\vec{\nu}\cdot\vec{a} = \frac{1}{2\pi}\frac{PQ}{P-Q}\ln\left(\frac{A_2}{A_1}\alpha\right). \tag{238}$$

In the limit when the volume of the associative cycle $\vec{\nu}\cdot\vec{a}$ is large, we can solve (237) and (238) order by order to obtain

$$\alpha \approx \frac{P^2}{Q^2}\left(1+\frac{6(P-Q)^2}{PQ\ln(\frac{A_2P^2}{A_1Q^2})}+\frac{(29P-7Q)(P-Q)^3}{P^2Q^2\ln^2(\frac{A_2P^2}{A_1Q^2})}\right) \tag{239}$$

together with

$$\vec{\nu}\cdot\vec{a} \approx \left(\frac{PQ\ln(\frac{A_2P^2}{A_1Q^2})}{2\pi(P-Q)}-\frac{3(P-Q)}{\pi\ln(\frac{A_2P^2}{A_1Q^2})} + \frac{11(P-Q)^2(P+Q)}{2\pi PQ\ln^2(\frac{A_2P^2}{A_1Q^2})}\right). \tag{240}$$

The moduli vevs at the barrier are then given by

$$s_i \approx \frac{3a_i}{7N_i}\left(\frac{PQ\ln(\frac{A_2P^2}{A_1Q^2})}{2\pi(P-Q)}-\frac{3(P-Q)}{\pi\ln(\frac{A_2P^2}{A_1Q^2})} + \frac{11(P-Q)^2(P+Q)}{2\pi PQ\ln^2(\frac{A_2P^2}{A_1Q^2})}\right). \tag{241}$$

In the leading order

$$s_i \approx \frac{3a_i}{7N_i}\left(\frac{PQ\ln(\frac{A_2P^2}{A_1Q^2})}{2\pi(P-Q)}\right) \tag{242}$$

and

$$\alpha \approx \frac{P^2}{Q^2}. \tag{243}$$

Using (242) and (243), the value of the potential at the barrier in the leading order is given by

$$V_b \approx m_p^4\frac{8A_2^2\pi^6}{7Q^4}\left(7(P^2-Q^2)^2+PQ\ln\left(\frac{A_2P^2}{A_1Q^2}\right)\times\left(7(P^2-Q^2)+PQ\ln\left(\frac{A_2P^2}{A_1Q^2}\right)\right)\right)\left(\frac{PQ}{P-Q}\times\ln\left(\frac{A_2P^2}{A_1Q^2}\right)\right)^{-7}\left(\frac{A_2P^2}{A_1Q^2}\right)^{-(2P/(P-Q))}\prod_{i=1}^{N}\left(\frac{7N_i}{3a_i}\right)^{3a_i}. \tag{244}$$

Recall that the value of the gravitino mass at the SUSY AdS extremum in the leading order is given by

$$m_{3/2} = m_p\sqrt{2}\pi^3A_2P\left|\frac{P-Q}{PQ}\right|\left(\frac{PQ}{P-Q}\ln\left(\frac{A_2P}{A_1Q}\right)\right)^{-7/2}\times\left(\frac{A_2P}{A_1Q}\right)^{-(P/(P-Q))}\prod_{i=1}^{N}\left(\frac{7N_i}{3a_i}\right)^{3a_i/2}. \tag{245}$$

Therefore, we can express the value of the potential at the barrier in the leading order as

$$V_b \approx m_p^2m_{3/2}^2\left(7(P^2-Q^2)^2+PQ\ln\left(\frac{A_2P^2}{A_1Q^2}\right)\left(7(P^2-Q^2)+PQ\ln\left(\frac{A_2P^2}{A_1Q^2}\right)\right)\right)\frac{4}{7Q^2(P-Q)^2}\left(\frac{P}{Q}\right)^{-(2P/(P-Q))}\times\left(\frac{\ln(\frac{A_2P}{A_1Q})}{\ln(\frac{A_2P^2}{A_1Q^2})}\right)^7. \tag{246}$$

Note that the above expression is independent of the number of moduli and parameters a_i and N_i.

This formula is very accurate when compared to the exact numerical values. For example, for the values of the parameters in Eq. (54), the numerically obtained result is

$$V_b \approx 51.55\times m_p^2m_{3/2}^2, \tag{247}$$

whereas from the leading order expression in (246) we get

$$V_b \approx 49.92\times m_p^2m_{3/2}^2. \tag{248}$$

In Fig. 17 below, we plotted the value of the scalar potential at the barrier in units of $m_p^2m_{3/2}^2$ as a function of P for $P-Q=3$ and $P-Q=1$ and two different values of the parameter $\rho \equiv \frac{A_2P}{A_1Q}$.

For the case of vacua with charged matter in the hidden sector, the situation is more complicated, as the potential depends on an additional field (meson). The height of the potential barrier changes as one moves along the meson and the moduli directions. To illustrate this with an example, we have done a numerical analysis for a manifold with two moduli and one meson field with the microscopic constants as in (136). Figure 18 shows a three-dimensional plot of the potential as a function of the moduli along the

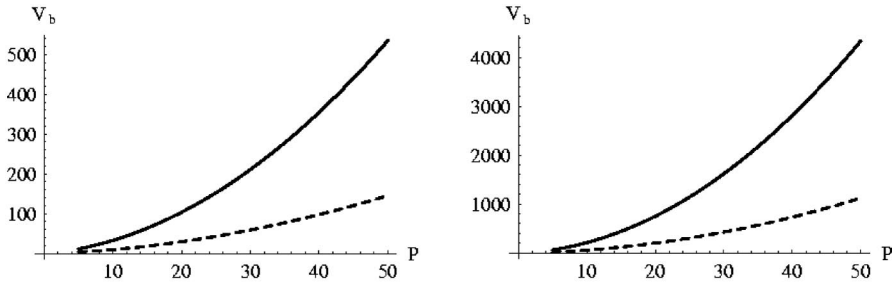

FIG. 17. Plots of the potential at the barrier in units of $m_p^2m_{3/2}^2$ as a function of P. The solid line corresponds to $\frac{A_2P}{A_1Q}=100$, while the dashed line corresponds to $\frac{A_2P}{A_1Q}=10$. Left panel: Plot for $P=Q+3$. Right panel: Plot for $P=Q+1$.

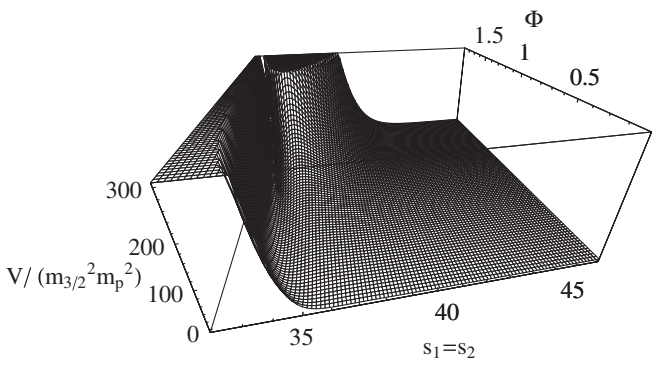

FIG. 18. Potential in units of $m_{3/2}^2 m_p^2$ plotted as a function of the meson field and the moduli along the slice $s_1 = s_2$, for a manifold with two moduli and the microscopic constants as in (136).

slice $s_1 = s_2$, and the meson field ϕ. In Fig. 19, in the left plot the potential is plotted along the slice $s_1 = s_2$ with the meson field equal to its value at the minimum (137), while in the right plot the potential is plotted along the slice $s_1 = s_2$ with the meson field equal to a value such that the height of the potential barrier is at its minimum.

VIII. PHENOMENOLOGY

In this section, we will begin the analysis of more detailed particle physics features of the vacua, with emphasis on the soft supersymmetry breaking parameters, since we are particularly interested in predicting collider physics observables that will be measured at the LHC.

The low energy physics observables are determined by the Kähler potential, the superpotential, and the gauge kinetic function of the effective $\mathcal{N} = 1$, $d = 4$ supergravity. The gauge kinetic function (f) has already been discussed. The Kähler potential and the superpotential can be written, in general, as follows:

$$K = \hat{K}(s_i, \phi_h, \bar{\phi}_h) + \tilde{K}_{\bar{\alpha}\beta}(s_i)\bar{\Phi}^{\bar{\alpha}}\Phi^{\beta} + Z_{\alpha\beta}(s_i, \phi_h)\Phi^{\alpha}\Phi^{\beta} + \ldots,$$
$$W = \hat{W}(z_i) + \mu'\Phi^{\alpha}\Phi^{\beta} + Y'_{\alpha\beta\gamma}\Phi^{\alpha}\Phi^{\beta}\Phi^{\gamma} + \ldots \qquad (249)$$

where Φ^{α} are the visible sector chiral matter fields, $\tilde{K}_{\bar{\alpha}\beta}$ is their Kähler metric, and $Y'_{\alpha\beta\gamma}$ are their *unnormalized* Yukawa couplings. ϕ^h denote the hidden sector matter fields. The first terms in K and W depend only on the bulk moduli and have already been studied earlier. In general, there can be a mass term (μ') in the superpotential, but as explained in [26], natural discrete symmetries can exist which forbid it, in order to solve the doublet-triplet splitting problem. The quantity $Z_{\alpha\beta}$ in the Kähler potential will be important for generating an effective μ term, as we will see later.

Since the vacua have low scale supersymmetry, the effective Lagrangian must be equivalent to the MSSM plus couplings involving possibly additional fields beyond the MSSM. For simplicity in this section we will assume an observable sector which is precisely the MSSM, although it would also be interesting to consider natural M theoretic extensions. The MSSM Lagrangian is characterized by the Yukawa and gauge couplings of the standard model and the soft supersymmetry breaking couplings. These are the scalar squared masses m_i^2, the trilinear couplings A_{ijk}, the μ and $B\mu$ mass parameters, and the gaugino masses. In M theory all of these couplings become functions of the various constants (A_i, N, P, Q, N_k) which are determined by the *particular* G_2 manifold X. In addition, because we are now discussing the observable sector, we have to explain the origin of observable sector gauge, Yukawa, and other couplings in M theory. As we have already explained, all gauge couplings are integer linear combinations of the N moduli, the N integers determining the homology class of the three-dimensional subspace of X which supports that particular gauge group. Furthermore, the entire superpotential is generated by membrane instantons, as we have already discussed. Therefore mass terms and Yukawa couplings in the superpotential are also determined by integer linear combinations of the moduli fields. Hence, in addition to the constants (A_i, N, P, Q, N_k) which determine the moduli potential, additional integers enter in determining the observable sector superpotential. Generically, though, we do not expect these integers to be large in the basis that the moduli Kähler metric is given by (6).

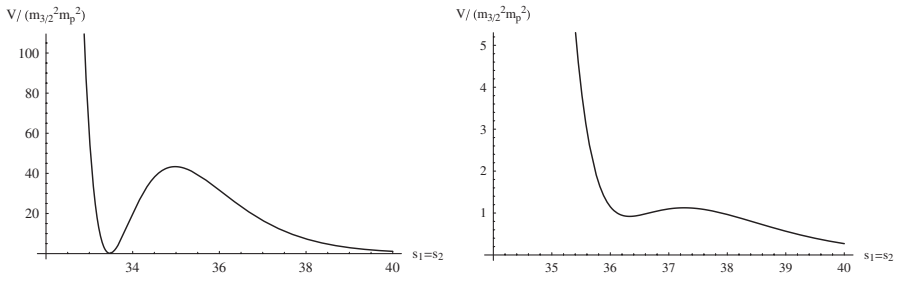

FIG. 19. Left panel: Potential in units of $m_{3/2}^2 m_p^2$ along the slice $s_1 = s_2$ for a manifold with two moduli with the meson field equal to its value at the minimum of the potential [as in (137)]. Right panel: Potential in units of $m_{3/2}^2 m_p^2$ along the slice $s_1 = s_2$ for a manifold with two moduli with the meson field $\phi = 0.102$ (this is such that the height of the potential barrier is at its minimum). The microscopic constants for both cases are the same as in (136).

We determine the values of the soft SUSY breaking couplings at $M_{\rm unif}$ in the standard way: The moduli fields, hidden sector matter fields, as well as their auxiliary fields are replaced by their *vevs* in the $\mathcal{N}=1$, $d=4$ SUGRA Lagrangian. One then takes the flat limit $M_p \to \infty$ with $m_{3/2}$ fixed. This gives a global SUSY Lagrangian with soft SUSY breaking terms [27]. Unfortunately, in M theory the matter Kähler potential is difficult to compute. This leads to theoretical uncertainties in the calculation of the scalar masses and A, B, and μ parameters. Fortunately though we are able to calculate the gaugino masses. Our main phenomenological result is that the tree-level gaugino masses are suppressed relative to the gravitino mass. After explaining this, we will go on to discuss the other soft terms in a certain, calculable limit.

A. Suppression of gaugino masses

Grand unification is particularly natural in G_2 vacua of M theory [19]. This implies that the gaugino masses at tree level (at the unification scale) are *universal*, i.e. the gauginos of the three SM gauge groups have the same mass. In order to compute the SM sector gaugino mass scale at tree level, we need the standard model gauge kinetic function, $f_{\rm sm}$. In general, this will be an integer linear combination of the moduli, with integers $N_i^{\rm sm}$, which is linearly independent of the hidden sector gauge kinetic function in general. The expression for the tree-level MSSM gaugino masses in general $\mathcal{N}=1$, $d=4$ SUGRA is given by

$$M_{1/2} = m_p \frac{e^{\hat{K}/2}\hat{K}^{n\bar{m}}F_{\bar{m}}\partial_n f_{\rm sm}}{2i{\rm Im}f_{\rm sm}}. \tag{250}$$

Note that the gauge kinetic function is independent of the hidden sector matter fields. Therefore, the large hidden sector matter F-term responsible for the dS minimum does not contribute to the gaugino masses at tree level. We will now proceed to evaluate this expression explicitly, both for the AdS and dS vacua. We will find that, generically, the gaugino masses are suppressed relative to the gravitino mass.

1. Gaugino masses in AdS vacua

Choosing the hidden sector to be pure SYM with gauge groups $SU(P)$ and $SU(Q)$, the normalized gaugino mass in these compactifications can be expressed as

$$M_{1/2} = -\frac{m_p e^{-i\gamma_W}}{8\sqrt{\pi}V_X^{3/2}}\left[\frac{4\pi}{3}\left(\frac{A_1}{P}e^{-(2\pi/P){\rm Im}f} - \frac{A_2}{Q}e^{-(2\pi/Q){\rm Im}f}\right)\times\frac{\sum_{i=1}^N N_i^{\rm sm}s_i\nu_i}{\sum_{i=1}^N N_i^{\rm sm}s_i} + A_1 e^{-(2\pi/P){\rm Im}f} - A_2 e^{-(2\pi/Q){\rm Im}f}\right] \tag{251}$$

where γ_W is the phase of the superpotential W. In the leading order, the last two terms in the brackets can be combined as

$$A_1 e^{-(2\pi/P){\rm Im}f} - A_2 e^{-(2\pi/Q){\rm Im}f} = A_2\left[\frac{P-Q}{Q}\right]\left[\frac{A_2 P}{A_1 Q}\right]^{-(P/(P-Q))}. \tag{252}$$

On the other hand, the two terms in the round brackets coming from the partial derivative of the superpotential cancel in the leading order. Therefore we need to take into account the first subleading order contribution (92). In this order, we obtain[8]

$$\left(\frac{A_1}{P}e^{-(2\pi/P){\rm Im}f} - \frac{A_2}{Q}e^{-(2\pi/Q){\rm Im}f}\right) = \frac{1}{2\pi}A_2\left[\frac{P-Q}{Q}\right]\left[\frac{A_2 P}{A_1 Q}\right]^{-(P/(P-Q))}\frac{B_A^{(c)}}{\mathcal{T}_A^{(c)}}. \tag{253}$$

From (252) and (253) we notice that the absolute value of the gaugino mass can now be conveniently expressed in terms of the gravitino mass (for a given value of A and c, as discussed in previous sections) as

$$|M_{1/2}|_A^{(c)} = \frac{2}{3}\frac{\sum_{i=1}^N a_i L_{A,k}^{(c)}(L_{A,k}^{(c)}+3/2)(N_i^{\rm sm}/N_i)}{\sum_{i=1}^N a_i L_{A,k}^{(c)}(N_i^{\rm sm}/N_i)} \times (m_{3/2})_A^{(c)}, \tag{254}$$

where we also used (79) and (85). Finally, using (73) and the first equation in (72), after some algebra we arrive at the following expression for the gaugino mass:

$$|M_{1/2}|_A^{(c)} = \left(\frac{4}{3}T_A^{(c)}+1\right)\frac{q-A}{q+\frac{T_A^{(c)}}{H_A^{(c)}}} \times (m_{3/2})_A^{(c)}, \tag{255}$$

where we have introduced a new quantity

$$q = \frac{\sum_{i=1}^N m_i a_i (N_i^{\rm sm}/N_i)}{\sum_{i=1}^N a_i (N_i^{\rm sm}/N_i)}, \tag{256}$$

such that the range of possible values for q is

$$-1 \le q \le 1. \tag{257}$$

Note that the general formula (255) which relates the gravitino and gaugino masses is completely independent of the number of moduli.

When all m_k have the same sign the gaugino mass in (255) automatically vanishes. This is expected since the solution when $A=\pm 1$ is the SUSY extremum. In Fig. 20 we have plotted absolute values of $(M_{1/2})_A^{(1)}$ and $(M_{1/2})_A^{(2)}$ as functions of q.

For a significant fraction of the space in both plots we have $(M_{1/2})_A^{(1,2)} \le 0.2(m_{3/2})_A^{(1,2)}$, so the gaugino masses are typically suppressed compared to the gravitino mass for these AdS vacua. Note also that the suppression factor in (255) is independent of the gravitino mass. This result is

[8]Recall that ${\rm Im}(f)_A^{(c)} \equiv \mathcal{T}_A^{(c)}$ [see (75)].

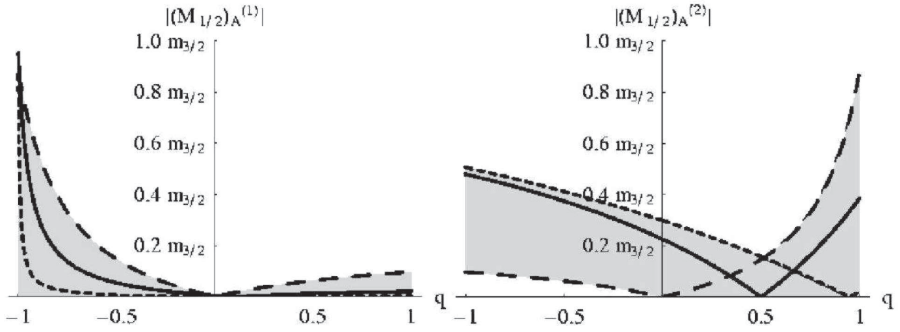

FIG. 20. Absolute values of $(M_{1/2})_A^{(1)}$ (left panel) and $(M_{1/2})_A^{(2)}$ (right panel) in units of gravitino mass as functions of q. As parameter A varies over $0 \leq A < 1/7$ (on the left) and $0 \leq A \leq 1$ (on the right), and the whole light gray region is covered. Left panel: $A = 0$ is depicted as the long-dashed line, $A = 1/9$ as the solid line, and $A = 5/36$ as the short-dashed line. Right panel: $A = 0$ is shown as the long-dashed line, $A = 0.5$ as the solid line, and $A = 0.95$ as the short-dashed line.

different from the small hierarchy between $M_{1/2}$ and $m_{3/2}$ in the type IIB flux vacua [10], where the gaugino mass is generically suppressed by $\ln(m_{3/2})$.

For the special case $A = 0$, system (72) yields two solutions with positive moduli. Therefore, there will be two different values for the gaugino mass corresponding to these solutions. After some algebra we obtain

$$|M_{1/2}|_0^{(1,2)} = \left(\frac{5-\sqrt{17}}{4}\right)\left|\frac{q}{q \pm \frac{-9+\sqrt{17}}{\sqrt{-26+10\sqrt{17}}}}\right| \times (m_{3/2})_0^{(1,2)} \sim 0.22\left|\frac{q}{q \mp 1.25}\right| \times (m_{3/2})_0^{(1,2)}. \quad (258)$$

Again, this relation is valid for any AdS vacuum with broken SUSY with $A = 0$ with an arbitrary number of moduli.

To check the accuracy of the approximate gaugino mass formula we again try the special case with two moduli $a_1 = a_2 = 7/6$ with the same choice of the constants as in (67) and the integer combination for the standard model gauge kinetic function $\{N_1^{\rm sm} = 2, N_2^{\rm sm} = 1\}$. In this case Eq. (258) for the absolute value of $M_{1/2}$ yields

$$(M_{1/2})_0^{(1)} = 164.4 \text{ GeV}, \qquad (M_{1/2})_0^{(2)} = 95 \text{ GeV}, \quad (259)$$

whereas the exact values computed numerically for the same choice of constants are

$$(M_{1/2})_0^{(1)} = 165.4 \text{ GeV}, \qquad (M_{1/2})_0^{(2)} = 97 \text{ GeV}. \quad (260)$$

This demonstrates a high degree of accuracy of our approximation, similar to that for the gravitino mass.

2. Gaugino masses in dS vacua

From the formula for the gaugino mass in (250), the gaugino mass for the dS vacua, in general, can be expressed as

$$M_{1/2} = \frac{e^{-i\gamma_W} m_p e^{\phi_0^2/2}}{8\sqrt{\pi} V_X^{3/2}}\left[\frac{2}{3}\tilde{y}\frac{\sum_{i=1}^N N_i^{\rm sm} s_i \nu_i}{\sum_{i=1}^N N_i^{\rm sm} s_i} + \tilde{x}\right] A_2 e^{-b_2 \vec{\nu}\cdot\vec{a}}$$
$$\Rightarrow M_{1/2} = -e^{-i\gamma_W}\left(\frac{2}{3}L_{1,+} + 1\right) m_{3/2}, \quad (261)$$

where in the second equality we used (122) and the fact that for these vacua $\nu_i = \nu$ for all $i = \overline{1, N}$, independent of i. Also, by including the minus sign we took into account that $m_{3/2} = e^{K/2}|\tilde{x}|A_2 e^{-b_2\vec{\nu}\cdot\vec{a}}$ but $\tilde{x} < 0$, since $Q - P \geq 3$. From (127) we can find $\tilde{L}_{1,+}$ including the first subleading contribution,

$$\tilde{L}_{1,+} \approx -\frac{3}{2} + \frac{3a\tilde{\alpha}b_1\tilde{y}}{14\tilde{x}\tilde{z}}\left(\frac{a\tilde{\alpha}}{\phi_0^2\tilde{x}} + 1\right). \quad (262)$$

For $\tilde{x}$, $\tilde{y}$, and $\tilde{z}$ in (262) we use the definitions (114) and substitute the approximate result (133) for $\tilde{\alpha}$. Then after substituting (262) into (261) and assuming that $Q - P \sim \mathcal{O}(1)$, in the limit when P is large the approximate tree-level MSSM gaugino mass is given by

$$M_{1/2} \approx -\frac{e^{-i\gamma_W}}{P\ln(\frac{A_1 Q}{A_2 P})}\left(1 + \frac{2}{\phi_0^2(Q-P)} + \frac{7}{\phi_0^2 P\ln(\frac{A_1 Q}{A_2 P})}\right) \times m_{3/2}, \quad (263)$$

where we use (134) to substitute for ϕ_0^2. It is important to note some features of the above equation. First, Eq. (263) is completely independent of the choice of integers $N_i^{\rm sm}$ for the standard model gauge kinetic function as well as the integers N_i for the hidden sector. Second, it is independent of the number of moduli N, and moreover, it is also independent of the particular details of the internal manifold described by the rational numbers a_i appearing in the Kähler potential (2). These properties imply that relation (263) is universal for all G_2 holonomy compactifications consistent with our approximations, independent of many internal details of the manifold. Furthermore, the denominator $P\ln(A_1 Q/A_2 P)$ turns out to be always greater than unity for choices of microscopic parameters consistent

with all constraints such as the supergravity regime constraint and the dS minimum constraint. In fact, for reasonable choices of parameters, it is typically of $\mathcal{O}(10–100)$. Since the expression in the round brackets in (263) is slowly varying and for the range under consideration is of $\mathcal{O}(1)$, we see that *gaugino masses are always suppressed relative to the gravitino for these dS vacua*.

After one imposes the constraint equation (191) [(207) when $Q - P = 3$] to make the cosmological constant very small, one can get rid of one of the constants in (263), and further simplify the expression for the universal tree-level gaugino mass parameters for the dS vacuum with a very small cosmological constant:

$$\begin{aligned} M_{1/2} &\approx -\frac{e^{-i\gamma_w}}{84}\left(1+\frac{2}{3\phi_0^2}+\frac{7}{84\phi_0^2}\right)\times m_{3/2} \\ &= -e^{-i\gamma_w}\frac{139+396\sqrt{3}}{34\,356}\times m_{3/2} \\ &\approx -e^{-i\gamma_w}0.024\times m_{3/2}. \end{aligned} \tag{264}$$

As in the more general case [Eq. (263)], the tree-level gaugino mass is suppressed compared to the gravitino mass, and the suppression factor can also be predicted.

One would like to understand the physical origin of the suppression of the gaugino masses at tree level, especially for the dS vacua which are phenomenologically relevant. As mentioned earlier, since the matter F-term does not contribute to the gaugino masses, the gaugino masses can only get contributions from the moduli F-terms, which, as explained in the last paragraph in Sec. VI D, vanish in the leading order of our approximation. The first subleading contribution is suppressed by the inverse power of the volume of the associative three-cycle, causing the gaugino masses to be suppressed relative to the gravitino. Since the inverse volume of this three-cycle is essentially α_{hidden}—the hidden sector gauge coupling in the UV—the suppression is due to the fact that the hidden sector is asymptotically free. In large volume type IIB compactifications, the moduli F-terms also vanish in the leading order, leading to suppressed gaugino masses as well [10]. However, in contrast to our case, there the subleading contribution is suppressed by the inverse power of the volume of the compactification manifold. Note that a large associative cycle on a G_2 manifold does *not* translate into a large volume compactification manifold. Thus, unlike large volume type IIB compactifications, these M theory vacua have a much higher compactification scale and hence are consistent with standard gauge coupling unification.

B. Other parameters and flavor issues

The trilinears, scalars, anomaly mediated contributions to gaugino masses, and the $B\mu$ parameter depend more on the microscopic details of the theory—the Yukawa couplings, the μ' parameter, and the Kähler metric for visible sector matter fields. The flavor structure of the Yukawa matrices as well as that of the Kähler metric for matter fields is crucial for estimating flavor changing effects. We will comment on these at appropriate places.

The (unnormalized) Yukawa couplings in these vacua arise from membrane instantons which connect singularities where chiral superfields are supported (if some singularities coincide, there could also be order 1 contributions). They are given by

$$Y'_{\alpha\beta\gamma} = C_{\alpha\beta\gamma}e^{i2\pi\sum_i l_i^{\alpha\beta\gamma}z^i} \tag{265}$$

where $C_{\alpha\beta\gamma}$ is an $\mathcal{O}(1)$ constant and $l_i^{\alpha\beta\gamma}$ are integers.

The moduli dependence of the matter Kähler metric is notoriously difficult to compute in generic string and M theory vacua, and the vacua under study here are no exception. The best we can do here is to consider the type IIA limit of these vacua. The matter Kähler metric has been computed in type IIA intersecting D6-brane vacua on toroidal orientifolds [28] building on earlier work [29]. Since chiral fermions living at intersections of D6-branes lift to chiral fermions supported at conical singularities in M theory [15,30], we will simply uplift the type IIA calculation to M theory. Thus the results of this section are strictly only valid in the type IIA limit.

Lifting the type IIA result to M theory, one gets (see the Appendix for details)

$$\begin{aligned} &\tilde{K}_{\bar{\alpha}\beta} = \delta_{\bar{\alpha}\beta}\prod_{i=1}^{n}\left(\frac{\Gamma(1-\theta_i^\alpha)}{\Gamma(\theta_i^\alpha)}\right)^{1/2}, \qquad \tan(\pi\theta_i^\alpha) = c_i^\alpha(s_i)^l; \\ &c_i^\alpha = \text{constant}; \qquad l = \text{rational number of } \mathcal{O}(1). \end{aligned} \tag{266}$$

In the type IIA toroidal orientifolds, the underlying symmetries always allow us to have a diagonal Kähler metric [28]. We have assumed for simplicity the Kähler metric to be diagonal in the analysis below. Now, we will write down the general expressions for the physical Yukawa couplings and the soft parameters—the trilinears and the scalars, and then estimate these in M theory compactifications. The μ and $B\mu$ parameters will be discussed in Sec. VIII E.

The Kähler potential for the chiral matter fields is noncanonical for any compactification in general. In determining physical implications however, it is much simpler to work in a basis with a canonical Kähler potential. So, to canonically normalize the matter field Kähler potential, we introduce the normalization matrix $\mathcal{Q}$:

$$\Phi \to \mathcal{Q}\cdot\Phi, \quad s.t. \quad \mathcal{Q}^\dagger\tilde{K}\mathcal{Q} = 1. \tag{267}$$

The $\mathcal{Q}$'s are themselves only defined up to a unitary transformation; i.e. $\mathcal{Q}' = \mathcal{Q}\cdot\mathcal{U}$ is also an allowed normalization matrix if $\mathcal{U}$ is unitary. If the Kähler metric is already diagonal ($\tilde{K}_{\bar{\alpha}\beta} = \tilde{K}_\alpha\delta_{\bar{\alpha}\beta}$), the normalization matrix can be simplified: $\mathcal{Q}_{\bar{\alpha}\beta} = (\tilde{K}_\alpha)^{-1/2}\delta_{\bar{\alpha}\beta}$. The normalized (physical) Yukawa couplings are [27]

$$Y_{\alpha\beta\gamma} = e^{\hat{K}/2}\frac{\hat{W}^\star}{|\hat{W}|}Y'_{\alpha'\beta'\gamma'}\mathcal{Q}_{\alpha'\alpha}\mathcal{Q}_{\beta'\beta}\mathcal{Q}_{\gamma'\gamma}. \quad (268)$$

It was shown in [31] that, in the class of theories with a hierarchical structure of the unnormalized Yukawa couplings (in the superpotential), the Kähler corrections to both masses and mixing angles of the SM particles are subdominant. In these compactifications, it is very natural to obtain a hierarchical structure of the unnormalized Yukawa couplings due to their exponential dependence on the various moduli and also because of some possible family symmetries; therefore one expects the effects of the Kähler corrections, which are less under control, to be subdominant. The expressions for the *unnormalized* trilinears and scalar masses are given by [27]

$$\begin{aligned} m'^2_{\tilde{\alpha}\beta} &= (m^2_{3/2}+V_0)\tilde{K}_{\tilde{\alpha}\beta} - e^{\hat{K}}F^{\bar{m}}(\partial_{\bar{m}}\partial_n\tilde{K}_{\tilde{\alpha}\beta} \\ &\quad - \partial_{\bar{m}}\tilde{K}_{\tilde{\alpha}\gamma}\tilde{K}^{\gamma\bar{\delta}}\partial_n\tilde{K}_{\bar{\delta}\beta})F^n, \\ A'_{\alpha\beta\gamma} &= \frac{\hat{W}^\star}{|\hat{W}|}e^{\hat{K}/2}F^m[\hat{K}_m Y'_{\alpha\beta\gamma} + \partial_m Y'_{\alpha\beta\gamma} \\ &\quad - (\tilde{K}^{\delta\bar{\rho}}\partial_n\tilde{K}_{\bar{\rho}\alpha}Y'_{\alpha\beta\gamma} + \alpha\leftrightarrow\gamma + \alpha\leftrightarrow\beta)]. \end{aligned} \quad (269)$$

The *normalized* scalar masses and trilinears are thus given by

$$\begin{aligned} m^2_{\tilde{\alpha}\beta} &= (\mathcal{Q}^\dagger\cdot m'^2\cdot\mathcal{Q})_{\tilde{\alpha}\beta}, \\ \tilde{A}_{\alpha\beta\gamma} &= A'_{\alpha'\beta'\gamma'}\mathcal{Q}_{\alpha'\alpha}\mathcal{Q}_{\beta'\beta}\mathcal{Q}_{\gamma'\gamma}. \end{aligned} \quad (270)$$

Let us discuss the implications for the soft terms, beginning with the anomaly mediated corrections to gaugino masses.

1. Anomaly mediated contributions to gaugino masses

We saw in Sec. VIII A that the gauginos are generically suppressed relative to the gravitino. Since anomaly mediated gaugino masses are also suppressed relative to the gravitino (by a loop factor), they are non-negligible compared to the tree-level contributions and have to be taken into account. Also, since anomaly mediated contributions for the three gauge groups are *nonuniversal*, these introduce nonuniversality in the gaugino masses at the unification scale.

The general expression for the anomaly mediated contributions is given by [32]

$$\begin{aligned} (M)^{\rm am}_a &= -\frac{g_a^2}{16\pi^2}\Big[-\Big(3C_a - \sum_\alpha C^\alpha_a\Big)e^{\hat{K}/2}W^* \\ &\quad + \Big(C_a - \sum_\alpha C^\alpha_a\Big)e^{\hat{K}/2}F^m\hat{K}_m \\ &\quad + 2\sum_\alpha (C^\alpha_a e^{\hat{K}/2}F^m\partial_m\ln(\tilde{K}_\alpha))\Big] \end{aligned} \quad (271)$$

where C_a and C^α_a are the Casimir invariants of the ath gauge group and α runs over the number of fields charged under the ath gauge group. For a given spectrum such as that of the MSSM, C_a and C^α_a are known.

We first compute the F-term contributions

$$\begin{aligned} e^{\hat{K}/2}F^i\hat{K}_i &= \frac{14}{3}e^{-i\gamma_W}\Big(\tilde{L}_{1,+}+\frac{3}{2}\Big)\times m_{3/2}, \\ e^{\hat{K}/2}F^\phi\hat{K}_\phi &= e^{-i\gamma_W}\Big(\frac{a\tilde{\alpha}}{\tilde{x}}+\phi_0^2\Big)\times m_{3/2}. \end{aligned} \quad (272)$$

Then, Eq. (271) gives

$$\begin{aligned} (M)^{\rm am}_a &= -e^{-i\gamma_W}\frac{\alpha_{\rm GUT}}{4\pi}\Big[-\Big(3C_a - \sum_\alpha C^\alpha_a\Big) \\ &\quad + \frac{14}{3}\Big(C_a - \sum_\alpha C^\alpha_a\Big)\Big(\tilde{L}_{1,+}+\frac{3}{2}\Big) + \Big(C_a - \sum_\alpha C^\alpha_a\Big) \\ &\quad \times\Big(\frac{a\tilde{\alpha}}{\tilde{x}}+\phi_0^2\Big) - \frac{4}{3}\Big(\tilde{L}_{1,+}+\frac{3}{2}\Big)\sum_\alpha C^\alpha_a\sum_i\frac{1}{2\pi} \\ &\quad \times (l\psi^\alpha_i\sin(2\pi\theta^\alpha_i))\Big]\times m_{3/2}, \end{aligned} \quad (273)$$

where

$$(\alpha_{\rm GUT})^{-1} = \sum_{i=1}^N s_i N_i^{\rm sm}, \quad (274)$$

and we have defined the quantity

$$\psi^\alpha_i(\theta^\alpha_i) \equiv \frac{d\ln(\tilde{K}_\alpha)}{d\theta^\alpha_i}, \quad (275)$$

where θ^α_i implicitly depends on the moduli. However, it is much simpler to keep the dependence as a function of θ^α_i, as is explained in the Appendix. Depending on the values of the Casimir invariants C_a and C^i_a for the three gauge groups, the anomaly mediated contribution can either add to or cancel the tree-level contributions. Here we also took into account that $m_{3/2} = e^{K/2}|\tilde{x}|A_2e^{-b_2\vec{\nu}\cdot\vec{a}}$ but $\tilde{x}<0$, since $Q-P\geq 3$. Using the expression for $\tilde{L}_{1,+}$ in (129) along with the definitions of $\tilde{x}$, $\tilde{y}$, and $\tilde{z}$ in (114) in terms of $\tilde{\alpha}$ in (133) and assuming that $Q-P\sim\mathcal{O}(1)$, in the limit when P is large we obtain

$$\begin{aligned} \tilde{L}_{1,+} &= -\frac{3}{2}+\frac{3}{2P\ln(\frac{A_1Q}{A_2P})}\Big(1+\frac{2}{(Q-P)\phi_0^2} \\ &\quad + \frac{7}{\phi_0^2P\ln(\frac{A_1Q}{A_2P})}\Big). \end{aligned} \quad (276)$$

Using (143) and substituting for ν from (132) into (143), together with $a=-2/P$, we can express

$$\frac{a\tilde{\alpha}}{\tilde{x}}+\phi_0^2 = \phi_0^2\Big(1+\frac{2}{(Q-P)\phi_0^2}+\frac{7}{\phi_0^2P\ln(\frac{A_1Q}{A_2P})}\Big). \quad (277)$$

Substituting (276) and (277) into (273) we obtain

$$(M)_a^{\rm am} = -e^{-i\gamma_W}\frac{\alpha_{\rm GUT}}{4\pi}\Bigg[-\Big(3C_a-\sum_\alpha C_a^\alpha\Big) + \Big(1+\frac{2}{(Q-P)\phi_0^2}+\frac{7}{\phi_0^2 P\ln(\frac{A_1Q}{A_2P})}\Big) \times\Bigg(\Big(C_a-\sum_\alpha C_a^\alpha\Big)\Big(\phi_0^2+\frac{7}{P\ln(\frac{A_1Q}{A_2P})}\Big) - \frac{2\sum_\alpha C_a^\alpha\sum_i \frac{1}{2\pi}(l\psi_i^\alpha\sin(2\pi\theta_i^\alpha))}{P\ln(\frac{A_1Q}{A_2P})}\Bigg)\Bigg]\times m_{3/2}. \quad (278)$$

Note that these M theory vacua do not have a no-scale structure. Therefore, the anomaly mediated gaugino masses are only suppressed by loop effects, in contrast to the type IIB compactifications, which exhibit a no-scale structure in the leading order [10], leading to an additional suppression of the anomaly mediated gaugino masses.

As before, when one imposes the constraint (207), the anomaly mediated gaugino mass contribution can be simplified further and is given by

$$(M)_a^{\rm am} = -\frac{\alpha_{\rm GUT}(e^{-i\gamma_W})}{4\pi}\Bigg[-\Big(3C_a-\sum_\alpha C_a^\alpha\Big) + \frac{29055+11374\sqrt{3}}{29448}\Big(C_a-\sum_\alpha C_a^\alpha\Big) - \frac{139+396\sqrt{3}}{17178}\sum_\alpha C_a^\alpha\sum_i\frac{1}{2\pi}(l\psi_i^\alpha\sin(2\pi\theta_i^\alpha))\Bigg]\times m_{3/2},$$

$$(M)_a^{\rm am} \approx -\frac{\alpha_{\rm GUT}(e^{-i\gamma_W})}{4\pi}\Bigg[-\Big(3C_a-\sum_\alpha C_a^\alpha\Big) + 1.6556\Big(C_a-\sum_\alpha C_a^\alpha\Big) - 0.048\sum_\alpha C_a^\alpha\sum_i\frac{1}{2\pi} \times(l\psi_i^\alpha\sin(2\pi\theta_i^\alpha))\Bigg]\times m_{3/2}. \quad (279)$$

From the left plot in Fig. 21 of the Appendix we note that $|\frac{1}{2\pi}(l\psi_i^\alpha\sin(2\pi\theta_i^\alpha))|<0.5$. In a generic case, we expect that parameters θ_i^α are all different and, as a result, the terms appearing inside the corresponding sum over i partially cancel each other. Thus, in a typical case we expect that

$$\Big|\sum_\alpha C_a^\alpha\sum_i\frac{1}{2\pi}(l\psi_i^\alpha\sin(2\pi\theta_i^\alpha))\Big|<1. \quad (280)$$

Neglecting the corresponding contribution in (279), taking $\alpha_{\rm GUT}=1/25$, and substituting the Casimirs for an MSSM spectrum, we obtain the following values in the leading order, up to an overall phase $e^{-i\gamma_W}$:

$$(M)_{U(1)}^{\rm am}\approx 0.013\,77\times m_{3/2},\quad (M)_{SU(2)}^{\rm am}\approx 0.023\,17\times m_{3/2},\quad (M)_{SU(3)}^{\rm am}\approx 0.025\,36\times m_{3/2}. \quad (281)$$

Finally, combining the tree-level (264) plus anomaly mediated (281) contributions, we obtain the following *non-universal* gaugino masses at the unification scale:

$$M_1\approx -10.24\times10^{-3}m_{3/2},\quad M_2\approx -0.84\times10^{-3}m_{3/2},\quad M_3\approx +1.35\times10^{-3}m_{3/2}. \quad (282)$$

We immediately notice remarkable cancellations for M_2 and M_3 between the tree-level and the anomaly mediated contributions. Recall that since the distribution of $m_{3/2}$ peaked at $m_{3/2}\sim\mathcal{O}(100)$ TeV, the possible range of gaugino masses is in the desirable range $m_{1/2}\sim\mathcal{O}(0.1\text{–}1)$ TeV. One of the consequences of these cancellations is a comparatively lighter gluino. Furthermore, since M_2 is a lot smaller than M_1, assuming R-parity conservation, the neutralino lightest supersymmetric particle (LSP) is expected to be W-ino-like. This is confirmed by explicitly RG evolving the gaugino masses to low scales, at least for the case when the cosmological constant is tuned to be very small.

One should be extremely cautious, however, since the predictive expressions above are only true if (280) is satisfied. The extra contribution neglected in the above estimates is given by

$$\Delta_a = 0.15\times10^{-3}\sum_\alpha C_a^\alpha\sum_i\frac{1}{2\pi}(l\psi_i^\alpha\sin(2\pi\theta_i^\alpha))\times m_{3/2}. \quad (283)$$

Because of the large cancellations between the tree-level and anomaly mediated contributions, it may happen that these corrections become important in a relatively small region of the overall parameter space, leading to a deviation from the above result thereby altering the pattern of gaugino masses. Further corrections may also come from varying $\alpha_{\rm GUT}$ as well as taking into account subleading corrections to the condition for the cosmological constant to be very small. In Sec. VIII C, the effects of subleading corrections to the very small cosmological constant condition on the gaugino masses will be analyzed. A thorough study of these issues will be done in [12].

2. Trilinears

The normalized trilinear can be written as

$$\tilde{A}_{\alpha\beta\gamma} = \frac{\hat{W}^\star}{|\hat{W}|} e^{\hat{K}/2}(\tilde{K}_\alpha \tilde{K}_\beta \tilde{K}_\gamma)^{-1/2}\Big(\sum_i e^{\hat{K}/2} F^m[\hat{K}_m Y'_{\alpha\beta\gamma} + \partial_m Y'_{\alpha\beta\gamma} - \partial_m \ln(\tilde{K}_\alpha \tilde{K}_\beta \tilde{K}_\gamma)]\Big)$$
$$= Y_{\alpha\beta\gamma}\Big(\sum_i e^{\hat{K}/2} F^m[\hat{K}_m + \partial_m \ln(Y'_{\alpha\beta\gamma}) - \partial_m \ln(\tilde{K}_\alpha \tilde{K}_\beta \tilde{K}_\gamma)]\Big). \quad (284)$$

As stated earlier, the subscripts $\{\alpha, \beta, \gamma\}$ stand for the visible chiral matter fields. For example, α can be the left-handed up quark doublet, β can be the right-handed up quark singlet, and γ can be the up-type Higgs doublet. Our present understanding of the microscopic details of these constructions does not allow us to compute the three individual trilinear parameters—corresponding to the up-type Yukawa, the down-type Yukawa, and the lepton Yukawa matrices, explicitly. One can only estimate the rough overall scale of the trilinears.

We see from (284) that the normalized trilinears are proportional to the Yukawa couplings since the Kähler metric is diagonal. If instead the off-diagonal entries in the Kähler metric are small but nonzero, it would lead to a slight deviation from the proportionality of the trilinears to the Yukawa couplings. In most phenomenological analyses, the trilinears $\tilde{A}$ are taken to be proportional to the Yukawas and the *reduced* trilinear couplings $A_{\alpha\beta\gamma} \equiv \tilde{A}_{\alpha\beta\gamma}/Y_{\alpha\beta\gamma}$ are used. We expect this to be true in these compactifications from above. If the Yukawa couplings are those of the standard model, then from (284) the normalized reduced trilinear coupling $A_{\alpha\beta\gamma}$ for de Sitter vacua, in general, is given by

$$A_{\alpha\beta\gamma} = e^{-i\gamma_W}\Big(1 + \frac{2}{(Q-P)\phi_0^2} + \frac{7}{\phi_0^2 P \ln(\frac{A_1 Q}{A_2 P})}\Big) \times \Big(\phi_0^2 + \frac{1}{P\ln(\frac{A_1 Q}{A_2 P})}\Big[7 + 2\ln\Big|\frac{C_{\alpha\beta\gamma}}{Y'_{\alpha\beta\gamma}}\Big| + \sum_i \frac{1}{2\pi}(l\psi_i^\alpha \sin(2\pi\theta_i^\alpha) + \alpha \to \beta + \alpha \to \gamma)\Big]\Big) \times m_{3/2}. \quad (285)$$

If we then use (268) together with (266) and $\mathcal{Q}_{\bar{\alpha}\beta} = (\tilde{K}_\alpha)^{-1/2}\delta_{\bar{\alpha}\beta}$, we obtain the following expression for the trilinears:

$$A_{\alpha\beta\gamma} = m_{3/2} e^{-i\gamma_W}\Big(1 + \frac{2}{(Q-P)\phi_0^2} + \frac{7}{\phi_0^2 P \ln(\frac{A_1 Q}{A_2 P})}\Big) \times \Big(\phi_0^2 + \frac{1}{P\ln(\frac{A_1 Q}{A_2 P})}\Big[7 + 2\ln\Big|\frac{C_{\alpha\beta\gamma}}{Y_{\alpha\beta\gamma}}\Big| - 3\ln(4\pi^{1/3}V_X) + \phi_0^2 - \sum_i\Big(\Big\{\frac{1}{2}\ln\Big(\frac{\Gamma(1-\theta_i^\alpha)}{\Gamma(\theta_i^\alpha)}\Big) - \frac{1}{2\pi} l\psi_i^\alpha \sin(2\pi\theta_i^\alpha)\Big\} + \alpha \to \beta + \alpha \to \gamma\Big)\Big]\Big). \quad (286)$$

Imposing the constraint equation (207) on the expression above, the reduced trilinears for a dS vacuum with a tiny cosmological constant are simplified to

$$A_{\alpha\beta\gamma} = e^{-i\gamma_W}\Big(\frac{69 + 22\sqrt{3}}{72} + \frac{139 + 396\sqrt{3}}{34\,356}\Big[7 + 2\ln\Big|\frac{C_{\alpha\beta\gamma}}{Y_{\alpha\beta\gamma}}\Big| - 7\ln\Big(\frac{14(P+3)}{N}\Big) + \frac{1}{72}(15 + 22\sqrt{3}) - 6\ln\Big(\frac{2}{\pi}\Big) - \sum_i\Big(\Big\{\frac{1}{2}\ln\Big(\frac{\Gamma(1-\theta_i^\alpha)}{\Gamma(\theta_i^\alpha)}\Big) - \frac{1}{2\pi} l\psi_i^\alpha \sin(2\pi\theta_i^\alpha)\Big\} + \alpha \to \beta + \alpha \to \gamma\Big)\Big]\Big) \times m_{3/2},$$
$$A_{\alpha\beta\gamma} \approx e^{-i\gamma_W}\Big(1.4876 + 0.024\Big[10.45 + 2\ln\Big|\frac{C_{\alpha\beta\gamma}}{Y_{\alpha\beta\gamma}}\Big| - 7\ln\Big(\frac{14(P+3)}{N}\Big) - \sum_i\Big(\Big\{\frac{1}{2}\ln\Big(\frac{\Gamma(1-\theta_i^\alpha)}{\Gamma(\theta_i^\alpha)}\Big) - \frac{1}{2\pi} l\psi_i^\alpha \sin(2\pi\theta_i^\alpha)\Big\} + \alpha \to \beta + \alpha \to \gamma\Big)\Big]\Big) \times m_{3/2}. \quad (287)$$

We see that compared to the gauginos, the trilinears depend on more constants. The quantity $\{\frac{1}{2}\ln(\frac{\Gamma(1-\theta_i^\alpha)}{\Gamma(\theta_i^\alpha)}) - \frac{1}{2\pi}(l\psi_i^\alpha \sin(2\pi\theta_i^\alpha)\}$ is of $\mathcal{O}(1)$. Therefore, in a generic situation, we expect the terms inside the sum in $\sum_i\{\frac{1}{2} \times \ln(\frac{\Gamma(1-\theta_i^\alpha)}{\Gamma(\theta_i^\alpha)}) - \frac{1}{2\pi}(l\psi_i^\alpha \sin(2\pi\theta_i^\alpha)\}$ to partially cancel each other and give an overall contribution much smaller than the first three terms inside the square brackets. Then, for known values of the physical Yukawa couplings and reasonable values of P and N, the trilinears generically turn out to be slightly larger than $m_{3/2}$.

3. Scalar masses

For an (almost) diagonal Kähler metric, the normalized scalar masses reduce to

$$(m^2_{\tilde{\alpha}\beta}) = [m^2_{3/2} + V_0 - e^{\hat{K}} F^{\bar{m}} F^n \partial_{\bar{m}}\partial_n \ln(\tilde{K}_\alpha)]\delta_{\bar{\alpha}\beta} \quad (288)$$

where we have used (267). Using (276) in (288), we obtain

the following expression for the scalar mass squared,

$$(m_\alpha^2) = V_0 + (m_{3/2}^2)\Big[1 - \frac{9}{4P^2(\ln(\frac{A_1Q}{A_2P}))^2}\Big(1 + \frac{2}{(Q-P)\phi_0^2} + \frac{7}{\phi_0^2 P \ln(\frac{A_1Q}{A_2P})}\Big)^2 \frac{1}{4\pi}\sum_i \{l^2\psi_{ii}^\alpha \sin^2(2\pi\theta_i^\alpha) + l^2\psi_i^\alpha \sin(4\pi\theta_i^\alpha) - 2l\psi_i^\alpha \sin(2\pi\theta_i^\alpha)\}\Big], \quad (289)$$

where we have defined another quantity:

$$\psi_{\bar{i}i}^\alpha(\theta_i^\alpha) \equiv \frac{d\psi_i^\alpha}{d\theta_i^\alpha}. \quad (290)$$

As in the case of the trilinears, only the overall scale of the scalars can be estimated, not the individual masses of different flavors of squarks and sleptons. Once the cosmological constant is made small by imposing the constraint (207), the scalars are given by

$$\begin{aligned}(m_\alpha^2) &= (m_{3/2}^2)\Big[1 - \frac{(139+396\sqrt{3})^2}{524593216}\frac{1}{4\pi}\sum_i \{l^2\psi_{ii}^\alpha \sin^2(2\pi\theta_i^\alpha) + l^2\psi_i^\alpha \sin(4\pi\theta_i^\alpha) - 2l\psi_i^\alpha \sin(2\pi\theta_i^\alpha)\}\Big] \\ &\approx (m_{3/2}^2)\Big[1 - \frac{0.0013}{4\pi}\sum_i \{l^2\psi_{ii}^\alpha \sin^2(2\pi\theta_i^\alpha) + l^2\psi_i^\alpha \sin(4\pi\theta_i^\alpha) - 2l\psi_i^\alpha \sin(2\pi\theta_i^\alpha)\}\Big] \\ &\approx m_{3/2}^2. \end{aligned} \quad (291)$$

Thus, to a high degree of accuracy, in the type IIA limit, the scalar masses for de Sitter vacua are flavor universal as well as flavor diagonal and independent of the details of the matter Kähler metric described by parameters θ_i. Moreover, to a very good approximation, they are equal to the gravitino mass. A natural expectation away from the type IIA limit is that the squark and slepton masses are always of order $m_{3/2}$. Since $m_{3/2}$ is of several TeV, the scalars are quite heavy, naturally suppressing flavor changing neutral currents (FCNCs).

C. Subleading corrections to the condition for a small cosmological constant and effects on phenomenology

In this subsection we would like to give a rough estimate of how the amount of tuning of the cosmological constant might affect the values of the soft parameters. In fact, the constraint (207) which sets the cosmological constant to zero in the leading order still results in a very large value of the cosmological constant $V_0 \sim 0.01 \times m_{3/2}^2 m_p^2$, once the subleading terms are taken into account. One can also do exact numerical computations for manifolds with a small number of moduli (say two).

Taking into account the terms in the subleading order as $\tilde{y} \to 0$, the potential at the minimum with respect to the moduli, as a function of the meson vev ϕ_0, is given by

$$V_0 = \frac{(A_2\tilde{x})^2}{64\pi V_X^3}\Big[\phi_0^4 + \Big(\frac{2a\tilde{\alpha}}{\tilde{x}} - 3 + \frac{1}{7}\Big(\frac{ab_1\tilde{\alpha}\,\tilde{y}}{\tilde{x}\,\tilde{z}}\Big)^2 \times \Big(\frac{a\tilde{\alpha}}{\phi_0^2\tilde{x}} + 1\Big)^2\Big)\phi_0^2 + \Big(\frac{a\tilde{\alpha}}{\tilde{x}}\Big)^2\Big]\frac{e^{\phi_0^2}}{\phi_0^2}\Big(\frac{A_1Q}{A_2P}\Big)^{-(2P/(Q-P))}. \quad (292)$$

Hence, vanishing of the cosmological constant corresponds to the vanishing of the combination

$$\phi_0^4 + \Big(\frac{2a\tilde{\alpha}}{\tilde{x}} - 3 + \frac{1}{7}\Big(\frac{ab_1\tilde{\alpha}\,\tilde{y}}{\tilde{x}\,\tilde{z}}\Big)^2\Big(\frac{a\tilde{\alpha}}{\phi_0^2\tilde{x}} + 1\Big)^2\Big)\phi_0^2 + \Big(\frac{a\tilde{\alpha}}{\tilde{x}}\Big)^2 = 0. \quad (293)$$

Recall that by imposing this condition in the leading order as $\tilde{y} \to 0$ we had demonstrated that the combination $P\ln(\frac{A_1Q}{A_2P})$ is fixed by

$$3 - \frac{8}{Q-P} - \frac{28}{P\ln(\frac{A_1Q}{A_2P})} = 0. \quad (294)$$

Thus, the leading order condition on $P\ln(\frac{A_1Q}{A_2P})$ obtained from (294) is given by

$$\Big(P\ln\Big(\frac{A_1Q}{A_2P}\Big)\Big)^{(0)} = \frac{28(Q-P)}{3(Q-P)-8}. \quad (295)$$

In this case, the meson vev ϕ_0^2 in the leading order is fixed at the value

$$(\phi_0^2)^{(0)} = -\frac{1}{8} + \frac{1}{Q-P} + \frac{1}{4}\sqrt{1 - \frac{2}{Q-P}} + \frac{2}{Q-P}\sqrt{1 - \frac{2}{Q-P}}. \quad (296)$$

The subleading corrections to $P\ln(\frac{A_1Q}{A_2P})$ can be found iteratively if we plug (296) into the subleading term $\sim\tilde{y}^2$ in (293) to obtain

$$\phi_0^4 + \Big(\frac{2a\tilde{\alpha}}{\tilde{x}} - 3 + \frac{1}{7}\Big(\frac{ab_1\tilde{\alpha}\,\tilde{y}}{\tilde{x}\,\tilde{z}}\Big)^2\Big(\frac{a\tilde{\alpha}}{(\phi_0^2)^{(0)}\tilde{x}} + 1\Big)^2\Big)\phi_0^2 + \Big(\frac{a\tilde{\alpha}}{\tilde{x}}\Big)^2 = 0. \quad (297)$$

Again, by setting the discriminant of the biquadratic polynomial in (297) to zero and using

$$\tilde{L}_{1,+} = -\frac{3}{2} + \frac{3}{2P\ln(\frac{A_1Q}{A_2P})}\Big(1 + \frac{2}{(Q-P)(\phi_0^2)^{(0)}}\Big), \quad (298)$$

we obtain the following condition on $P\ln(\frac{A_1Q}{A_2P})$:

$$3 - \frac{8}{Q-P} - \frac{28}{P\ln(\frac{A_1Q}{A_2P})} + \frac{7}{(P\ln(\frac{A_1Q}{A_2P}))^2} \times \left(3 - \frac{4}{(\phi_0^4)^{(0)}(Q-P)^2} + \frac{4}{(\phi_0^2)^{(0)}(Q-P)}\right) = 0. \tag{299}$$

To compute the first subleading order correction to $P\ln(\frac{A_1Q}{A_2P})$ we express

$$P\ln\left(\frac{A_1Q}{A_2P}\right) = \frac{28(Q-P)}{3(Q-P)-8} + \delta^{(1)}, \tag{300}$$

where the first term in (300) corresponds to the leading order expression in (295) and $\delta^{(1)}$ is the subleading order correction. Hence, plugging (300) into (299) and keeping the terms linear in $\delta^{(1)}$, after some algebra we obtain

$$\delta^{(1)} = \frac{(2 + (\phi_0^2)^{(0)}(Q-P))(2 - 3(\phi_0^2)^{(0)}(Q-P))}{4(\phi_0^4)^{(0)}(Q-P)^2}. \tag{301}$$

Therefore, after including the first subleading order, the condition on the cosmological constant to vanish results in the following constraint:

$$P\ln\left(\frac{A_1Q}{A_2P}\right) = \frac{28(Q-P)}{3(Q-P)-8} + \frac{(2+(\phi_0^2)^{(0)}(Q-P))(2-3(\phi_0^2)^{(0)}(Q-P))}{4(\phi_0^4)^{(0)}(Q-P)^2}. \tag{302}$$

In particular, for the case when $Q - P = 3$ we obtain

$$P\ln\left(\frac{A_1Q}{A_2P}\right) = 84 - 0.9977 \approx 83.002, \tag{303}$$

which yields a $\sim$1% correction to the leading order. We have confirmed that for a case when the compactification manifold has two moduli, numerically imposing the constraint that the cosmological constant has the observed value implies

$$P\ln\left(\frac{A_1Q}{A_2P}\right) \approx 82.9958, \tag{304}$$

which agrees with (303) to a very high degree of accuracy.

One would now like to estimate the effects of tuning the cosmological constant to its observed value on phenomenological quantities. The quantity most sensitive to such corrections is the gravitino mass, since it is proportional to $(\frac{A_1Q}{A_2P})^{-(P/(Q-P))}$ and can therefore change by a factor of order 1. Of course, this hardly affects the distributions of scales of $m_{3/2}$, and the emergence of the TeV scale peak remains very robust. Moving on to gaugino masses, recall that the tree-level gaugino mass is given by

$$M_{1/2} \approx -\frac{e^{-i\gamma_W}}{P\ln(\frac{A_1Q}{A_2P})}\left(1 + \frac{2}{\phi_0^2(Q-P)} + \frac{7}{\phi_0^2 P\ln(\frac{A_1Q}{A_2P})}\right) \times m_{3/2}, \tag{305}$$

which for $Q - P = 3$ and the leading order constraint $(P\ln(\frac{A_1Q}{A_2P}))^{(0)} = 84$ resulted (up to an overall phase) in

$$(M_{1/2})^{(0)} \approx -0.0240 \times m_{3/2}. \tag{306}$$

Including the first subleading correction in (303), the tree-level gaugino mass (up to an overall phase) is given by

$$M_{1/2} \approx -\frac{1}{83}\left(1 + \frac{2}{3(\phi_0^2)^{(0)}} + \frac{7}{84(\phi_0^2)^{(0)}}\right) \times m_{3/2} = -0.0243 \times m_{3/2}, \tag{307}$$

resulting in a $\sim$1% correction to the leading order expression in (306). For a case when the compactification manifold has two moduli, the numerically obtained result is given by

$$M_{1/2} \approx -0.0242 \times m_{3/2}, \tag{308}$$

again confirming the high accuracy of the approximate result in (307). Recall that when the leading order constraint $P\ln(\frac{A_1Q}{A_2P}) \approx 84$ is satisfied the value of the cosmological constant is

$$V_0 \sim 0.01 m_{3/2}^2 m_p^2 \sim (\mathcal{O}(10^{10} - 10^{11})\ \text{GeV})^4 \tag{309}$$

for $m_{3/2} \sim \mathcal{O}$(10–100) TeV. Thus, while the cosmological constant changes by many orders of magnitude as it is tuned to its observed value, the tuning has a very small effect on the tree-level gaugino mass. However, due to the cancellation between the tree-level and the anomaly mediated contributions, the correction to the tree-level gaugino mass computed above may be important and, therefore, has been taken into account.

Finally, the $\sim$1% correction to the leading order $(P\ln(\frac{A_1Q}{A_2P}))^{(0)}$ due to the tuning of the cosmological constant has almost no effect on the anomaly mediated gaugino masses, trilinears, and the scalars. This is because the terms proportional to $1/P\ln(\frac{A_1Q}{A_2P})$ and $1/(P\ln(\frac{A_1Q}{A_2P}))^2$ are subleading. These considerations indicate that a leading order tuning of the cosmological constant is enough to allow reliable particle physics phenomenology.

D. Radiative electroweak symmetry breaking

It is very important to check whether the soft supersymmetry breaking parameters in these vacua naturally give rise to radiative electroweak symmetry breaking (REWSB) at low scales. In order to check that, one has to first RG evolve the scalar Higgs mass parameters $m^2_{H_u}$ and $m^2_{H_d}$ from the high scale to low scales. Then one has to check whether, for a given $\tan\beta$, there exists a value of μ which satisfies the EWSB conditions. At the one-loop level, we find that EWSB occurs quite generically in the parameter space. This can be understood as follows. The gaugino mass contributions to the RG equation (RGE) for $m^2_{H_u}$ push the value of $m^2_{H_u}$ up while the top Yukawa coupling, third generation squark masses and the top trilinear pull it down. The suppression of the gaugino mass relative to the gravitino mass causes it to have a negligible effect on the RGE evolution of $m^2_{H_u}$. On the other hand, the masses of squarks and A-terms are both of $\mathcal{O}(m_{3/2})$, which guarantees that $m^2_{H_u}$ is negative at the low scale. Typically, $m^2_{H_u}$ is proportional to $-m^2_{3/2}$, up to a factor less than 1 depending on $\tan\beta$. Thus, the EWSB condition can be easily satisfied with a μ parameter also of the order $m_{3/2}$. Note that large A-terms [of $\mathcal{O}(m_{3/2})$] are crucial for obtaining EWSB. Having large squark masses and small A-terms cannot guarantee EWSB, as is known from the focus point region in mSUGRA. Also, one has to ensure that the third generation squarks have positive squared masses, which we have checked. From the point of view of low scale effective theory, EWSB appears to be fine-tuned; however, a better understanding of the underlying microscopic theory may help justify the choice of parameters. We will report a detailed analysis of these issues in [12].

E. The μ and $B\mu$ problem

We will not have much to say about the μ terms here, leaving a detailed phenomenological study for our future work [12]. We will, however, take this opportunity to highlight the main theoretical issues. The normalized μ and $B\mu$ parameters are

$$\mu = \left(\frac{\hat{W}^\star}{|\hat{W}|} e^{\hat{K}/2}\mu' + m_{3/2}Z - e^{\hat{K}/2}F^{\bar{m}}\partial_{\bar{m}}Z\right)(\tilde{K}_{H_u}\tilde{K}_{H_d})^{-1/2},$$

$$\begin{aligned} B\mu = (\tilde{K}_{H_u}\tilde{K}_{H_d})^{-1/2}\Big\{&\frac{\hat{W}^\star}{|\hat{W}|} e^{\hat{K}/2}\mu'(e^{\hat{K}/2}F^m \\ &\times [\hat{K}_m + \partial_m \ln\mu'] - m_{3/2}) + (2m^2_{3/2} + V_0)Z \\ &- m_{3/2}F^{\bar{m}}\partial_{\bar{m}}Z + m_{3/2}F^m[\partial_m Z - Z\partial_m \ln(\tilde{K}_{H_u}\tilde{K}_{H_d})] \\ &- F^{\bar{m}}F^n[\partial_{\bar{m}}\partial_n Z - \partial_{\bar{m}}Z\partial_n \ln(\tilde{K}_{H_u}\tilde{K}_{H_d})]\Big\}. \end{aligned} \quad (310)$$

We see from above that the values of the physical μ and $B\mu$ parameters depend crucially on many of the microscopic details, e.g. if the theory gives rise to a nonzero superpotential μ' parameter and/or if a nonzero bilinear coefficient Z is present in the Kähler potential for the Higgs fields. From Sec. VIII D, we see that one requires a μ term of $\mathcal{O}(m_{3/2})$ to get consistent radiative EWSB. This is possible for e.g. when one has a vanishing μ' parameter and an $\mathcal{O}(1)$ Higgs bilinear coefficient Z, among other possibilities.

F. Dark matter

For dS vacua with a small cosmological constant, $M_2 \ll M_1$ at low scale. In addition, since μ should be of $\mathcal{O}(m_{3/2})$ for consistent EWSB as seen in Sec. VIII D, both M_2 and M_1 are much less than μ. Hence, the LSP is W-ino-like. As was discussed in Sec. VIII C, the tuning of the cosmological constant has little effect on the gaugino masses, thereby preserving the gaugino mass hierarchy. It is well known that W-inos coannihilate quite efficiently as the universe cools down. Since the W-ino masses in these vacua are $\mathcal{O}(100)$ GeV, the corresponding thermal relic density after they freeze out is very small. However, there could be nonthermal contributions to the dark matter as well, e.g. the decay of moduli fields into the LSP after the LSP freezes out. In addition, one should remember that the above result for a W-ino LSP is obtained after imposing the requirement of a small cosmological constant. It would be interesting to analyze the more general case where the results may change. We leave a full analysis of these possibilities for the future [12].

G. Correlations

As we have seen, the parameters of the MSSM depend on the ''microscopic constants'' determined by a given G_2 manifold and can be explicitly calculated, in principle. Therefore, the parameters obtained are correlated with each other, in general. For instance, we saw that the gaugino and gravitino masses are related. By scanning over the allowed values of the microscopic constants within the space of G_2 manifolds, one obtains a particular subspace of the parameter space of the MSSM at the unification scale. For a given spectrum and gauge group, the RG evolution of these parameters to low scales can also be determined unambiguously, leading to correlations in soft parameters at the low scale. Finally, these correlations in the soft parameters will lead to correlations in the space of actual observables (for, e.g., the LHC signature space) as well. In other words, the predictions of these vacua will only occupy a *finite* region of the observable signature space at, say, the LHC. Since two different theoretical constructions will have different correlations in general, this will in turn lead to different patterns of signatures at the LHC, allowing us to distinguish among different classes of string/M theory vacua (at least in principle). These issues, in particular, the systematics of the distinguishing procedure, have been explained in detail in [33].

H. Signatures at the LHC

The subject of predicting signatures at the LHC for a given class of string vacua requires considerable analysis. Here, we will make some preliminary comments, with a detailed analysis to appear in [12].

The scale of soft parameters is determined by the gravitino mass. We saw in Sec. VII D that requiring the cosmological constant to be very small by imposition of a constraint equation [Eq. (191)] fixes the overall scale of superpartner masses to be of $\mathcal{O}(1-100)$ TeV. Once the overall scale is fixed, the pattern of soft parameters at $M_{\rm unif}$ is crucial in determining the signatures at the LHC. As explained earlier, these M theory vacua give rise to a specific pattern of soft parameters at $M_{\rm unif}$. We find nonuniversal gaugino masses which are suppressed relative to the gravitino mass. We furthermore expect that the scalar masses and trilinears are of the same order as the gravitino. The μ and $B\mu$ parameters are not yet understood. For phenomenological analysis however, we may fix them by imposing consistent EWSB.

One can get a sense of the broad pattern of signatures at the LHC from the pattern of soft parameters. Since gaugino masses are suppressed and because the anomaly contribution to the gluino mass parameter approximately *cancels* the tree-level contribution, one would generically get comparatively light gluinos in these constructions, much lighter than the scalars, which would give rise to a large number of events for many signatures, in particular, many events with same-sign dileptons and trileptons in excess of the SM and many events with large missing energy, even for a modest luminosity of 10 fb^{-1}. Since the gauginos are lighter than the squarks and sleptons, gluino pair production is likely to be the dominant production mechanism. The LSP will be a neutralino for the same reason, assuming R parity is conserved.

It is also possible to distinguish the class of vacua obtained above from those obtained in type IIB compactifications, by the pattern of signatures at the LHC. For the large volume type IIB vacua, the scalars are lighter than the gluino [34], while for the Kallosh, Kachru, Linde, Trivedi (KKLT) type IIB vacua, the scalars are comparable to the gluino [35]. This implies that squark-gluino production and squark pair production are the dominant production mechanisms at the LHC. Since the LHC is a pp collider, up-type squarks are preferentially produced from t-channel valence u-quark annihilation if they are reasonably light, leading to a charge asymmetry which is preserved in cascade decays all the way to the final state with leptons. On the other hand, for the class of M theory vacua described here, since gluino pair production is the dominant mechanism and the decays of the gluino are charge symmetric (it is a Majorana particle), the M theory vacua predict a much smaller charge asymmetry in the number of events with one or two leptons and ≥ 2 jets compared to the type IIB vacua.

I. The moduli and gravitino problems

The cosmological moduli and gravitino problems can exist if moduli and gravitino masses are too light in gravity mediated SUSY breaking theories. Naively, after the end of inflation, the moduli fields coherently oscillate, dominating the energy density of the universe. Since the interactions of the moduli are suppressed by the Planck scale (m_p), their decay rates are small, perhaps leading to the onset of a radiation dominated universe at very low temperature [$T_R \sim \mathcal{O}(10^{-3})$ MeV for moduli of $\mathcal{O}(100$ GeV–5 TeV)], compared to what is required for successful big bang nucleosynthesis (BBN).

To check if the moduli and gravitino problem can be resolved in these M theory compactifications, one has to first compute the masses of the moduli. After doing this, we will use the results to discuss the moduli and gravitino problems.

The geometric moduli s_i appear in the Lagrangian with a kinetic term given by

$$\sum_{i=1}^{N} \frac{3a_i}{4s_i^2}\,\partial_\mu s_i \partial^\mu s_i, \tag{311}$$

which is noncanonical. The canonically normalized moduli χ_i are

$$\chi_i \equiv \sqrt{\frac{3a_i}{2}} \ln s_i. \tag{312}$$

The complete mass matrix including the mixed meson-moduli entries is given by

$$\begin{aligned}
(m_\chi^2)_{ij} &= \frac{2\nu^2 (a_i a_j)^{1/2}}{3N_i N_j}\,\frac{\partial^2 V}{\partial s_i \partial s_j}, \\
(m^2)_{i\phi_0} &= \sqrt{\frac{2a_i}{3}}\,\frac{\nu}{N_i}\,\frac{\partial^2 V}{\partial s_i \partial \phi_0}, \\
(m^2)_{\phi_0\phi_0} &= \frac{\partial^2 V}{\partial \phi_0^2},
\end{aligned} \tag{313}$$

where we took into account the fact that $\frac{\partial V}{\partial s_i} = 0$, $\frac{\partial V}{\partial \phi_0} = 0$ at the extremum and that $\nu_i = \nu$ for all $i = \overline{1, N}$. A fairly straightforward but rather tedious computation yields the following structure of the mass matrix:

$$\begin{aligned}
(m_\chi^2)_{ij} &= ((a_i a_j)^{1/2} K_1 + \delta_{ij} K_2) \times m_{3/2}^2, \\
(m^2)_{i\phi_0} &= (a_i)^{1/2} K_3 \times m_{3/2}^2, \\
(m^2)_{\phi_0\phi_0} &= K_4 \times m_{3/2}^2,
\end{aligned} \tag{314}$$

where, in the large ν approximation, K_1, K_2, K_3, K_4 are given by

$$
\begin{aligned}
K_1 &\approx \frac{112}{27}\left(\frac{\tilde{z}}{\tilde{x}}\right)^2 \nu^4 \approx \frac{48}{343}\left(\frac{Q}{P}\right)^2 \frac{(P\ln(\frac{A_1Q}{A_2P}))^4}{(Q-P)^4}, \\
K_2 &= -\frac{40}{9}(\tilde{L}_{1,+})^2 - \frac{56}{3}L_{1,+} - 8 - 2\phi_0^2\left(\frac{a\tilde{\alpha}}{\tilde{x}\phi_0^2}+1\right)^2 \\
&\approx 10 - \frac{8}{Q-P} - \frac{8}{(Q-P)^2\phi_0^2} - 2\phi_0^2 - \frac{36}{P\ln(\frac{A_1Q}{A_2P})}\left(1+\frac{2}{(Q-P)\phi_0^2}\right), \\
K_3 &\approx -\sqrt{\frac{2}{3}}\frac{56ab_1\tilde{\alpha}\,\tilde{z}}{9\phi_0\tilde{x}^2}\nu^3 \approx \sqrt{\frac{2}{3}}\left(\frac{48}{49}\right)\left(\frac{Q}{P}\right)^2 \frac{(P\ln(\frac{A_1Q}{A_2P}))^3}{(Q-P)^4\phi_0}, \qquad K_4 \approx \frac{32}{7}\frac{(Q\ln(\frac{A_1Q}{A_2P}))^2}{(Q-P)^4\phi_0^2}.
\end{aligned}
\tag{315}
$$

Using condition $P\ln(\frac{A_1Q}{A_2P}) = 84$ to tune the cosmological constant together with $Q - P = 3$, we obtain from (315)

$$
K_1 \approx 86\,016\left(\frac{Q}{P}\right)^2, \qquad K_2 \approx 3.83, \qquad K_3 \approx 6815\left(\frac{Q}{P}\right)^2, \qquad K_4 \approx 540\left(\frac{Q}{P}\right)^2. \tag{316}
$$

We can diagonalize the matrix (314) in two steps. We first construct a set of orthogonal (unnormalized) $N+1$ vectors given by

$$
\vec{x}_1 = \begin{pmatrix} \sqrt{a_1} \\ -\frac{a_1}{\sqrt{a_2}} \\ 0 \\ \cdot \\ \cdot \\ \cdot \\ 0 \\ 0 \end{pmatrix}, \qquad \vec{x}_2 = \begin{pmatrix} \sqrt{a_1} \\ \sqrt{a_2} \\ -\frac{a_1+a_2}{\sqrt{a_3}} \\ 0 \\ \cdot \\ \cdot \\ 0 \\ 0 \end{pmatrix}, \ldots, \qquad \vec{x}_{N-1} = \begin{pmatrix} \sqrt{a_1} \\ \sqrt{a_2} \\ \sqrt{a_3} \\ \cdot \\ \cdot \\ \cdot \\ -\frac{\sum_{i=1}^{N-1} a_i}{\sqrt{a_N}} \\ 0 \end{pmatrix}, \qquad \vec{x}_N = \begin{pmatrix} \sqrt{a_1} \\ \sqrt{a_2} \\ \sqrt{a_3} \\ \cdot \\ \cdot \\ \cdot \\ \sqrt{a_N} \\ 0 \end{pmatrix}, \qquad \vec{x}_{N+1} = \begin{pmatrix} 0 \\ 0 \\ 0 \\ \cdot \\ \cdot \\ \cdot \\ 0 \\ 1 \end{pmatrix}.
$$

Next, we normalize the above vectors and construct an orthogonal $(N+1)\times(N+1)$ matrix,

$$
\mathcal{R} = \left(\frac{\vec{x}_1}{|\vec{x}_1|}, \frac{\vec{x}_2}{|\vec{x}_2|}, \ldots, \frac{\vec{x}_{N+1}}{|\vec{x}_{N+1}|}\right). \tag{317}
$$

By applying the orthogonal transformation $\mathcal{R}$, the mass matrix in (314) is converted into a block-diagonal form given by

$$
\begin{pmatrix}
K_2 & 0 & \ldots & 0 & 0 & 0 \\
0 & K_2 & \ldots & 0 & 0 & 0 \\
\cdot & \cdot & \cdots & \cdot & \cdot & \cdot \\
\cdot & \cdot & \cdots & \cdot & \cdot & \cdot \\
\cdot & \cdot & \cdots & \cdot & \cdot & \cdot \\
0 & 0 & \ldots & K_2 & 0 & 0 \\
0 & 0 & \ldots & 0 & \frac{7}{3}K_1 + K_2 & \sqrt{\frac{7}{3}}K_3 \\
0 & 0 & \ldots & 0 & \sqrt{\frac{7}{3}}K_3 & K_4
\end{pmatrix}.
$$

Hence, the first $N-1$ eigenvalues are given by

$$
\lambda_i = K_2 \quad \text{for } i = 1, \ldots, N-1. \tag{318}
$$

Diagonalizing the 2×2 block is then trivial and boils down to solving a simple quadratic equation. Since for typical values of Q and P we have

$$
\frac{K_3}{K_1} \lesssim 0.07 \quad \text{and} \quad \frac{K_2}{K_1} \ll 1, \tag{319}
$$

the corresponding eigenvalues are given by

$$
\lambda_N \approx \frac{7}{3}K_1, \qquad \lambda_{N+1} \approx K_4 - \frac{K_3^2}{K_1}. \tag{320}
$$

Because of the significant cancellation due to the minus sign in λ_{N+1} we have to go beyond the leading order approximation in (316) when computing K_1, K_3, and K_4. For dS vacua with a nearly zero cosmological constant, we have verified numerically that the corresponding eigenvalue is always positive, confirming that we have obtained a stable minimum. The $N-1$ degenerate light states have masses given by

$$
\begin{aligned}
M_k &\approx \sqrt{K_2} \times m_{3/2} \approx 1.96 \times m_{3/2}, \\
k &= 1, \ldots, N-1,
\end{aligned}
\tag{321}
$$

independent of any parameters of the model. For dS vacua with a very small cosmological constant, numerical computations for the choice $P = 27$, $Q = 30$ give the following masses for the remaining two states:

$$
M_N \approx 600 \times m_{3/2}, \qquad M_{N+1} \approx 2.82 \times m_{3/2}. \tag{322}
$$

Note that all the masses are independent of the number of moduli N as well as the rationals a_i.

Since the gravitino mass distribution peaks at $\mathcal{O}(100)$ TeV, which is also in the phenomenologically relevant range, and the light moduli are roughly twice as

heavy compared to the gravitino, the moduli masses are heavy enough to be consistent with BBN constraints. A detailed study of this issue will appear in [12].

IX. SUMMARY AND CONCLUSIONS

A major goal of string/M theory is to find solutions that incorporate the standard model, important clues to physics beyond the SM such as gauge coupling unification, and in addition explain phenomena the SM cannot explain. The most important unsolved problem is explaining the value of the weak scale (at or below about a TeV) purely in terms of the Planck scale of $\mathcal{O}(10^{19}$ GeV) or some other fundamental scale, the hierarchy problem. One obstacle to solving the hierarchy problem is that all the moduli that characterize the string theory vacuum must be stabilized for a meaningful solution.

In fluxless M theory vacua the entire effective potential is generated by nonperturbative effects and depends upon all the moduli. In this paper we have studied this potential in detail for a particular form of the Kähler potential when the nonperturbative effects are dominated by strong gauge dynamics in the hidden sector and when such vacua are amenable to the supergravity approximation. In the simplest case, we studied G_2 manifolds giving rise to two hidden sectors. The resulting scalar potential has AdS vacua—most of them with broken supersymmetry and one supersymmetric. Then we studied the cases in which there was also charged matter in the hidden sector under the plausible assumption that the matter Kähler potential has weak moduli dependence. In these cases the potential receives positive contributions from nonvanishing F-term vevs for the hidden sector matter leading to a unique de Sitter minimum. The de Sitter minimum is obtained without adding any ''uplifting'' terms, such as those coming from antibranes, which explicitly break supersymmetry. With the form of the Kähler potential given by (1), we have explicitly shown that all moduli are stabilized by the potential generated by strong dynamics in the hidden sector.

In the de Sitter minimum we computed $m_{3/2}$ and found that a significant fraction of solutions have $m_{3/2}$ in the TeV region, even though the Planck scale is the only dimensionful parameter in the theory. The suppression of $m_{3/2}$ is due to the old idea of dimensional transmutation, which has also been used in heterotic string theory. The 11-dimensional M theory scale turns out to be slightly above the gauge unification scale but below the Planck scale. The absence of fluxes is significant for simultaneously having $m_{3/2} \sim$ TeV naturally and M_{11} not far below the Planck scale.

The problem of why the cosmological constant is not large is of course not solved by this approach. We do however understand to a certain extent what properties of G_2 manifolds are required in order to solve it. We suggest that one can set the value of the potential at the minimum to zero at tree level and proceed to do phenomenology with the superpartners whose masses are described by the softly broken Lagrangian. One particularly nice feature is that we are able to explicitly demonstrate that the soft-breaking terms are not sensitive to the *precise* value of the potential at the minimum. A tree-level tuning of the cosmological constant is enough to determine the phenomenology.

When we set the value of the potential at the minimum to zero at tree level a surprising result occurs. Doing so gives a nontrivial condition on the solutions. When this condition is imposed on $m_{3/2}$, for generic G_2 manifolds it turns out that the resulting values of $m_{3/2}$ are all in the TeV region. Thus we do not have to independently set V_0 to zero *and* set $m_{3/2}$ to the TeV region, as has been required in previous approaches.

A more detailed study of the phenomenology of these vacua, particularly for LHC and for dark matter, is underway and will be reported in a future paper. In the present paper we presented the relevant soft-breaking Lagrangian parameters and mentioned a few broad and generic features of the phenomenology, for both our generic solutions and for the case where V_0 is set to zero at tree level. We presented a standard supergravity calculation of the soft-breaking Lagrangian parameters, and found that the scalar masses m_α, and also the trilinears, are approximately equal to $m_{3/2}$, to the extent that our assumptions about the matter Kähler potential are valid. Remarkably, the tree-level gaugino masses are suppressed by a factor of $\mathcal{O}$(10–100). This suppression is present for all G_2 manifolds giving the type of de Sitter minimum described here. For calculating the tree-level gaugino masses the matter Kähler potential does not enter, so the obtained values at tree level are reliable. Because the gaugino suppression is large, the anomaly mediated mass contributions are comparable to the tree-level ones, and significant cancellations can occur. Gluinos are generically quite light, and should be produced copiously at the LHC and perhaps even at the Tevatron—this is an unavoidable prediction of our approach. We have also checked that radiative electroweak symmetry breaking occurs over a large part of the space of G_2 manifolds, and that the lightest neutralino is a good dark matter candidate. It will be exciting to pursue a number of additional phenomenological issues in our approach, including inflation, baryogenesis, flavor and CP-violation physics, Yukawa couplings, and neutrino masses.

The approach we describe here apparently offers a framework that can simultaneously address many important questions, from formal ones to cosmological ones to phenomenological ones (apart from the cosmological constant problem, which might be solved in a different way). Clearly, however, much work remains to be done. In particular, a much deeper understanding of G_2 manifolds is required to better understand some of the assumptions we made about the Kähler potential of these vacua.

ACKNOWLEDGMENTS

The authors appreciate helpful conversations with and suggestions from Jacob Bourjaily, Lisa Everett, Sergei Gukov, Renata Kallosh, James Liu, Joseph Lykken, David Morrissey, Brent Nelson, Aaron Pierce, Fernando Quevedo, Diana Vaman, Lian-Tao Wang, and James Wells. G. L. K. and P. K. thank the Kavli Institute for Theoretical Physics (KITP), UCSB for its hospitality where part of the research was conducted. The research of G. L. K. and P. K. is supported in part by the U.S. Department of Energy and in part by the National Science Foundation under Grant No. PHY99-07949. The research of K. B. and J. S. is supported in part by the Department of Energy.

APPENDIX A: KÄHLER METRIC FOR VISIBLE CHIRAL MATTER IN M THEORY

As stated in Sec. VIII B, we will generalize the result obtained for the Kähler metric for visible sector chiral matter fields in toroidal orientifold constructions in type IIA [28] to that in M theory. The result obtained for the Kähler metric for the (twisted) chiral matter fields (ϕ_α) in the supergravity limit ($\alpha' \to 0$) in [28] is

$$\tilde{K}^0_{\bar{\alpha}\beta} = \prod_{i=1}^{3}\left(\frac{\Gamma(1-\theta_i^\alpha)}{\Gamma(\theta_i^\alpha)}\right)^{1/2}\delta_{\bar{\alpha}\beta},$$
$$\tan(\pi\theta_i^\alpha) = \frac{U_2^i}{U_1^i + q_i^\alpha/p_i^\alpha}; \qquad U^i \equiv U_1^i + iU_2^i, \tag{A1}$$

where $i = 1, 2, 3$ denote the number of moduli in the specific type IIA example, $\{p, q\}$ are integers, and U^i are the complex structure moduli in type IIA in the geometrical basis. As mentioned before, we will restrict to factorized rectangular tori with commuting magnetic fluxes, for which $U_1^i = 0$. Then

$$\tan(\pi\theta_i^\alpha) = \frac{p_i^\alpha}{q_i^\alpha}U_2^i. \tag{A2}$$

The first step towards the generalization is to identify the G_2 moduli in terms of type IIA toroidal moduli by imposing consistency between results of type IIA and M theory. The consistency check is the formula for κ^2—the physically measured four-dimensional gravitational coupling. We have

$$\kappa^2 = \frac{\kappa_{11}^2}{\mathrm{Vol}(X_7)}, \qquad M \text{ theory [19]};$$
$$\kappa^2 = \frac{\kappa_{10}^2 g_s^2}{\mathrm{Vol}(X_6)}, \quad \text{IIA string theory (Eq. 18.2.2 of [37])}, \tag{A3}$$

where X_7 and X_6 are the volumes of the internal seven-manifold and six-manifold (in type IIA), respectively. The M theory gravitational coupling κ_{11}^2 and the string theory gravitational coupling κ_{10}^2 can be written in terms of the string coupling in type IIA ($g_s \equiv e^{\phi_{10}^A}$) and α':

$$\kappa_{11}^2 = \tfrac{1}{2}(2\pi)^8 g_s^3 (\alpha')^{9/2} \text{ [19]},$$
$$\kappa_{10}^2 = \tfrac{1}{2}(2\pi)^7 \alpha'^4 \quad \text{(Eq. 13.3.24 of [37])}. \tag{A4}$$

Also, the volumes of X_7 and X_6 (for a type IIA toroidal orientifold) can be written as

$$\mathrm{Vol}(X_7) = V_X l_M^7 \quad \text{where } V_X = \prod_{i=1}^{N}(s_i)^{a_i}; \qquad \frac{l_M^9}{4\pi} = \kappa_{11}^2 \text{ [18]},$$
$$\mathrm{Vol}(X_6) = (2\pi R_1^{(1)})(2\pi R_2^{(1)})(2\pi R_1^{(2)})(2\pi R_2^{(2)}) \times (2\pi R_1^{(3)})(2\pi R_2^{(3)}). \tag{A5}$$

Using (A4), we get

$$l_M = 2\pi\alpha'^{1/2} g_s^{1/3}, \tag{A6}$$

which gives rise to the following expression for κ in M theory:

$$\kappa^2 = \frac{\pi\alpha' g_s^{2/3}}{V_X}. \tag{A7}$$

In type IIA string theory, the definition of the type IIA moduli T_i and U_i in terms of the geometry of the torus is given below. We will stick to the case of a factorized T^6, rectangular tori, and commuting magnetic fluxes (in the type IIB dual) for simplicity, in which case only the imaginary parts of the moduli are important:

$$\mathrm{Im}(T)^i \equiv T_2^{(i)} = \frac{R_2^{(i)}}{R_1^{(i)}}, \quad \mathrm{Im}(U)^i \equiv U_2^{(i)} = \frac{R_1^{(i)} R_2^{(i)}}{\alpha'}; \quad i = 1, 2, 3, \tag{A8}$$

where $R_1^{(i)}$, $R_2^{(i)}$ are the radii of the ith type IIA torus along the x and y axes, respectively.

Now, from (A3)–(A5) and (A8) we get

$$\kappa^2 = \frac{\pi\alpha' g_s^2}{U_2^{(1)} U_2^{(2)} U_2^{(3)}}. \tag{A9}$$

Combining (A7) and (A9) gives

$$V_X = \frac{U_2^{(1)} U_2^{(2)} U_2^{(3)}}{g_s^{4/3}}. \tag{A10}$$

The above formula [Eq. (A10)] is quite general and should always hold,[9] since it has been derived by requiring consistency between formulas for the physically measured gravitational coupling constant. Identifying the individual G_2 moduli, however, is harder and model dependent. In the next subsection, we will do the mapping for the case of a simple toroidal G_2 orbifold (T^7/Z_3) considered in [36], where it can be shown that Eq. (A10) is satisfied.

[9]Within the limits of the type IIA setup considered.

1. Particular case

In [36], the definitions of the G_2 moduli [Eq. (2.4)] and the Kähler potential [Eq. (2.10)] are not given in a dimensionless form. Therefore, we will make them dimensionless as is done in [18]. So, we have

$$s^i \equiv \frac{a^i}{l_M^3} = \frac{\int_{C^i} \tilde{\phi}}{l_M^3}; \qquad K = -3\ln\left(\frac{\mathrm{Vol}(X_7)}{l_M^7}\right) + \text{constant}. \tag{A11}$$

The volume of the manifold and the moduli in this compactification are explicitly given as [36]

$$\begin{aligned} &\mathrm{Vol}(X_7) = \prod_{i=1}^{7} R_i; \qquad a^1 = R_1R_2R_7; \qquad a^2 = R_1R_3R_6; \\ &a^3 = R_1R_4R_5; \qquad a^4 = R_2R_3R_5; \qquad a^5 = R_2R_4R_6; \\ &a^6 = R_3R_4R_7; \qquad a^7 = R_5R_6R_7. \end{aligned} \tag{A12}$$

From (A12), we can write $\mathrm{Vol}(X_7) = (a^1a^2a^3a^4a^5a^6a^7)^{1/3}$, which implies that $V_X = \prod_{i=1}^{7}(s_i)^{1/3}$. Therefore, in the notation of [18], $a_i = 1/3$; $i = 1, 2, \ldots, 7$. We will identify the M theory circle radius as R_7; the remaining six radii can just be identified as the x and y radii of the three tori in type IIA:

$$\begin{aligned} &R_1 = (2\pi)R_1^{(1)}; \qquad R_2 = (2\pi)R_2^{(1)}; \qquad R_3 = (2\pi)R_1^{(2)}; \\ &R_4 = (2\pi)R_2^{(2)}; \qquad R_5 = (2\pi)R_1^{(3)}; \qquad R_6 = (2\pi)R_2^{(3)}; \\ &R_7 = (2\pi)g_s\alpha'^{1/2}. \end{aligned} \tag{A13}$$

With these identifications, and using (A6), we can write the individual G_2 moduli in terms of the type IIA moduli:

$$\begin{aligned} &s^1 = U_2^{(1)}; \qquad s^6 = U_2^{(2)}; \qquad s^7 = U_2^{(3)}; \\ &s_2 = \frac{1}{g_s}\left(\frac{T_2^{(3)}U_2^{(1)}U_2^{(2)}U_2^{(3)}}{T_2^{(1)}T_2^{(2)}}\right)^{1/2}; \\ &s_3 = \frac{1}{g_s}\left(\frac{T_2^{(2)}U_2^{(1)}U_2^{(2)}U_2^{(3)}}{T_2^{(1)}T_2^{(3)}}\right)^{1/2}; \\ &s_4 = \frac{1}{g_s}\left(\frac{T_2^{(1)}U_2^{(1)}U_2^{(2)}U_2^{(3)}}{T_2^{(2)}T_2^{(3)}}\right)^{1/2}; \\ &s_5 = \frac{1}{g_s}(T_2^{(1)}T_2^{(2)}T_2^{(3)}U_2^{(1)}U_2^{(2)}U_2^{(3)})^{1/2}. \end{aligned}$$

Therefore, we get

$$V_X = \prod_{i=1}^{7}(s^i)^{1/3} = \frac{U_2^{(1)}U_2^{(2)}U_2^{(3)}}{g_s^{4/3}} \tag{A14}$$

which is the same as (A10). So, for the particular case, this suggests the following generalization:

$$\tilde{K}_\alpha = \prod_{i=1,6,7}\left(\frac{\Gamma(1-\theta_i^\alpha)}{\Gamma(\theta_i^\alpha)}\right)^{1/2}, \quad \tan(\pi\theta_i^\alpha) = \frac{p_i^\alpha}{q_i^\alpha}s_i; \quad i = 1, 6, 7. \tag{A15}$$

2. General case

For more general G_2 manifolds with many moduli, the precise map of the individual moduli is not completely clear. However, it seems plausible that the complex structure moduli appearing in the Kähler metric in type IIA map to a subset of the G_2 moduli in a similar way, as in the particular case.

Therefore, we use the following expression for the Kähler metric for visible chiral matter fields in M theory:

$$\begin{aligned} &\tilde{K}_\alpha = \prod_{i=1}^{p}\left(\frac{\Gamma(1-\theta_i^\alpha)}{\Gamma(\theta_i^\alpha)}\right)^{1/2}; \\ &i = 1, 2, \ldots, p \le N(\equiv N); \\ &\tan(\pi\theta_i^\alpha) = c_i^\alpha(s_i)^l; \qquad c_i^\alpha = \text{constant}; \\ &l = \text{rational number of } \mathcal{O}(1). \end{aligned} \tag{A16}$$

The derivatives of the Kähler metric with respect to the moduli are very important, as they appear in the soft scalar masses, the trilinears, as well as the anomaly mediated gaugino masses, as seen from Sec. VIII B. The first derivatives appear in the trilinears and anomaly mediated gaugino masses, while the second derivatives appear in the scalar masses. For the metric in (A16), these can be written as follows:

$$\begin{aligned} &\partial_n \ln(\tilde{K}_\alpha) = \psi_n^\alpha\left(\frac{\partial\theta_n^\alpha}{\partial z^n}\right); \\ &\psi_n^\alpha(\theta_n^\alpha) \equiv \frac{1}{2}\frac{d}{d\theta_n^\alpha}\ln\left(\frac{\Gamma(1-\theta_n^\alpha)}{\Gamma(\theta_n^\alpha)}\right); \\ &\partial_{\bar{m}}\partial_n \ln(\tilde{K}_\alpha) = \delta_{\bar{m}n}\left[\psi_{\bar{n}n}^\alpha\left(\frac{\partial\theta_n^\alpha}{\partial\bar{z}^n}\right)\left(\frac{\partial\theta_n^\alpha}{\partial z^n}\right) + \psi_n^\alpha\left(\frac{\partial^2\theta_n^\alpha}{\partial\bar{z}^n\partial z^n}\right)\right]; \\ &\psi_{\bar{m}n}^\alpha(\theta_n^\alpha) \equiv \frac{d}{d\theta_m^\alpha}\psi_n^\alpha. \end{aligned} \tag{A17}$$

The functions ψ_n^α and $\psi_{\bar{n}n}^\alpha$ depend on the angular variable θ_n^α, which in turn depends on the moduli. The first and second derivatives of θ_n^α with respect to z_n are given by

$$\begin{aligned} &\frac{\partial\theta_n^\alpha}{\partial z^n} = \frac{1}{2i}\frac{\partial\theta_n^\alpha}{\partial s^n} = \frac{l}{4\pi i s^n}\sin(2\pi\theta_n^\alpha), \\ &\frac{\partial^2\theta_n^\alpha}{\partial\bar{z}^n\partial z^n} = \frac{1}{4}\frac{\partial^2\theta_n^\alpha}{\partial(s^n)^2} \\ &\qquad = \frac{l}{16\pi(s^n)^2}[l\sin(4\pi\theta_n^\alpha) - 2\sin(2\pi\theta_n^\alpha)]. \end{aligned} \tag{A18}$$

The dependence of the soft parameters in Sec. VIII B on θ_n^α is extremely simple. Instead of reexpressing the dependence on θ_n^α in terms of the moduli, it is much more

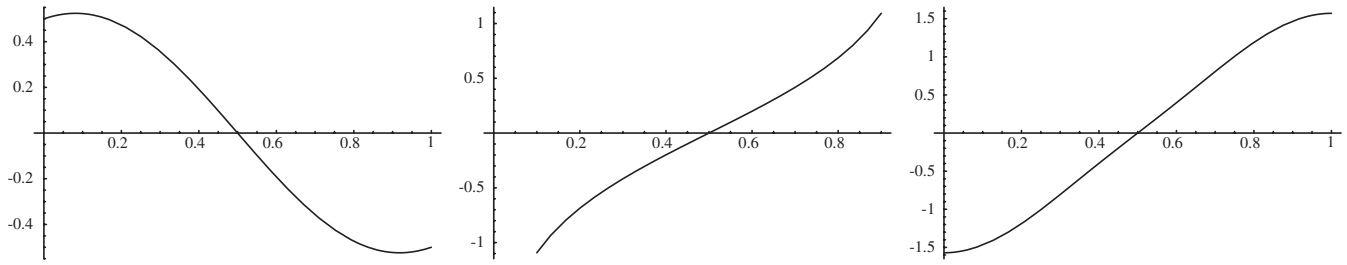

FIG. 21. Left panel: F as a function of θ_n^α. Middle panel: G as a function of θ_n^α. Right panel: H as a function of θ_n^α (for $l = 1$). From [28], $\theta_n \in [0, 1)$.

convenient to retain the dependence on θ_n^α, as $\theta_n^\alpha \in [0, 1)$ [28] and the variation of relevant functions with θ_n^α in the allowed range can be plotted easily. In particular, the function $F(\theta_n^\alpha) \equiv \frac{1}{2\pi}\{\psi_n^\alpha \sin(2\pi\theta_n^\alpha)\}$ appears in the expression for the anomaly mediated gaugino masses [Eq. (279)] and the trilinears [Eq. (287)], the function $G(\theta_n^\alpha) \equiv \ln(\frac{\Gamma(1-\theta_n^\alpha)}{\Gamma(\theta_n^\alpha)})$ appears in the expression for the trilinears [Eq. (287)] and the function $H(\theta_n^\alpha) \equiv \frac{1}{4\pi} \times \{l^2\psi_{\bar{n}n}^\alpha \sin^2(2\pi\theta_n^\alpha) + l^2\psi_n^\alpha \sin(4\pi\theta_n^\alpha) - 2l\psi_n^\alpha \sin(2\pi\theta_n^\alpha)\}$ appears in the expression for the scalars [Eq. (291)]. The variation of these functions with θ_n^α is quite mild as seen from Fig. 21.

Since the functions F, G, and H vary very mildly with θ_n^α and are $\mathcal{O}(1)$ in the whole range, it is reasonable to replace the above functions by $\mathcal{O}(1)$ numbers, as is done in Sec. VIII B. This is justified since we are only interested in estimating the rough overall scales of various soft parameters.

[1] P. Candelas, G. T. Horowitz, A. Strominger, and E. Witten, Nucl. Phys. **B258**, 46 (1985); E. Witten, Nucl. Phys. **B258**, 75 (1985).
[2] M. R. Douglas and S. Kachru, Rev. Mod. Phys. **79**, 733 (2007).
[3] S. B. Giddings, S. Kachru, and J. Polchinski, Phys. Rev. D **66**, 106006 (2002).
[4] S. Kachru, R. Kallosh, A. Linde, and S. P. Trivedi, Phys. Rev. D **68**, 046005 (2003).
[5] H. L. Verlinde, Nucl. Phys. **B580**, 264 (2000); C. S. Chan, P. L. Paul, and H. L. Verlinde, Nucl. Phys. **B581**, 156 (2000).
[6] L. Randall and R. Sundrum, Phys. Rev. Lett. **83**, 3370 (1999).**83**, 4690 (1999).
[7] O. DeWolfe, A. Giryavets, S. Kachru, and W. Taylor, J. High Energy Phys. 07 (2005) 066; J. P. Derendinger, C. Kounnas, P. M. Petropoulos, and F. Zwirner, Nucl. Phys. **B715**, 211 (2005).
[8] B. S. Acharya, arXiv:hep-th/0212294.
[9] S. Gukov, S. Kachru, X. Liu, and L. McAllister, Phys. Rev. D **69**, 086008 (2004); V. Braun and B. A. Ovrut, J. High Energy Phys. 07 (2006) 035.
[10] J. P. Conlon and F. Quevedo, J. High Energy Phys. 06 (2006) 029.
[11] P. Binetruy, M. K. Gaillard, and B. D. Nelson, Nucl. Phys. **B604**, 32 (2001).
[12] B. S. Acharya, K. Bobkov, G. L. Kane, P. Kumar, and J. Shao (unpublished).
[13] B. Acharya, K. Bobkov, G. Kane, P. Kumar, and D. Vaman, Phys. Rev. Lett. **97**, 191601 (2006).
[14] B. S. Acharya, arXiv:hep-th/0011089.
[15] M. Atiyah and E. Witten, Adv. Theor. Math. Phys. **6**, 1 (2003); arXiv:hep-th/0107177.
[16] B. S. Acharya and E. Witten, arXiv:hep-th/0109152.
[17] B. S. Acharya and S. Gukov, Phys. Rep. **392**, 121 (2004).
[18] B. S. Acharya, F. Denef, and R. Valandro, J. High Energy Phys. 06 (2005) 056.
[19] T. Friedmann and E. Witten, Adv. Theor. Math. Phys. **7**, 577 (2003); arXiv:hep-th/0211269.
[20] D. Krefl and D. Lust, J. High Energy Phys. 06 (2006) 023; R. Kallosh and A. Linde, J. High Energy Phys. 12 (2004) 004; J. J. Blanco-Pillado, R. Kallosh, and A. Linde, J. High Energy Phys. 05 (2006) 053.
[21] D. D. Joyce, *Compact Manifolds with Special Holonomy* (Oxford University Press, New York, 2000); A. Kovalev, arXiv:math.dg/0012189.
[22] V. Braun, Y. H. He, B. A. Ovrut, and T. Pantev, J. High Energy Phys. 05 (2006) 043; B. A. Ovrut, Fortschr. Phys. **54**, 160 (2006); V. Bouchard and R. Donagi, Phys. Lett. B **633**, 783 (2006); V. Bouchard, M. Cvetic, and R. Donagi, Nucl. Phys. **B745**, 62 (2006).
[23] O. Lebedev, H. P. Nilles, and M. Ratz, Phys. Lett. B **636**, 126 (2006).
[24] N. Seiberg, Phys. Rev. D **49**, 6857 (1994); Phys. Lett. B **318**, 469 (1993).
[25] D. Finnell and P. Pouliot, Nucl. Phys. **B453**, 225 (1995).
[26] E. Witten, arXiv:hep-ph/0201018.
[27] H. P. Nilles, Phys. Rep. **110**, 1 (1984); A. Brignole, L. E. Ibanez, and C. Munoz, arXiv:hep-ph/9707209.
[28] M. Bertolini, M. Billo, A. Lerda, J. F. Morales, and R.

Russo, Nucl. Phys. **B743**, 1 (2006).
[29] M. Cvetic and I. Papadimitriou, Phys. Rev. D **68**, 046001 (2003); **70**, 029903(E) (2004); D. Lust, P. Mayr, R. Richter, and S. Stieberger, Nucl. Phys. **B696**, 205 (2004).
[30] M. Cvetic, G. Shiu, and A. M. Uranga, arXiv:hep-th/0111179.
[31] S. F. King, I. N. R. Peddie, G. G. Ross, L. Velasco-Sevilla, and O. Vives, J. High Energy Phys. 07 (2005) 049.
[32] M. K. Gaillard, B. D. Nelson, and Y. Y. Wu, Phys. Lett. B **459**, 549 (1999); J. A. Bagger, T. Moroi, and E. Poppitz, J. High Energy Phys. 04 (2000) 009.
[33] G. L. Kane, P. Kumar, and J. Shao, J. Phys. G **34**, 1993 (2007).
[34] J. P. Conlon, S. S. Abdussalam, F. Quevedo, and K. Suruliz, arXiv:hep-th/0610129.
[35] K. Choi, A. Falkowski, H. P. Nilles, and M. Olechowski, Nucl. Phys. **B718**, 113 (2005); K. Choi, K. S. Jeong, and K. i. Okumura, J. High Energy Phys. 09 (2005) 039; K. Choi, K. S. Jeong, T. Kobayashi, and K. i. Okumura, Phys. Lett. B **633**, 355 (2006); R. Kitano and Y. Nomura, Phys. Lett. B **631**, 58 (2005); A. Pierce and J. Thaler, J. High Energy Phys. 09 (2006) 017; H. Baer, E. K. Park, X. Tata, and T. T. Wang, J. High Energy Phys. 08 (2006) 041.
[36] A. Lukas and S. Morris, Phys. Rev. D **69**, 066003 (2004).
[37] J. Polchinski, *String Theory* Vol. II (Cambridge University Press, Cambridge, England, 2003).